

# Analysis of Dalitz decays with intrinsic parity violating interactions in resonance chiral perturbation theory

Daiji Kimura,<sup>1,\*</sup> Takuya Morozumi,<sup>2,3,†</sup> and Hiroyuki Umeeda<sup>4,‡</sup>

<sup>1</sup>*National Institute of Technology, Ube College, Ube Yamaguchi 755-8555, Japan*

<sup>2</sup>*Graduate School of Science, Hiroshima University,*

*Higashi-Hiroshima 739-8526, Japan*

<sup>3</sup>*Core of Research for the Energetic Universe,*

*Hiroshima University, Higashi-Hiroshima 739-8526, Japan*

<sup>4</sup>*Graduate School of Science and Engineering,*

*Shimane University, Matsue 690-8504, Japan*

(Dated: December 9, 2024)

## Abstract

Observables of light hadron decays are analyzed in a model of chiral Lagrangian which includes resonance fields of vector mesons. In particular, transition form factors are investigated for Dalitz decays of  $V \rightarrow Pl^+l^-$  and  $P \rightarrow \gamma l^+l^-$  ( $V = 1^-, P = 0^-$ ). Moreover, the differential decay width of  $P \rightarrow \pi^+\pi^-\gamma$  and the partial widths of  $P \rightarrow 2\gamma, V \rightarrow P\gamma, \eta' \rightarrow V\gamma, \phi(1020) \rightarrow \omega(782)\pi^0$  and  $V \rightarrow 3P$  are also calculated. In this study, we consider a model which contains octet and singlet fields as representation of SU(3). As an extension of chiral perturbation theory, we include 1-loop ordered interaction terms. For both pseudoscalar and vector meson, we evaluate mixing matrices in which isospin/SU(3) breaking is taken into account. Furthermore, intrinsic parity violating interactions are considered with singlet fields. For parameter estimation, we carry out  $\chi^2$  fittings in which a spectral function of  $\tau$  decays, vector meson masses, decay widths of  $V \rightarrow P\gamma$  and transition form factor of  $V \rightarrow Pl^+l^-$  are utilized as input data. Using the estimated parameter region in the model, we give predictions for decay widths and transition form factors of intrinsic parity violating decays. As further model predictions, we calculate the transition form factors of  $\phi(1020) \rightarrow \pi^0 l^+l^-$  and  $\eta'(958) \rightarrow \gamma l^+l^-$  in the vicinity of resonance regions, taking account of the contribution for intermediate  $\rho(770)$  and  $\omega(782)$ .

---

\* E-mail: kimurad@ube-k.ac.jp

† E-mail: morozumi@hiroshima-u.ac.jp

‡ E-mail: umeeda@riko.shimane-u.ac.jp

# CONTENTS

I. Introduction	4
II. The model with SU(3) octets and singlets	6
A. Neutral vector meson	9
B. 1-loop correction to decay width of $V \rightarrow PP$	12
1. $K^* \rightarrow K\pi$ and $\rho^\pm \rightarrow \pi^\pm\pi^0$	12
2. $V \rightarrow \pi^+\pi^-$ ( $V = \omega, \phi$ ) and $\phi \rightarrow K^+K^-(K^0\bar{K}^0)$	13
C. Mixing between photon and vector meson	16
D. Pseudoscalar	17
III. Intrinsic parity violation	18
A. Intrinsic parity violating operators with vector mesons	19
B. Intrinsic parity violating decays	20
1. $V \rightarrow P\gamma$ and $P \rightarrow V\gamma$	20
2. $\phi \rightarrow \omega\pi^0$	24
3. $P \rightarrow 2\gamma$	25
4. $P \rightarrow \gamma l^+ l^-$	26
5. $V \rightarrow Pl^+ l^-$	27
6. $V \rightarrow P\pi^+\pi^-$	28
7. $P \rightarrow \pi^+\pi^-\gamma$	29
IV. Numerical analysis	29
A. Parameter fit	30
1. $\tau^- \rightarrow K_s\pi^-\nu$	30
2. Mass and width of vector mesons	33
3. Intrinsic parity violating decays	35
B. Model prediction	41
V. Summary and discussion	51
Acknowledgement	53
A. Counter terms	53

B. Power counting with SU(3) breaking and singlets	55
C. 1-loop correction to self-energy for $K^{*+}, K^{*0}$ and $\rho^+$	58
D. Proof of the relation for $V - A$ mixing vertex	61
E. 1-loop correction to self-energy for $\pi^+, K^+$ and $K^0$	62
F. 1-loop correction to self-energy for neutral pseudoscalars	63
G. 1-loop correction to decay constants of $\pi^+$ and $K^+$	66
H. Wess-Zumino-Witten term	67
I. Form factors at $O(p^4)$ for $\tau^- \rightarrow K_s \pi^- \nu$ decay	67
References	70

## I. INTRODUCTION

Decays of light hadrons play a crucial role to investigate low-energy behavior of quantum chromodynamics (QCD), and are measured extensively in experiments. In particular, Dalitz decays such as  $P \rightarrow \gamma l^+ l^-$  and  $V \rightarrow P l^+ l^-$  provide rich resources as hadronic observables. Using these experimental data, we can test the validity of QCD effective theories which include resonances of vector meson. As a recent result, high-precision data of transition form factors (TFFs) for  $\omega \rightarrow \pi^0 \mu^+ \mu^-$  and  $\eta \rightarrow \gamma \mu^+ \mu^-$  are measured by the NA60 collaboration [1] in proton-nucleus (p-A) collisions. Moreover, the measurement of the branching ratio and the TFF of  $\eta' \rightarrow \gamma e^+ e^-$  has been carried out by the BES III collaboration [2].

In order to describe dynamics of light hadrons, we adopt a model of chiral Lagrangian which includes vector mesons. In this model, chiral octets and singlets are introduced as representation of SU(3). There are some models [3–5], which incorporate vector mesons and the other resonances. In this study, we develop the framework so that one can include chiral correction to processes in which vector mesons and/or pseudoscalars are involved. On the basis of power counting of superficial degree of divergence, 1-loop order counter terms, which correspond to  $O(p^4)$ , are introduced [6]. Finite parts of the coefficients of the counter terms are estimated in the fitting procedure with the experimental observables in the same way as the chiral perturbation theory (ChPT). Once those parameters are determined, one can predict other observables such as TFFs and decay widths.

This effective dynamics of hadrons is applicable to a variety of phenomena, *e.g.*, hadronic  $\tau$  decays. As experimental results, a spectral function of  $\tau^- \rightarrow \pi^0 \pi^- \nu$  decay is measured in the experiments [7–9]. As for decays including kaons, a mass spectrum of  $\tau^- \rightarrow K^- \pi^0 \nu$  is observed in the BaBar experiment [10] while one of  $\tau^- \rightarrow K_S \pi^- \nu$  is measured in the Belle experiment [11]. In Ref. [12, 13], the branching ratios of  $\tau$  decays including  $\eta$  are reported. As theoretical study, the spectral function of  $\tau^- \rightarrow K_S \pi^- \nu$  decay is fitted with a resonance field of  $K^*(892)^-$  [6]. The review for  $\tau$  decays is given in Ref. [14].

For vector mesons, we calculate quantum correction to self-energies to obtain a 1-loop corrected mass matrix. The mixing matrix, which is an orthogonal matrix to diagonalize the mass matrix, is determined in the procedure of diagonalization. After diagonalizing the mass matrix, the relevant mass eigenstates play the role as resonance fields of  $\rho(770)$ ,  $\omega(782)$  and  $\phi(1020)$ . In our formulation, SU(3)/isospin breaking contribution in the self-energies is

taken into account in the mixing matrix for vector mesons. We also consider kinetic mixing of neutral vector mesons, which arises from 1-loop correction to the self-energies. Including such mixing contribution, we obtain analytic formulae of the widths for  $V \rightarrow PP$  decays. Furthermore, we consider mixing between vector meson and photon, which also comes from 1-loop correction to self-energies. As analyzed explicitly in this paper, we find that the  $V - \gamma$  mixing plays a crucial role in processes such as radiative decays. For pseudoscalars, we also take account of quantum correction to self-energies. We use parametrization in which the 1-loop correction to mass matrix elements is accounted. The mixing matrix for pseudoscalars is determined so as to diagonalize the 1-loop corrected mass matrix. Using this formulation, we consider SU(3)/isospin breaking in the  $3 \times 3$  mixing matrix for  $\pi^0, \eta$  and  $\eta'$ .

In processes such as  $P \rightarrow 2\gamma$  and radiative decays of  $V \rightarrow P\gamma$ , intrinsic parity (IP) [15] is violated. It is well-known that intrinsic parity violation (IPV) in models with vector mesons is categorized as two types: The first one is the Wess-Zumino-Witten (WZW) term, which results from quantum anomaly of SU(3) symmetry [16, 17]. The second one comes from the presence of resonance fields for vector mesons, as originally suggested in the framework of hidden local symmetry (HLS) [18, 19].

For IP violating interactions in the model, we introduce operators including SU(3) singlet fields, in addition to ones suggested in Refs. [18–20]. As shown in our numerical result, inclusion of the singlet-induced IP violating operators plays an important role in the framework of the octet+singlet scheme, typically for  $\eta' \rightarrow 2\gamma$ .

Using the introduced operators, we write formulae of the IP violating decays of hadrons. In particular, the expressions of (differential) decay widths and electromagnetic TFFs are shown. These formulae are useful for thorough analysis to test the validity of the model.

In this paper, the observables of IP violating decays are analyzed in our model. For the HLS model, a numerical result for IP violating decay widths is given in Refs. [20, 21], with SU(3) breaking effect in IP violating interactions. Radiative decays are analyzed with  $VP\gamma$  vertices in Ref. [22]. Moreover, numerical analyses of the TFFs are given in Refs. [23–28].

In our analysis,  $\chi^2$  fittings are carried out to estimate parameters in the model. As input data in the fittings, the spectral function in  $\tau^- \rightarrow K_S \pi^- \nu$  decay measured by the Belle collaboration [11] are used. Furthermore, we also utilize the data of masses for the vector mesons, which are precisely determined in experiments. For parameter estimation of coefficients of IP violating operators, the data of partial widths for radiative decays and

TFFs of  $V \rightarrow Pl^+l^-$  decays are used. As shown in the numerical result, one can find a parameter region which is consistent with experimental data for the TFFs.

Using the estimated parameter region, model prediction for hadron decays is presented in this work. Specifically, we give predictions for (1) the electromagnetic TFFs of  $P \rightarrow \gamma l^+l^-$ , (2) the partial decay widths of  $P \rightarrow \gamma l^+l^-$ ,  $P \rightarrow \pi^+\pi^-\gamma$ ,  $\phi \rightarrow \omega\pi^0$  and  $V \rightarrow Pl^+l^-$ , (3) the differential decay widths of  $P \rightarrow \pi^+\pi^-\gamma$ , (4) the TFFs of  $\rho^0 \rightarrow \pi^0 l^+l^-$ ,  $\rho^0 \rightarrow \eta l^+l^-$ ,  $\omega \rightarrow \eta l^+l^-$  and  $\phi \rightarrow \eta' l^+l^-$  and (5) the branching ratio and the partial widths of  $V \rightarrow \pi^0\pi^+\pi^-$ . As discussed in the latter part of this paper, the TFFs for  $\phi \rightarrow \pi^0 l^+l^-$  and  $\eta' \rightarrow \gamma l^+l^-$  have a peak region around which di-lepton invariant mass is close to the pole of  $\omega$ .

Remaining part of this paper is organized as follows: In Sec. II, the model is introduced and 1-loop ordered interactions are given with SU(3) octets and singlets. The quantum correction to self-energies of vector mesons are also shown. Using the 1-loop corrected propagators, we write the width of  $V \rightarrow PP$  decay, including the contribution of kinetic mixing. The  $V - \gamma$  vertex, which arises from 1-loop order interactions, is also shown. The mixing matrix for  $\pi^0$ ,  $\eta$  and  $\eta'$ , in which 1-loop correction is accounted, is introduced. In Sec. III, IP violating interaction terms are given. The formulae of decay widths for IP violating modes are explicitly shown. In Sec. IV, the results of numerical analysis are presented. We show the fitting result of the invariant mass distribution of  $\tau$  decay. Physical masses of vector mesons are also fitted in this section. Moreover, we estimate coefficients of the IP violating operators, via experimental data of hadron decays. We give the model prediction for decay widths, TFFs and differential decay widths for IP violating decays. Finally, Sec. V is devoted to summary and discussion.

## II. THE MODEL WITH SU(3) OCTETS AND SINGLETS

In this section, we introduce a model of chiral Lagrangian with vector mesons [6]. In this paper, we extend the previous one so that it includes  $\phi$  meson and electromagnetic mass of

pseudoscalar mesons as follows,

$$\mathcal{L}_\chi = \mathcal{L}_P + \mathcal{L}_V + \mathcal{L}_c, \quad (1)$$

$$\begin{aligned} \mathcal{L}_P = & \frac{f^2}{4} \text{Tr}(D_\mu U D^\mu U^\dagger) + B \text{Tr}[M(U + U^\dagger)] + C \text{Tr} Q U Q U^\dagger \\ & + \frac{1}{2} \partial_\mu \eta_0 \partial^\mu \eta_0 - \frac{1}{2} M_{00}^2 \eta_0^2 - i g_{2p} \eta_0 \text{Tr}[M(U - U^\dagger)], \end{aligned} \quad (2)$$

$$\begin{aligned} \mathcal{L}_V = & -\frac{1}{2} \text{Tr} F_V^{\mu\nu} F_{V\mu\nu} + M_V^2 \text{Tr} \left( V_\mu - \frac{\alpha_\mu}{g} \right)^2 + g_{1V} \phi_\mu^0 \text{Tr} \left\{ \left( V^\mu - \frac{\alpha^\mu}{g} \right) \left( \frac{\xi M \xi + \xi^\dagger M \xi^\dagger}{2} \right) \right\} \\ & - \frac{1}{4} F_{V\mu\nu}^0 F_V^{0\mu\nu} + \frac{1}{2} M_{0V}^2 \phi_\mu^0 \phi^{0\mu}, \end{aligned} \quad (3)$$

where

$$\alpha_\mu = \frac{1}{2i} (\xi^\dagger D_{L\mu} \xi + \xi D_{R\mu} \xi^\dagger), \quad (4)$$

$$D_{L(R)\mu} = \partial_\mu + i A_{L(R)\mu}, \quad (5)$$

$$U = \xi^2 = \exp \left( \frac{2i\pi}{f} \right), \quad (6)$$

$$D_\mu U = \partial_\mu U + i A_{L\mu} U - i U A_{R\mu}, \quad (7)$$

$$M = \text{diag}(m_u, m_d, m_s), \quad (8)$$

$$F_{V\mu\nu} = \partial_\mu V_\nu - \partial_\nu V_\mu + ig[V_\mu, V_\nu], \quad (9)$$

$$F_{V\mu\nu}^0 = \partial_\mu \phi_\nu - \partial_\nu \phi_\mu, \quad (10)$$

$$Q = \text{diag} \left( \frac{2}{3}, -\frac{1}{3}, -\frac{1}{3} \right). \quad (11)$$

The Lagrangian is divided into three parts in Eq. (1), which consist of the parts of pseudoscalars, vector mesons, and 1-loop order counter terms. As fields of pseudoscalar, the octet matrix and the singlet field are contained in Eq. (2).  $\eta_0$  is  $U(1)_A$  pseudoscalar and its mass is given as  $M_{00}$ . The term denoted as  $C \text{Tr} Q U Q U^\dagger$  in Eq. (2) is the electromagnetic correction to ChPT. This term describes the effect of virtual photon [29], and affects the mass of the charged pseudoscalar. Vector mesons are introduced as  $SU(3)$  octet and singlet in Eq. (3). Vector meson matrix for octet is denoted by  $V_\mu$ , and its mass is given as  $M_V$ , while the field  $\phi_\mu^0$  denotes  $SU(3)$  singlet vector meson.

In the following, we present how 1-loop counter terms given as  $\mathcal{L}_c$  are introduced for chiral Lagrangian with vector mesons and pseudoscalar singlet. The form of 1-loop counter terms depends on the tree-level Lagrangian and is obtained with power counting of the superficial degree of divergence in the loop calculation. The tree-level Lagrangian is constructed based

on the expansion with respect to derivatives and chiral SU(3) breaking. The Lagrangian includes either the second derivatives or an insertion of chiral SU(3) breaking. The interaction Lagrangian which satisfies such criteria is extracted from Eqs. (2, 3),

$$\begin{aligned}\mathcal{L}_0 = & \frac{f^2}{4} \text{Tr} D_\mu U D^\mu U^\dagger + M_V^2 \text{Tr} \left( V_\mu - \frac{\alpha_\mu}{g} \right)^2 \\ & + B \text{Tr}(M(U + U^\dagger)) - i g_{2p} \eta_0 \text{Tr}(M(U - U^\dagger)).\end{aligned}\quad (12)$$

Note that  $\mathcal{L}_0$  does not include the parts which are written only with vector mesons and singlet pseudoscalars. With  $\mathcal{L}_0$ , the divergent parts of the 1-loop correction is extracted and the counter terms are given in Eq. (A1). As proven in App. B, the counter terms satisfy the power counting rule, which enables us to specify the structure of them. Based on the discussion, in Eq. (1), we have included a singlet-octets vector mesons mixing term as a finite counter term.

The counter terms for the self-energy for vector mesons and  $V - \gamma$  mixing can be summarized as the effective counter terms [6],

$$\begin{aligned}\mathcal{L}_c^{eff} = & -\frac{1}{2} Z_V^{(1)} \text{Tr}(\mathcal{F}_{V\mu\nu} \mathcal{F}_V^{\mu\nu}) \\ & + C_1 \text{Tr} \left[ \frac{\xi \chi \xi + \xi^\dagger \chi^\dagger \xi^\dagger}{2} \left( V_\mu - \frac{\alpha_\mu}{g} \right)^2 \right] + C_2 \text{Tr} \left( \frac{\xi \chi \xi + \xi^\dagger \chi^\dagger \xi^\dagger}{2} \right) \text{Tr} \left[ \left( V_\mu - \frac{\alpha_\mu}{g} \right)^2 \right] \\ & + C_4 \text{Tr} \mathcal{F}_V^{\mu\nu} (F_{L\mu\nu}^0 + F_{R\mu\nu}^0),\end{aligned}\quad (13)$$

$$\chi = \frac{4BM}{f^2}.\quad (14)$$

where all the field strength are Abelian part defined by,  $\mathcal{F}_{V\mu\nu} = \partial_\mu V_\nu - \partial_\nu V_\mu$  and  $F_{L(R)\mu\nu}^0 = \partial_\mu A_{L(R)\nu} - \partial_\nu A_{L(R)\mu}$ .  $Z_V^{(1)}$  and  $C_i$  ( $i = 1, 2, 4$ ) are renormalization constants and they are written in terms of the coefficients in Eq. (A1),

$$\begin{aligned}Z_V^{(r)(1)} = & K_3^{(r)} (g_{\rho\pi\pi})_{\text{tr}}^2, \quad C_1^{(r)} = 2K_4^{(r)} (g_{\rho\pi\pi})_{\text{tr}}^2, \\ C_2^{(r)} = & 2K_5^{(r)} (g_{\rho\pi\pi})_{\text{tr}}^2, \quad C_4^{(r)} = -\frac{(g_{\rho\pi\pi})_{\text{tr}}}{2} \left( K_2^{(r)} - K_3^{(r)} \frac{M_V^2}{2g^2 f^2} \right),\end{aligned}\quad (15)$$

$$(g_{\rho\pi\pi})_{\text{tree}} = \frac{M_V^2}{2gf^2}.\quad (16)$$

The coefficients of the effective counter terms in Eq. (15) include the divergent part and the finite part. The finite parts are denoted with suffix  $(r)$ . Both divergent and finite parts of  $K_i$  are recorded in Eq. (A4).



In Eq. (16),  $(g_{\rho\pi\pi})_{\text{tree}}$  denotes a tree-level vertex for  $\rho\pi\pi$  coupling. We also define the 1-loop ordered  $\rho\pi\pi$  coupling,

$$g_{\rho\pi\pi} = \frac{M_V^2}{2gf_\pi^2}. \quad (17)$$

### A. Neutral vector meson

In this subsection, we diagonalize the mass matrix for neutral vector mesons and obtain the mass eigenstates which correspond to  $(\rho, \omega, \phi)$ . The mixing matrix between  $(\rho_0, \omega_8, \phi_0)$  and mass eigenstates determines the interaction among the physical states. The inverse propagator for the vector mesons is,

$$\frac{1}{2}V^{\mu I}D_{\mu\nu IJ}^{-1}V^{\nu J}, \quad (18)$$

where  $V^I$  denotes the eigenstate for the mass matrix,  $V_\mu^T = (V_\mu^1, V_\mu^2, V_\mu^3) = (\rho_\mu, \omega_\mu, \phi_\mu)$ . The mixing matrix  $O_V$  relates the mass eigenstates to SU(3) basis in the following,

$$V_\mu^0 = \begin{pmatrix} \rho_\mu^0 \\ \omega_\mu^8 \\ \phi_\mu^0 \end{pmatrix} = O_V V_\mu. \quad (19)$$

In Eq. (18),  $D_{\mu\nu}^{-1} = O_V^T D_{\mu\nu}^{0-1} O_V$  contains the self-energy correction,

$$D_{\mu\nu}^{0-1} = g_{\mu\nu} \begin{pmatrix} M_\rho^2 & M_{V\rho 8}^2 & M_{V0\rho}^2 \\ M_{V\rho 8}^2 & M_{V88}^2 & M_{V08}^2 \\ M_{V0\rho}^2 & M_{V08}^2 & M_{0V}^2 \end{pmatrix} + Q_{\mu\nu} \begin{pmatrix} \delta B_\rho(Q^2) & \delta B_{\rho 8}(Q^2) & 0 \\ \delta B_{\rho 8}(Q^2) & \delta B_{88}(Q^2) & 0 \\ 0 & 0 & 1 \end{pmatrix}, \quad (20)$$

$$Q_{\mu\nu} = Q_\mu Q_\nu - g_{\mu\nu} Q^2, \quad (21)$$

$$\delta B_\rho = Z_V^r(\mu) + g_{\rho\pi\pi}^2 (4M_\pi^r + M_{K^+}^r + M_{K^0}^r), \quad (22)$$

$$\delta B_{\rho 8} = \sqrt{3}g_{\rho\pi\pi}^2 \Delta M_{K^+K^0}^r, \quad (23)$$

$$\delta B_{88} = Z_V^r(\mu) + 3g_{\rho\pi\pi}^2 (M_{K^+}^r + M_{K^0}^r), \quad (24)$$

where  $\Delta M_{K^+K^0}^r = M_{K^+}^r - M_{K^0}^r$ . In Eqs. (22, 24),  $Z_V^r$  denotes the coefficient of kinetic term of octet vector meson defined as  $1 + Z_V^{r(1)}$ .  $M_P^r$  are the loop functions of vector mesons,

$$M_P^r = \frac{1}{12} \left[ \left( 1 - \frac{4M_P^2}{Q^2} \right) \bar{J}_P - \frac{1}{16\pi^2} \ln \frac{M_P^2}{\mu^2} - \frac{1}{48\pi^2} \right], \quad (25)$$

$$\bar{J}_P = \begin{cases} -\frac{1}{16\pi^2} \sqrt{1 - \frac{4M_P^2}{Q^2}} \ln \frac{1 + \sqrt{1 - \frac{4M_P^2}{Q^2}}}{1 - \sqrt{1 - \frac{4M_P^2}{Q^2}}} + \frac{1}{8\pi^2} + i \frac{1}{16\pi} \sqrt{1 - \frac{4M_P^2}{Q^2}}, & (Q^2 \geq 4M_P^2), \\ \frac{1}{8\pi^2} \left( 1 - \sqrt{\frac{4M_P^2}{Q^2}} - 1 \arctan \frac{1}{\sqrt{\frac{4M_P^2}{Q^2} - 1}} \right), & (Q^2 \leq 4M_P^2), \end{cases}$$

where  $\mu$  is a renormalization scale. In the numerical analysis, we fix it as  $\mu = m_{K^{*+}}$ . The elements in the mass matrix (20) are given by,

$$M_\rho^2 = M_V^2 + C_1^r M_\pi^2 + C_2^r (2\bar{M}_K^2 + M_\pi^2) - 4g_{\rho\pi\pi}^2 \left( \mu_\pi + \frac{\bar{\mu}_K}{2} \right) f^2, \quad (26)$$

$$M_{V88}^2 = M_V^2 + C_1^r \frac{4\bar{M}_K^2 - M_\pi^2}{3} + C_2^r (2\bar{M}_K^2 + M_\pi^2) - 6g_{\rho\pi\pi}^2 \bar{\mu}_K f^2, \quad (27)$$

$$M_{V\rho 8}^2 = \frac{1}{\sqrt{3}} \{ C_1^r \Delta_{K^+K^0} - 3g_{\rho\pi\pi}^2 \Delta\mu_K f^2 \}, \quad (28)$$

$$M_{V0\rho}^2 = \frac{\hat{g}_{1V}}{4} \Delta_{K^+K^0}, \quad (29)$$

$$M_{V08}^2 = -\frac{\hat{g}_{1V}}{2\sqrt{3}} \Delta_{K\pi}, \quad (30)$$

with

$$\mu_P = \frac{M_P^2}{32\pi^2 f^2} \ln \left( \frac{M_P^2}{\mu^2} \right), \quad \bar{\mu}_K = \frac{\mu_{K^+} + \mu_{K^0}}{2}, \quad (31)$$

$$\bar{M}_K^2 = \frac{M_{K^+}^2 + M_{K^0}^2}{2}, \quad M_\pi^2 = M_{\pi^+}^2 = M_{\pi^0}^2, \quad (32)$$

$$\hat{g}_{1V} = \frac{f^2 g_{1V}}{B}, \quad \Delta\mu_K = \mu_{K^+} - \mu_{K^0}, \quad (33)$$

$$\Delta_{PQ} = M_P^2 - M_Q^2, \quad \Delta_{K\pi} = \bar{M}_K^2 - M_\pi^2. \quad (34)$$

We calculate the mass of the neutral vector mesons,  $\rho, \omega$  and  $\phi$ . The first term in Eq. (20) is diagonalized as,

$$D_{\mu\nu}^{-1} = g_{\mu\nu} \mathcal{M}^2 + \delta B_V(Q^2) Q_{\mu\nu}, \quad (35)$$

$$\mathcal{M}^2 = \text{diag}(\mathcal{M}_1^2, \mathcal{M}_2^2, \mathcal{M}_3^2), \quad (36)$$

where  $\delta B_V(Q^2)$  is a  $3 \times 3$  matrix,

$$\delta B_V(Q^2) = O_V^T \delta B(Q^2) O_V. \quad (37)$$

The propagator for the neutral vector mesons is denoted as,

$$D^{\mu\nu} = g^{\mu\nu} D_0 + Q^\mu Q^\nu D_L, \quad (38)$$

$$D_0 = (\mathcal{M}^2 - Q^2 \delta B_V)^{-1}, \quad (39)$$

$$D_L = \frac{1}{Q^2} \left( \frac{1}{\mathcal{M}^2} - \frac{1}{\mathcal{M}^2 - Q^2 \delta B_V} \right). \quad (40)$$

In the following, we expand the propagator in Eq. (38) with respect to the off-diagonal parts of  $\delta B_V$ ,

$$(D_{\mu\nu})_{IJ} = \begin{cases} g_{\mu\nu} - \frac{Q_\mu Q_\nu}{\mathcal{M}_I^2} \delta B_{VI} \\ \mathcal{M}_I^2 - Q^2 \delta B_{VI} \end{cases}, \quad (I = J) \quad (41)$$

$$-Q_{\mu\nu} \frac{1}{\mathcal{M}_I^2 - Q^2 \delta B_{VI}} \delta B_{VIJ} \frac{1}{\mathcal{M}_J^2 - Q^2 \delta B_{VJ}}, \quad (I \neq J)$$

where  $I, J = 1, 2, 3$  and  $\delta B_{VI}$  denotes the diagonal part in the matrix in Eq. (37). If one neglects the off-diagonal parts of  $\delta B_V$ , the above propagator becomes diagonal matrix given in the first line in Eq. (41). The pole mass squared is defined as the momentum squared where the real part of the denominator of the propagator vanishes in the following as,

$$\mathcal{M}_I^2 - m_I^2 \text{Re} \delta B_{VI}(m_I^2) = 0. \quad (42)$$

The denominator of the propagator in Eq. (41) is expanded in the vicinity of the pole mass,

$$\begin{aligned} \mathcal{M}_I^2 - Q^2 \text{Re} \delta B_{VI}(Q^2) &= m_I^2 \text{Re} \delta B_{VI}(m_I^2) - Q^2 \text{Re} \delta B_{VI}(Q^2) \\ &\simeq (m_I^2 - Q^2) \frac{dQ^2 \text{Re} \delta B_{VI}(Q^2)}{dQ^2} \Big|_{Q^2=m_I^2}. \end{aligned} \quad (43)$$

We define the wave function renormalization of neutral vector meson,

$$Z_I^{-1} = \frac{dQ^2 \text{Re} \delta B_{VI}(Q^2)}{dQ^2} \Big|_{Q^2=m_I^2} = \text{Re} \delta B_{VI}(m_I^2) + m_I^2 \frac{d \text{Re} \delta B_{VI}(Q^2)}{dQ^2} \Big|_{Q^2=m_I^2}. \quad (44)$$

Thus, in the vicinity of the pole mass, the propagator takes the following form,

$$(D_{\mu\nu})_{II} \simeq Z_I \frac{g_{\mu\nu} - \frac{Q_\mu Q_\nu}{m_I^2} \left( 1 + i \frac{\text{Im} \delta B_{VI}(m_I^2)}{\text{Re} \delta B_{VI}(m_I^2)} \right)}{m_I^2 - Q^2 - i m_I \Gamma_I}, \quad (45)$$

where the definitions of the pole mass and width are given as,

$$m_I^2 = \frac{\mathcal{M}_I^2}{\text{Re} \delta B_{VI}(m_I^2)}, \quad (46)$$

$$\Gamma_I = m_I Z_I \text{Im} \delta B_{VI}(m_I^2). \quad (47)$$

## B. 1-loop correction to decay width of $V \rightarrow PP$

In this subsection, we derive the formulae for width of vector meson decay into two pseudoscalars. We compute the 1-loop diagrams which are shown in Fig. II.1. For neutral vector mesons,  $\rho, \omega$  and  $\phi$ , the contribution of the kinetic mixing is also taken into account, in addition to the diagrams in Fig. II.1.

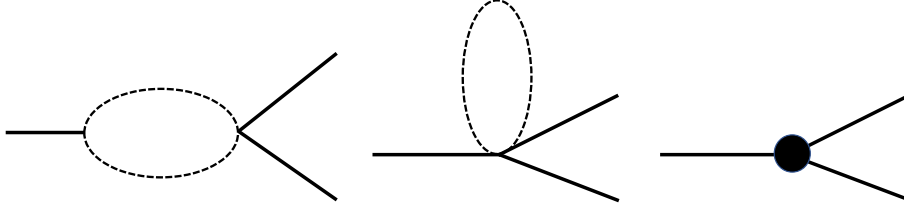


FIG. II.1. 1-loop ordered Feynman diagrams for  $V \rightarrow PP$  decays. A black circle indicates a vertex of the 1-loop ordered counter term.

### 1. $K^* \rightarrow K\pi$ and $\rho^\pm \rightarrow \pi^\pm \pi^0$

The amplitude for  $V \rightarrow P\pi$  is written as the sum of the tree-level amplitude and 1-loop correction,

$$\mathcal{M}(V \rightarrow P\pi) = \epsilon^{\mu*} q_\mu (\hat{g}_{VP\pi} + \Delta g_{VP\pi}), \quad (48)$$

where  $\hat{g}_{VP\pi}$  denotes the tree-level coupling and  $\Delta g_{VP\pi}$  is 1-loop correction. We denote  $q = p_P - p_\pi$ . Firstly, we consider the case that  $V$  and  $P$  consist of the same quark flavor contents. For  $V = K^{*+(0)}$  and  $P = K^{+(0)}$ , they are given as,

$$\begin{aligned} \hat{g}_{K^{*+}K^+\pi^0} &= \frac{(g_{\rho\pi\pi})_{\text{tree}}}{2} \sqrt{Z_{K^+} Z_{\pi^+}} = \frac{M_V^2}{4g f_K f_\pi} \\ \Delta g_{K^{*+}K^+\pi^0} &= \frac{C_2^r (2M_K^2 + M_\pi^2) + C_1^r M_K^2}{4g f^2} \\ &\quad - \frac{3(g_{\rho\pi\pi})_{\text{tree}}}{4f^2} \left( 1 - \frac{M_V^2}{2g^2 f^2} \right) \{ -(M_{K\pi}^r + M_{K\eta_8}^r) m_{K^*}^2 + (L_{K\pi}^r + L_{K\eta_8}^r) \} \\ &\quad - \frac{3(g_{\rho\pi\pi})_{\text{tree}}^2}{8g} (2\mu_K + \mu_\pi + \mu_\eta) + \frac{C_3^r}{8f^2} m_{K^*}^2. \end{aligned} \quad (49)$$

In the isospin limit, one can find the relations,  $\hat{g}_{K^{*+}K^0\pi^+} = \sqrt{2}\hat{g}_{K^{*+}K^+\pi^0}$  and  $\Delta g_{K^{*+}K^0\pi^+} = \sqrt{2}\Delta g_{K^{*+}K^+\pi^0}$ , are satisfied. Therefore, the decay width of  $K^{*+} \rightarrow K^0\pi^+$  is two times larger

than that of  $K^{*+} \rightarrow K^+\pi^0$ . For  $V = \rho^+$  and  $P = \pi^+$ , the couplings are given as,

$$\begin{aligned}\hat{g}_{\rho\pi\pi} &= (g_{\rho\pi\pi})_{\text{tree}} Z_{\pi^+} \sqrt{Z_{\rho^+}} = \frac{M_V^2}{2gf_\pi^2} \sqrt{Z_{\rho^+}}, \\ \Delta g_{\rho\pi\pi} &= \frac{C_2^r(2M_K^2 + M_\pi^2) + C_1^r M_\pi^2}{2gf^2} \\ &\quad + \frac{(g_{\rho\pi\pi})_{\text{tree}}}{f^2} \left(1 - \frac{M_V^2}{2g^2 f^2}\right) (2M_{\pi\pi}^r + M_{KK}^r) m_\rho^2 \\ &\quad - \frac{(g_{\rho\pi\pi})_{\text{tree}}}{g} (\mu_K + 2\mu_\pi) + \frac{C_3^r}{4f^2} m_\rho^2.\end{aligned}\tag{50}$$

In the above calculation, the isospin breaking effect is not taken into account. Using the 1-loop corrected couplings, we obtain the partial decay width for  $V \rightarrow P\pi$ ,

$$\Gamma[V \rightarrow P\pi] = \frac{\nu_{P\pi}(m_V^2)^3}{48\pi} \frac{\hat{g}_{VP\pi}^2}{m_V^5} \left(1 + 2\text{Re} \left( \frac{\Delta g_{VP\pi}}{\hat{g}_{VP\pi}} \right)\right),\tag{51}$$

$$\nu_{P\pi}(Q^2) = \sqrt{Q^4 - Q^2(M_P^2 + M_\pi^2) + (M_P^2 - M_\pi^2)^2}.\tag{52}$$

Using the isospin relation of  $K^*$  decays, one can find,

$$\Gamma[K^{*+} \rightarrow K^+\pi^0] + \Gamma[K^{*+} \rightarrow K^0\pi^+] = \frac{\nu_{K\pi}(m_{K^*}^2)^3}{16\pi} \frac{\hat{g}_{K^{*+}K^+\pi^0}^2}{m_{K^*}^5} \left(1 + 2\text{Re} \left( \frac{\Delta g_{K^{*+}K^+\pi^0}}{\hat{g}_{K^{*+}K^+\pi^0}} \right)\right).\tag{53}$$

## 2. $V \rightarrow \pi^+\pi^-$ ( $V = \omega, \phi$ ) and $\phi \rightarrow K^+K^-(K^0\bar{K}^0)$

In this subsection, we study the decay width of  $V \rightarrow PP$ , including the effect of kinetic mixing. First,  $V \rightarrow \pi^+\pi^-$  ( $V = \omega, \phi$ ) is investigated. Since the two pions in the final state are p wave and form an isotriplet, the decays of  $\omega$  and  $\phi$  occur due to isospin breaking. There are two major contributions to the isospin breaking amplitude. The first one is due to a partial component of isotriplet state ( $\rho^0$ ) in the mass eigenstate of  $\omega(\phi)$ . This effect is incorporated as the mixing matrix of the neutral vector mesons. Another contribution comes from the non-vanishing decay amplitude for isosinglet due to isospin breaking. In our model, incomplete cancellation between 1-loop diagram of charged kaon and one of neutral kaon leads to such contribution. The decay amplitudes for octet states  $\rho^0, \omega^8$  and a singlet

state  $\phi^0$  are given as,

$$\begin{aligned}
T(\rho^0 \rightarrow \pi^+ \pi^-) &= -(g_{\rho\pi\pi})_{\text{tree}} q_\mu \epsilon^{\mu*}, \\
T(\omega^8 \rightarrow \pi^+ \pi^-) &= \frac{\sqrt{3}}{2} (g_{\rho\pi\pi})_{\text{tree}} \epsilon^{\mu*} q_\mu \left( -(H_{K^+} - H_{K^0}) \right. \\
&\quad \left. + \frac{M_V^2}{2g^2 f^2} (H_{K^+} - H_{K^0} + \mu_{K^+} - \mu_{K^0}) - \frac{2C_1^r}{3} \frac{M_{K^+}^2 - M_{K^0}^2}{M_V^2} \right), \\
T(\phi^0 \rightarrow \pi^+ \pi^-) &= -\frac{\hat{g}_{1V}}{8g f^2} (M_{K^+}^2 - M_{K^0}^2) = -(g_{\rho\pi\pi})_{\text{tree}} \hat{g}_{1V} \frac{M_{K^+}^2 - M_{K^0}^2}{4M_V^2} q_\mu \epsilon^{\mu*}. \tag{54}
\end{aligned}$$

The effective Lagrangian for the singlet and octet states is given as,

$$\mathcal{L} = i((g_{\rho\pi\pi})_{\text{tree}} \rho^{0\mu} + g_{\omega\pi\pi} \omega^{8\mu} + g_{\phi\pi\pi} \phi^{0\mu}) \left( \pi^+ \overleftrightarrow{\partial}_\mu \pi^- \right), \tag{55}$$

where coupling constants are defined as,

$$\begin{aligned}
g_{\omega\pi\pi} &= \frac{\sqrt{3}}{2} (g_{\rho\pi\pi})_{\text{tree}} \left( H_{K^+} - H_{K^0} \right. \\
&\quad \left. - \frac{M_V^2}{2g^2 f^2} (H_{K^+} - H_{K^0} + \mu_{K^+} - \mu_{K^0}) + \frac{2C_1^r}{3} \frac{M_{K^+}^2 - M_{K^0}^2}{M_V^2} \right), \\
g_{\phi\pi\pi} &= (g_{\rho\pi\pi})_{\text{tree}} \hat{g}_{1V} \frac{M_{K^+}^2 - M_{K^0}^2}{4M_V^2}. \tag{56}
\end{aligned}$$

Next one can rewrite the Lagrangian in terms of the mass eigenstates using their relations with the octet and singlet states,

$$\begin{pmatrix} \rho_\mu^0 \\ \omega_\mu^8 \\ \phi_\mu^0 \end{pmatrix} = O_V \begin{pmatrix} \sqrt{Z_1} & 0 & 0 \\ 0 & \sqrt{Z_2} & 0 \\ 0 & 0 & \sqrt{Z_3} \end{pmatrix} \begin{pmatrix} \rho_{\mu R} \\ \omega_{\mu R} \\ \phi_{\mu R} \end{pmatrix}. \tag{57}$$

Substituting the above equation, one obtains the effective Lagrangian for renormalized mass eigenstates  $(V_\mu^1 \ V_\mu^2 \ V_\mu^3) = (\rho_{R\mu} \ \omega_{R\mu} \ \phi_{R\mu})$ ,

$$\begin{aligned}
\mathcal{L}|_{V\pi^+\pi^-} &= i((g_{\rho\pi\pi})_{\text{tree}} O_{V1I} + g_{\omega\pi\pi} O_{V2I} + g_{\phi\pi\pi} O_{V3I}) \sqrt{Z_I} V_\mu^I \left( \pi^+ \overleftrightarrow{\partial}^\mu \pi^- \right) \\
&= i(g_{\rho\pi\pi})_{\text{tree}} \Pi_I \sqrt{Z_I} V_\mu^I \left( \pi^+ \overleftrightarrow{\partial}^\mu \pi^- \right), \tag{58}
\end{aligned}$$

$$\Pi_I = O_{V1I} + \frac{g_{\omega\pi\pi}}{(g_{\rho\pi\pi})_{\text{tree}}} O_{V2I} + \frac{g_{\phi\pi\pi}}{(g_{\rho\pi\pi})_{\text{tree}}} O_{V3I}. \tag{59}$$

To evaluate the partial decay width for  $V^I \rightarrow PP$ , kinetic mixing in the decay process, i.e.,  $V^I \rightarrow V^J \rightarrow PP$ , should be taken into account. Using the renormalized fields, we can express the kinetic mixing terms,

$$\mathcal{L}_{\text{KM}} = \frac{1}{2} \begin{pmatrix} \rho_\mu^R & \omega_\mu^R & \phi_\mu^R \end{pmatrix} Q^{\mu\nu} \begin{pmatrix} 0 & \delta B_{V12} & \delta B_{V13} \\ \delta B_{V12} & 0 & \delta B_{V23} \\ \delta B_{V13} & \delta B_{V23} & 0 \end{pmatrix} \begin{pmatrix} \rho_\nu^R \\ \omega_\nu^R \\ \phi_\nu^R \end{pmatrix}. \tag{60}$$

In the above Lagrangian, we set the wave function renormalization  $Z_I = 1$ , since  $\delta B_{VIJ}$  ( $I \neq J$ ) is 1-loop order contribution.

The  $T$ -matrix elements for  $V \rightarrow PP$  decays are,

$$\begin{aligned} T[V^I \rightarrow \pi^+ \pi^-] &= -g_{V^I \pi^+ \pi^-}^{\text{eff}} (q \cdot \epsilon^*), \quad (I = 2, 3) \\ T[\phi \rightarrow K^+ K^-] &= -g_{\phi K^+ K^-}^{\text{eff}} (q \cdot \epsilon^*), \\ T[\phi \rightarrow K^0 \bar{K}^0] &= -g_{\phi K^0 \bar{K}^0}^{\text{eff}} (q \cdot \epsilon^*), \end{aligned} \quad (61)$$

where  $q = p_{+(0)} - p_{-(0)}$ . Including the contribution of kinetic mixing, the effective couplings in Eq. (61) are given as,

$$g_{V^I \pi^+ \pi^-}^{\text{eff}} = g_{\rho \pi \pi} \left[ \Pi_I \sqrt{Z_I} + m_I^2 \sum_{J \neq I} \Pi_J \frac{\delta B_{VJI}}{\mathcal{M}_J^2 - m_I^2 \delta B_{VJ}(m_I^2)} \right], \quad (62)$$

$$g_{\phi K^+ K^-}^{\text{eff}} = g_{\rho \pi \pi} \left( \frac{f_\pi}{f_K} \right)^2 \left[ \sqrt{Z_3} \Pi_3^{K^+} + m_\phi^2 \sum_{J \neq 3} \Pi_J^{K^+} \frac{\delta B_{VJ3}}{\mathcal{M}_J^2 - m_\phi^2 \delta B_{VJ}(m_3^2)} \right], \quad (63)$$

$$g_{\phi K^0 \bar{K}^0}^{\text{eff}} = g_{\rho \pi \pi} \left( \frac{f_\pi}{f_K} \right)^2 \left[ \sqrt{Z_3} \Pi_3^{K^0} + m_\phi^2 \sum_{J \neq 3} \Pi_J^{K^0} \frac{\delta B_{VJ3}}{\mathcal{M}_J^2 - m_\phi^2 \delta B_{VJ}(m_3^2)} \right], \quad (64)$$

$$\Pi_I^{K^+} = \frac{O_{V1I}}{2} + \frac{\sqrt{3}}{2} O_{V2I} + \frac{\hat{g}_{1V}(M_{\pi^+}^2 - M_{K^0}^2)}{4M_V^2} O_{V3I}, \quad (65)$$

$$\Pi_I^{K^0} = -\frac{O_{V1I}}{2} + \frac{\sqrt{3}}{2} O_{V2I} + \frac{\hat{g}_{1V}(M_{\pi^+}^2 - M_{K^+}^2)}{4M_V^2} O_{V3I}. \quad (66)$$

Ignoring the isospin breaking effect, we note that  $T[\rho^0 \rightarrow \pi^+ \pi^-]$  is the same as the amplitude of  $\rho^+ \rightarrow \pi^+ \pi^0$  which was studied in the previous subsection. In Eqs. (62-64), the second terms denote the kinetic mixing effects for  $V^I \rightarrow V^J \rightarrow PP$  decay process and  $\mathcal{M}_J$  ( $J = 1, 2, 3$ ) is the eigenvalue for the vector meson mass matrix, which differs from the physical masses,  $m_\rho, m_\omega$  or  $m_\phi$ . However, within the accuracy, one can set  $\mathcal{M}_J = m_J$  since their difference arises from only the wavefunction renormalization. One can obtain the partial widths for  $V \rightarrow PP$  decay,

$$\Gamma[V^I \rightarrow PP] = \frac{m_I |g_{VPP}^{\text{eff}}|^2}{48\pi} \left( 1 - \frac{4M_P^2}{m_I^2} \right)^{\frac{3}{2}}, \quad (67)$$

where  $g_{VPP}^{\text{eff}}$  is the coupling associated with Eqs. (62-64).

### C. Mixing between photon and vector meson

In this subsection, the mixing between photon and vector mesons is analyzed. The contributing diagrams for  $V - A$  mixing in 1-loop order are exhibited in Fig. II.2. The  $V - \gamma$



FIG. II.2. Feynman diagrams for the two-point function of the mixing of photon and vector meson. Wavy lines imply vector meson while bold wavy lines indicate the vector mesons.

conversion vertex is denoted as,

$$\mathcal{L}_\chi|_{V\gamma} = V_\mu^{0I} \Pi^{\mu\nu V^{0I}A} A_\nu = V_\mu^I \Pi^{\mu\nu V^I A} A_\nu, \quad (68)$$

$$\Pi_{\mu\nu}^{V^I A} = O_V^T \Pi_{\mu\nu}^{V^{0I} A}. \quad (69)$$

In the basis of  $SU(3)$ , the two-point functions in the l.h.s. of Eq. (68) are given as,

$$\Pi_{\mu\nu}^{V^{0I}A} = e g_{\mu\nu} \Pi^{V^{0I}A} + e Q_{\mu\nu} \Pi_T^{V^{0I}A}, \quad (70)$$

$$\begin{aligned} \Pi^{\rho_0 A} = \frac{1}{g} \left\{ -M_V^2 + 4g_{\rho\pi\pi}^2 \left( \mu_\pi + \frac{\mu_{K^+}}{2} \right) f^2 \right. \\ \left. - C_1^r \left( M_\pi^2 + \frac{\Delta_{K^+K^0}}{3} \right) - C_2^r (2\bar{M}_K^2 + M_\pi^2) \right\}, \end{aligned} \quad (71)$$

$$\Pi_T^{\rho_0 A} = g_{\rho\pi\pi} \left( 1 - \frac{M_V^2}{2g^2 f^2} \right) (4M_\pi^r + 2M_{K^+}^r) - 2C_4^r, \quad (72)$$

$$\begin{aligned} \Pi^{\omega_8 A} = \frac{1}{\sqrt{3}g} \left\{ -M_V^2 + 6g_{\rho\pi\pi}^2 \mu_{K^+} f^2 \right. \\ \left. - C_1^r \left( \frac{4\bar{M}_K^2 - M_\pi^2}{3} + \Delta_{K^+K^0} \right) - C_2^r (2\bar{M}_K^2 + M_\pi^2) \right\}, \end{aligned} \quad (73)$$

$$\Pi_T^{\omega_8 A} = 2\sqrt{3}g_{\rho\pi\pi} \left( 1 - \frac{M_V^2}{2g^2 f^2} \right) M_{K^+}^r - \frac{2}{\sqrt{3}}C_4^r, \quad (74)$$

$$\Pi^{\phi_0 A} = \frac{\hat{g}_{1V}}{g} \left( \frac{\Delta_{K\pi}}{6} - \frac{\Delta_{K^+K^0}}{4} \right), \quad (75)$$

$$\Pi_T^{\phi_0 A} = 0. \quad (76)$$



One can find that  $g^{\mu\nu}$  part in Eq. (70) is related to the matrix elements of the 1-loop corrected neutral vector meson masses in Eqs. (26, 27, 30),

$$\Pi^{V^0 A} = -\frac{1}{g} \begin{pmatrix} M_\rho^2 + \frac{1}{\sqrt{3}} M_{V\rho 8}^2 \\ M_{V\rho 8}^2 + \frac{1}{\sqrt{3}} M_{V88}^2 \\ M_{V0\rho}^2 + \frac{1}{\sqrt{3}} M_{V08}^2 \end{pmatrix}. \quad (77)$$

One can write the two-point functions in Eq. (69),

$$\Pi^{VA} = O_V^T \Pi^{V^0 A} = -\frac{1}{g} \begin{pmatrix} \mathcal{M}_1^2 & 0 & 0 \\ 0 & \mathcal{M}_2^2 & 0 \\ 0 & 0 & \mathcal{M}_3^2 \end{pmatrix} \begin{pmatrix} O_{V11} + \frac{1}{\sqrt{3}} O_{V21} \\ O_{V12} + \frac{1}{\sqrt{3}} O_{V22} \\ O_{V13} + \frac{1}{\sqrt{3}} O_{V23} \end{pmatrix}. \quad (78)$$

The derivation of Eq. (78) is shown in App. D. Thus, the mixing vertices for  $V - \gamma$  in Eq. (68) are expressed as,

$$\mathcal{L}_\chi|_{V\gamma} = -\frac{e\mathcal{M}_I^2}{g} \eta_I V_\mu^I A^\mu, \quad (79)$$

$$\eta_I = O_{V1I} + \frac{1}{\sqrt{3}} O_{V2I}. \quad (80)$$

#### D. Pseudoscalar

In this subsection, the structures of a mixing matrix and decay constants for pseudoscalars are given. We take account of 1-loop correction to both mixing and the decay constants.

The basis for an SU(3) eigenstate is written in terms of mass eigenstates as,

$$\begin{pmatrix} \pi_3 \\ \eta_8 \\ \eta_0 \end{pmatrix} = \sqrt{Z} O \begin{pmatrix} \pi^0 \\ \eta \\ \eta' \end{pmatrix}, \quad (81)$$

where  $O$  denotes an orthogonal matrix which diagonalizes a mass matrix of pseudoscalars.  $\sqrt{Z}$  in Eq. (81) is a matrix which canonically rescales 1-loop corrected kinetic terms for pseudoscalars. The result of 1-loop correction to the mass terms for charged particles is summarized in App. E, while one to the mass matrix for neutral particles is shown in App.

F. The 1-loop expression of  $\sqrt{Z}$  is recorded in Eq. (F8). We denote the mixing matrix as,

$$\begin{aligned}
O &= \begin{pmatrix} \cos \theta_2 & \sin \theta_2 & 0 \\ -\sin \theta_2 & \cos \theta_2 & 0 \\ 0 & 0 & 1 \end{pmatrix} \begin{pmatrix} 1 & 0 & 0 \\ 0 & \cos \theta_1 & \sin \theta_1 \\ 0 & -\sin \theta_1 & \cos \theta_1 \end{pmatrix} \begin{pmatrix} \cos \theta_3 & \sin \theta_3 & 0 \\ -\sin \theta_3 & \cos \theta_3 & 0 \\ 0 & 0 & 1 \end{pmatrix} \\
&= \begin{pmatrix} \cos \theta_2 \cos \theta_3 - \cos \theta_1 \sin \theta_2 \sin \theta_3 & \cos \theta_2 \sin \theta_3 + \cos \theta_1 \sin \theta_2 \cos \theta_3 & \sin \theta_1 \sin \theta_2 \\ -\sin \theta_2 \cos \theta_3 - \cos \theta_1 \cos \theta_2 \sin \theta_3 & -\sin \theta_2 \sin \theta_3 + \cos \theta_1 \cos \theta_2 \cos \theta_3 & \sin \theta_1 \cos \theta_2 \\ \sin \theta_1 \sin \theta_3 & -\sin \theta_1 \cos \theta_3 & \cos \theta_1 \end{pmatrix}, \quad (82)
\end{aligned}$$

where ranges of the mixing angles in Eq. (82) are defined as,

$$-\pi \leq \theta_1 \leq 0, \quad -\pi \leq \theta_2 \leq \pi, \quad -\pi \leq \theta_3 \leq \pi. \quad (83)$$

The mixing angles denoted as  $\theta_2$  and  $\theta_3$  are almost 0 or  $\pi$  due to isospin breaking. In Eq. (82), if we take the limit where  $\theta_{2,3} \rightarrow 0$  or  $\pi$ , one can find that  $\theta_1$  corresponds to a  $2 \times 2$  mixing angle for  $\eta_8 - \eta_0$ . Hence, in order to calculate a mixing angle for  $\eta - \eta'$  in the  $3 \times 3$  mixing matrix, we use the value of  $\theta_1$  in Eq. (82).

For decay constants of  $\pi^+$  and  $K^+$ , we also consider the 1-loop quantum correction. As stated in App. G, the ratio of a pion decay constant to one for kaon is determined with wave function renormalization of pseudoscalars [6],

$$\frac{f_{K^+}}{f_{\pi^+}} = \sqrt{\frac{Z_{\pi^+}}{Z_{K^+}}} \sim 1 + 4 \frac{M_{K^+}^2 - M_{\pi^+}^2}{f^2} L_5^r + \frac{c}{4} (5\mu_{\pi^+} - 3\mu_{88} - 2\mu_{K^+}), \quad (84)$$

where  $c$  is defined as,

$$c = 1 - \frac{M_V^2}{g^2 f^2}. \quad (85)$$

### III. INTRINSIC PARITY VIOLATION

In this section, we discuss IPV in the model. As well as ChPT, quantum anomaly of chiral symmetry causes an IP violating interaction. The expression of the WZW term is given in Eq. (H1). In addition to this operator, IP violating interaction terms, which come from the resonance field of vector mesons, are introduced. Subsequently, we write the formula of widths, TFFs, differential widths for IP violating decays.

### A. Intrinsic parity violating operators with vector mesons

Since SU(3) singlet fields are contained in the model, IP violating operators with singlets should be taken into account. We consider such singlet-induced operators within invariance of SU(3) symmetry. Imposing the charge conjugation (C) symmetry, one can obtain the operators in the model,

$$\mathcal{L}_1 = i\epsilon^{\mu\nu\rho\sigma}\text{Tr}[\alpha_{L\mu}\alpha_{L\nu}\alpha_{L\rho}\alpha_{R\sigma} - (R \leftrightarrow L)], \quad (86)$$

$$\mathcal{L}_2 = i\epsilon^{\mu\nu\rho\sigma}\text{Tr}[\alpha_{L\mu}\alpha_{R\nu}\alpha_{L\rho}\alpha_{R\sigma}], \quad (87)$$

$$\mathcal{L}_3 = \epsilon^{\mu\nu\rho\sigma}\text{Tr}[gF_{V\mu\nu}\{\alpha_{L\rho}\alpha_{R\sigma} - (R \leftrightarrow L)\}], \quad (88)$$

$$\mathcal{L}_4 = \frac{1}{2}\epsilon^{\mu\nu\rho\sigma}\text{Tr}[(\hat{F}_{L\mu\nu} + \hat{F}_{R\mu\nu})\{\alpha_{L\rho}, \alpha_{R\sigma}\}], \quad (89)$$

$$\mathcal{L}_5 = \epsilon^{\mu\nu\rho\sigma}F_{V\mu\nu}^0\text{Tr}[\alpha_{L\rho}\alpha_{R\sigma} - (R \leftrightarrow L)], \quad (90)$$

$$\mathcal{L}_6 = \frac{\eta_0}{f}\epsilon^{\mu\nu\rho\sigma}\text{Tr}F_{V\mu\nu}F_{V\rho\sigma}, \quad (91)$$

$$\mathcal{L}_7 = \frac{\eta_0}{f}\epsilon^{\mu\nu\rho\sigma}F_{V\mu\nu}^0F_{V\rho\sigma}^0, \quad (92)$$

$$\mathcal{L}_8 = \epsilon^{\mu\nu\rho\sigma}\text{Tr}(\hat{F}_{L\mu\nu} + \hat{F}_{R\mu\nu})\phi_\rho^0\frac{\alpha_{L\sigma} - \alpha_{R\sigma}}{2}, \quad (93)$$

$$\mathcal{L}_9 = \frac{\eta_0}{f}\epsilon^{\mu\nu\rho\sigma}\text{Tr}(\hat{F}_{L\mu\nu} + \hat{F}_{R\mu\nu})F_{V\rho\sigma}, \quad (94)$$

$$\mathcal{L}_{10} = \frac{\eta_0}{f}\epsilon^{\mu\nu\rho\sigma}\text{Tr}(\hat{F}_{L\mu\nu} + \hat{F}_{R\mu\nu})(\hat{F}_{L\rho\sigma} + \hat{F}_{R\rho\sigma}), \quad (95)$$

where  $\epsilon^{0123} = -\epsilon_{0123} = +1$  and,

$$\hat{F}_{L\mu\nu} = \xi^\dagger F_{L\mu\nu} \xi, \quad (96)$$

$$\hat{F}_{R\mu\nu} = \xi F_{R\mu\nu} \xi^\dagger, \quad (97)$$

$$F_{L(R)\mu\nu} = \partial_\mu A_{L(R)\nu} - \partial_\nu A_{L(R)\mu} + i[A_{L(R)\mu}, A_{L(R)\nu}], \quad (98)$$

$$\alpha_{L\mu} = \alpha_\mu + \alpha_{\perp\mu} - gV_\mu, \quad (99)$$

$$\alpha_{R\mu} = \alpha_\mu - \alpha_{\perp\mu} - gV_\mu, \quad (100)$$

$$\alpha_{\perp\mu} = \frac{1}{2i}(\xi^\dagger D_{L\mu} \xi - \xi D_{R\mu} \xi^\dagger). \quad (101)$$

In Eqs. (86-88),  $\mathcal{L}_{1-3}$  are introduced in Refs. [18, 19] while  $\mathcal{L}_4$  is considered in Ref. [20]. We introduced  $\mathcal{L}_{5-10}$ , which are written with singlets of  $\eta_0$  or  $\phi_0$ . In Eqs. (86-95), we required that the operators should be Hermite.

In contrast to our work, the singlet fields are contained as a component of chiral nonet matrix in Ref. [20] and  $\mathcal{L}_i (i = 5 - 10)$  is not included in that work. Chiral SU(3) breaking

effect in IP violating interactions is introduced with spurion field method in Ref. [20], while the operators in Eqs. (86-95) are invariant under SU(3) transformation.

The IP violating interactions in our model are denoted as,

$$\mathcal{L}_{\text{IPV}} = \mathcal{L}_{\text{WZ}} + \sum_{i=1}^{10} c_i^{\text{IP}} \mathcal{L}_i. \quad (102)$$

In Eq. (102), the coefficients of the operators,  $c_i^{\text{IP}}$  ( $i = 1-10$ ), are free parameters. As carried out in Sec. IV, these parameters are estimated via experimental data which are sensitive to IPV. In the following subsections, with the interaction in Eq. (102), the formulae of IP violating decay modes are explicitly written.

## B. Intrinsic parity violating decays

### 1. $V \rightarrow P\gamma$ and $P \rightarrow V\gamma$

In this subsection, IP violating decays of  $V \rightarrow P\gamma$  and  $P \rightarrow V\gamma$  are investigated. Diagrams contributing to  $V \rightarrow P\gamma$  and  $P \rightarrow V\gamma$  are listed in Fig. III.1. Interaction vertices of

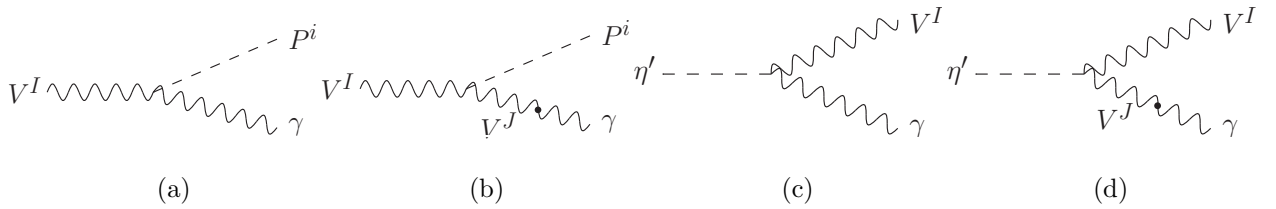


FIG. III.1. Diagrams contributing to the decay width for: (a)-(b)  $V^I \rightarrow P^i\gamma$  and (c)-(d)  $\eta' \rightarrow V\gamma$ .

vector meson are shown as,

$$\mathcal{L}_{\text{IPV}}|_{VP\gamma} = -\frac{e}{f_\pi} \chi_{iI} \epsilon^{\mu\nu\rho\sigma} \partial_\mu V_\nu^I \partial_\rho P^i A_\sigma, \quad (103)$$

$$\mathcal{L}_{\text{IPV}}|_{VVP} = \frac{g}{f_\pi} \theta_{iIJ} \epsilon^{\mu\nu\rho\sigma} \partial_\mu V_\nu^I \partial_\rho P^i V_\sigma^J, \quad (104)$$

$$\begin{aligned} \mathcal{L}_{\text{IPV}}|_{V^+P^-\gamma + \text{h.c.}} &= \frac{2eg}{3f_\pi} c_{34}^- \epsilon^{\mu\nu\rho\sigma} (\partial_\mu \rho_\nu^+ \partial_\rho \pi^- + \partial_\mu \rho_\nu^- \partial_\rho \pi^+) A_\sigma \\ &\quad + \frac{2eg}{3f_K} c_{34}^- \epsilon^{\mu\nu\rho\sigma} (\partial_\mu K_\nu^{*+} \partial_\rho K^- + \partial_\mu K_\nu^{*-} \partial_\rho K^+) A_\sigma \\ &\quad - \frac{4eg}{3f_K} c_{34}^- \epsilon^{\mu\nu\rho\sigma} (\partial_\mu K_\nu^* \partial_\rho \bar{K}^0 + \partial_\mu \bar{K}_\nu^* \partial_\rho K^0) A_\sigma, \end{aligned} \quad (105)$$

$$\begin{aligned} \mathcal{L}_{\text{IPV}}|_{V^-P^+V^0 + \text{h.c.}} &= \frac{g}{f_\pi} \gamma_I \epsilon^{\mu\nu\rho\sigma} (\partial_\mu \rho_\nu^+ \partial_\rho \pi^- + \partial_\mu \rho_\nu^- \partial_\rho \pi^+) V_\sigma^I \\ &\quad + \frac{g}{f_K} L_I \epsilon^{\mu\nu\rho\sigma} (\partial_\mu K_\nu^{*+} \partial_\rho K^- + \partial_\mu K_\nu^{*-} \partial_\rho K^+) V_\sigma^I \\ &\quad - \frac{g}{f_K} \varphi_I \epsilon^{\mu\nu\rho\sigma} (\partial_\mu K_\nu^* \partial_\rho \bar{K}^0 + \partial_\mu \bar{K}_\nu^* \partial_\rho K^0) V_\sigma^I, \end{aligned} \quad (106)$$

where  $i, I$  and  $J$  run from 1 to 3 and  $c_{34}^- = c_3^{\text{IP}} - c_4^{\text{IP}}$ . In Eqs. (103-104, 106), fields of mass eigenstate are denoted for vector mesons as  $(V^1, V^2, V^3) = (\rho, \omega, \phi)$  and for pseudoscalars as  $(P^1, P^2, P^3) = (\pi^0, \eta, \eta')$ , respectively. The coefficients,  $\chi_{iI}$  in Eq. (103), describes the vertex of each component, *e.g.*,  $\chi_{11}$  for  $\rho\pi^0\gamma$  vertex and  $\chi_{12}$  for  $\omega\pi^0\gamma$  vertex. Note that the vertex coefficient of  $\rho\omega\pi^0$  is proportional to  $\theta_{121} + \theta_{112}$  in Eq. (104) since an operator with  $I = 1, J = 2$  and another operator with  $I = 2, J = 1$  give the same amplitude. The coefficients of the vertices in Eqs. (103-106) are given as,

$$\begin{aligned} V^I P^i \gamma : \chi_{iI} &= -\frac{2g}{3} c_{34}^- \left[ \left( O_{1i} + \sqrt{3} \sqrt{\frac{Z_2^\pi}{Z_1^\pi}} O_{2i} \right) O_{V1I} + \left( \sqrt{3} O_{1i} - \sqrt{\frac{Z_2^\pi}{Z_1^\pi}} O_{2i} \right) O_{V2I} \right] \\ &\quad - 4c_5^{\text{IP}} \left( O_{1i} + \frac{1}{\sqrt{3}} \sqrt{\frac{Z_2^\pi}{Z_1^\pi}} O_{2i} \right) O_{V3I} + 2c_8^{\text{IP}} \left( O_{1i} + \frac{1}{\sqrt{3}} \sqrt{\frac{Z_2^\pi}{Z_1^\pi}} O_{2i} \right) O_{V3I} \\ &\quad + 2c_9^{\text{IP}} \sqrt{\frac{1}{Z_1^\pi}} O_{3i} \left( O_{V1I} + \frac{1}{\sqrt{3}} O_{V2I} \right), \end{aligned} \quad (107)$$

$$\begin{aligned} V^I V^J P^i : \theta_{iIJ} &= -\frac{2gc_3^{\text{IP}}}{\sqrt{3}} \left[ \left( 2O_{1i} O_{V1I} - \sqrt{\frac{Z_2^\pi}{Z_1^\pi}} O_{2i} O_{V2I} \right) O_{V2J} + \sqrt{\frac{Z_2^\pi}{Z_1^\pi}} O_{2i} O_{V1I} O_{V1J} \right] \\ &\quad - 4c_5^{\text{IP}} \left( O_{1i} O_{V3I} O_{V1J} + \sqrt{\frac{Z_2^\pi}{Z_1^\pi}} O_{2i} O_{V3I} O_{V2J} \right) \\ &\quad - \frac{2c_6^{\text{IP}}}{g} \sqrt{\frac{1}{Z_1^\pi}} O_{3i} (O_{V1I} O_{V1J} + O_{V2I} O_{V2J}) - \frac{4c_7^{\text{IP}}}{g} \sqrt{\frac{1}{Z_1^\pi}} O_{3i} O_{V3I} O_{V3J}, \end{aligned} \quad (108)$$

$$\rho^+ \pi^- V^I + \text{h.c.} : \gamma_I = -\frac{4gc_3^{\text{IP}}}{\sqrt{3}} O_{V2I} - 4c_5^{\text{IP}} O_{V3I}, \quad (109)$$

$$K^{*+} K^- V^I + \text{h.c.} : L_I = -2gc_3^{\text{IP}} \left( O_{V1I} - \frac{1}{\sqrt{3}} O_{V2I} \right) - 4c_5^{\text{IP}} O_{V3I}, \quad (110)$$

$$K^{*0} \bar{K}^0 V^I + \text{h.c.} : \varphi_I = -2gc_3^{\text{IP}} \left( O_{V1I} + \frac{1}{\sqrt{3}} O_{V2I} \right) + 4c_5^{\text{IP}} O_{V3I}. \quad (111)$$

Vector mesons can decay into  $P\gamma$  directly with the operator in Eq. (103).  $VP\gamma$  vertex is absent in Ref. [20] since the relation  $c_3^{\text{IP}} = c_4^{\text{IP}}$  is adopted. Meanwhile, IP violating  $VVP$  operator in Eq. (104) also causes  $V \rightarrow P\gamma$  with the  $V - \gamma$  conversion vertex in Eq. (79). The notation of propagators for neutral vector meson is given as,

$$iD_{\mu\nu}^J(Q) = ig_{\mu\nu} D^J(Q^2) + iQ_\mu Q_\nu D_L^J(Q^2), \quad (J = 1, 2, 3), \quad (112)$$

where  $J = 1, 2, 3$  is assigned with the propagator of  $\rho, \omega$  and  $\phi$ , respectively. In the calculation of the  $V - \gamma$  conversion decay  $V \rightarrow PV^* \rightarrow P\gamma$ , the term proportional to  $D_L^J(0)$  vanishes since the momentum product  $Q_\mu Q_\nu$  is eliminated when multiplied with antisymmetric tensor. Consequently, the conversion process  $V \rightarrow PV^* \rightarrow P\gamma$  is proportional to the contribution from the metric tensor part of intermediate vector mesons. With Eq. (78), one can find that the following relation is satisfied,

$$D^J(0) \cdot \left( -\frac{e\mathcal{M}_J^2}{g} \eta_J \right) = -\frac{e}{g} \eta_J. \quad (113)$$

Although vector meson propagator is shown apparently in Fig. III.1(b), the dependence on the mass cancels out in Eq. (113).

Decay amplitudes are obtained from the operators in Eqs. (103-106) as,

$$\mathcal{M}_{V^I \rightarrow P^i \gamma} = X_{iI} \epsilon^{\mu\nu\rho\sigma} p_\mu^\gamma p_\nu^P \epsilon_\rho^V \epsilon_\sigma^{\gamma*} \quad (114)$$

$$\mathcal{M}_{\rho^+ \rightarrow \pi^+ \gamma} = X_{\rho^+} \epsilon^{\mu\nu\rho\sigma} p_\mu^\gamma p_\nu^{\pi^+} \epsilon_\rho^{\rho^+} \epsilon_\sigma^{\gamma*}, \quad (115)$$

$$\mathcal{M}_{K^{*+} \rightarrow K^+ \gamma} = X_{K^{*+}} \epsilon^{\mu\nu\rho\sigma} p_\mu^\gamma p_\nu^{K^+} \epsilon_\rho^{K^{*+}} \epsilon_\sigma^{\gamma*} \quad (116)$$

$$\mathcal{M}_{K^{*0} \rightarrow K^0 \gamma} = X_{K^{*0}} \epsilon^{\mu\nu\rho\sigma} p_\mu^\gamma p_\nu^{K^0} \epsilon_\rho^{K^{*0}} \epsilon_\sigma^{\gamma*}, \quad (117)$$

$$\mathcal{M}_{\eta' \rightarrow V^I \gamma} = X_{3I} \epsilon^{\mu\nu\rho\sigma} p_\mu^V p_\nu^{\gamma*} \epsilon_\rho^V \epsilon_\sigma^{\gamma*}, \quad (I = 1, 2) \quad (118)$$

$$X_{iI} = \frac{e\sqrt{Z_I}}{f_\pi} \bar{\chi}_{iI}, \quad (119)$$

$$\bar{\chi}_{iI} = \chi_{iI} - \sum_{J=1}^3 \bar{\theta}_{IJ} \eta_J, \quad (\bar{\theta}_{IJ} = \theta_{IJ} + \theta_{JI}) \quad (120)$$

$$\begin{aligned} &= \frac{2gc_{34}^+}{\sqrt{3}} \left[ \left( \sqrt{\frac{Z_2^\pi}{Z_1^\pi}} O_{2i} + \frac{1}{\sqrt{3}} O_{1i} \right) O_{V1I} + \left( O_{1i} - \frac{1}{\sqrt{3}} \sqrt{\frac{Z_2^\pi}{Z_1^\pi}} O_{2i} \right) O_{V2I} \right] \\ &+ \frac{2c_{69}}{g} \sqrt{\frac{1}{Z_1^\pi}} O_{3i} (O_{V1I} + \frac{1}{\sqrt{3}} O_{V2I}) + 2c_8^{\text{IP}} \left( O_{1i} + \frac{1}{\sqrt{3}} \sqrt{\frac{Z_2^\pi}{Z_1^\pi}} O_{2i} \right) O_{V3I}, \end{aligned} \quad (121)$$

$$X_{\rho^+} = \frac{e\sqrt{Z_\rho}}{f_\pi} \left( -\frac{2g}{3} c_{34}^- - \sum_{J=1}^3 \gamma_J \eta_J \right) = \frac{2eg\sqrt{Z_\rho}}{3f_\pi} c_{34}^+, \quad (122)$$

$$X_{K^{*+}} = \frac{e\sqrt{Z_{K^*}}}{f_K} \left( -\frac{2g}{3} c_{34}^- - \sum_{J=1}^3 L_J \eta_J \right) = \frac{2eg\sqrt{Z_{K^*}}}{3f_K} c_{34}^+, \quad (123)$$

$$X_{K^{*0}} = \frac{e\sqrt{Z_{K^*}}}{f_K} \left( \frac{4g}{3} c_{34}^- + \sum_{J=1}^3 \varphi_J \eta_J \right) = -\frac{4eg\sqrt{Z_{K^*}}}{3f_K} c_{34}^+, \quad (124)$$

where  $c_{34}^+ = c_3^{\text{IP}} + c_4^{\text{IP}}$  and  $c_{69} = 2c_6^{\text{IP}} + gc_9^{\text{IP}}$ . The coefficient of neutral meson decay amplitude denoted as  $X_{iI}$  in Eq. (119) includes the factor  $(\sqrt{Z_1}, \sqrt{Z_2}, \sqrt{Z_3}) = (\sqrt{Z_\rho}, \sqrt{Z_\omega}, \sqrt{Z_\phi})$ , which comes from the wave function renormalization of an external vector line in Fig. III.1. In Eqs. (122, 123), we assume that the wave function renormalization of charged vector meson is equal to one for neutral vector meson, *i.e.*,  $\sqrt{Z_{\rho^+}} = \sqrt{Z_\rho}$  and  $\sqrt{Z_{K^*}} = \sqrt{Z_{K^{*+}}}$ , which is valid in the isospin limit. One can write the partial decay width of  $V \rightarrow P\gamma$  and  $P \rightarrow V\gamma$

with  $X$ 's in Eqs. (119, 122-124) as,

$$\Gamma[V^I \rightarrow P^i \gamma] = \frac{1}{96\pi} X_{iI}^2 m_I^3 \left(1 - \frac{M_{P^i}^2}{m_I^2}\right)^3, \quad (125)$$

$$\Gamma[\rho^+ \rightarrow \pi^+ \gamma] = \frac{1}{96\pi} X_{\rho^+}^2 m_{\rho^+}^3 \left(1 - \frac{M_{\pi^+}^2}{m_{\rho^+}^2}\right)^3, \quad (126)$$

$$\Gamma[K^{*+} \rightarrow K^+ \gamma] = \frac{1}{96\pi} X_{K^{*+}}^2 m_{K^{*+}}^3 \left(1 - \frac{M_{K^+}^2}{m_{K^{*+}}^2}\right)^3, \quad (127)$$

$$\Gamma[K^{*0} \rightarrow K^0 \gamma] = \frac{1}{96\pi} X_{K^{*0}}^2 m_{K^{*0}}^3 \left(1 - \frac{M_{K^0}^2}{m_{K^{*0}}^2}\right)^3, \quad (128)$$

$$\Gamma[\eta' \rightarrow V^I \gamma] = \frac{1}{32\pi} X_{3I}^2 M_{\eta'}^3 \left(1 - \frac{m_I^2}{M_{\eta'}^2}\right)^3. \quad (I = 1, 2) \quad (129)$$

The pseudoscalar decay width in Eq. (129) is analogous to one for  $V \rightarrow P\gamma$  given in Eqs. (125-128) and its coefficient is different by a factor 1/3 which comes from spin average of vector meson. One can find that  $\Gamma[V^I \rightarrow P^i \gamma]$  and  $\Gamma[\rho^+ \rightarrow \pi^+ \gamma]$  in Eqs. (125-126) provide the relation,

$$\left| \frac{X_{iI}}{X_{\rho^+}} \right| = \sqrt{\frac{\Gamma_{V^I \rightarrow P^i \gamma}}{\Gamma_{\rho^+ \rightarrow \pi^+ \gamma}} \frac{m_I^3}{m_{\rho^+}^3} \left( \frac{m_{\rho^+}^2 - M_{\pi^+}^2}{m_I^2 - M_{P^i}^2} \right)^3}. \quad (130)$$

In the above relation, the ratio of the effective coupling for  $V^I \rightarrow P^i \gamma$  to one for  $\rho^+ \rightarrow \pi^+ \gamma$  is written in terms experimental data on r.h.s. Using Eqs. (125-126), we can rewrite l.h.s. in Eq. (130),

$$\begin{aligned} \left| \frac{X_{iI}}{X_{\rho^+}} \right| &= \sqrt{\frac{Z_I}{Z_{\rho^+}}} \left| O_{1i}(O_{V1I} + \sqrt{3}O_{V2I}) + \sqrt{\frac{Z_2^\pi}{Z_1^\pi}} O_{2i}(\sqrt{3}O_{V1I} - O_{V2I}) \right. \\ &\quad \left. + \frac{\sqrt{3}c_{69}}{g^2 c_{34}^+} \sqrt{\frac{1}{Z_1^\pi}} O_{3i}(\sqrt{3}O_{V1I} + O_{V2I}) + \frac{\sqrt{3}c_8^{\text{IP}}}{g c_{34}^+} \left( \sqrt{3}O_{1i} + \sqrt{\frac{Z_2^\pi}{Z_1^\pi}} O_{2i} \right) O_{V3I} \right|. \end{aligned} \quad (131)$$

In the above relation, the effective coupling is written in terms of model parameters. We use the relations in Eqs. (130, 131) for the numerical analysis of  $\chi^2$  fitting.

## 2. $\phi \rightarrow \omega \pi^0$

In this subsection, an IP violating process of  $\phi \rightarrow \omega \pi^0$  is analyzed. The contributing operator to  $\phi \rightarrow \omega \pi^0$  is given in Eq. (104), and the diagram is shown in Fig. III.2. The



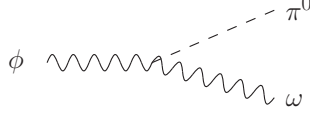


FIG. III.2. Diagram contributing to the IP violating decay of  $\phi \rightarrow \omega\pi^0$ .

transition amplitude of  $\phi \rightarrow \omega\pi^0$  is written as,

$$\mathcal{M}_{\phi \rightarrow \omega\pi^0} = X_{\phi \rightarrow \omega\pi^0} \epsilon^{\mu\nu\rho\sigma} p_\mu^\omega p_\nu^{\pi^0} \epsilon_\rho^\phi \epsilon_\sigma^{\omega*}, \quad (132)$$

$$X_{\phi \rightarrow \omega\pi^0} = -\frac{g\sqrt{Z_\phi Z_\omega}}{f_\pi} \bar{\theta}_{123}. \quad (133)$$

The contribution coming from  $V - \gamma$  conversion is negligible since it gives rise to  $\mathcal{O}(\alpha)$  correction. In Eq. (133), the factor of wave function renormalization of external vectors is included. Thus, the partial decay width of  $\phi \rightarrow \omega\pi^0$  is,

$$\Gamma[\phi \rightarrow \omega\pi^0] = \frac{1}{96\pi} X_{\phi \rightarrow \omega\pi^0}^2 \times \left( \frac{\sqrt{m_\phi^4 + m_\omega^4 + M_{\pi^0}^4 - 2(m_\phi^2 m_\omega^2 + m_\omega^2 M_{\pi^0}^2 + M_{\pi^0}^2 m_\phi^2)}}{m_\phi} \right)^3. \quad (134)$$

### 3. $P \rightarrow 2\gamma$

In this subsection, we evaluate partial decay widths of the IP violating process given as  $P^i \rightarrow 2\gamma$ . The IP violating interaction terms yield contribution to  $P\gamma\gamma$  vertex as,

$$\mathcal{L}_{\text{IPV}}|_{P^i\gamma\gamma} = -\frac{e^2}{f_\pi} h_i \epsilon^{\mu\nu\rho\sigma} P^i \partial_\mu A_\nu \partial_\rho A_\sigma, \quad (135)$$

$$h_i = \left( \frac{1}{8\pi^2} + \frac{4c_4^{\text{IP}}}{3} \right) \left( O_{1i} + \frac{1}{\sqrt{3}} \sqrt{\frac{Z_2^\pi}{Z_1^\pi}} O_{2i} \right) - \frac{32}{3} c_{10}^{\text{IP}} \sqrt{\frac{1}{Z_1^\pi}} O_{3i}, \quad (136)$$

where the first term proportional to  $1/8\pi^2$  in Eq. (136) implies the contribution from the WZW term. Diagrams of the decay of  $P^i \rightarrow 2\gamma$  are given in Fig. III.3. With the operators

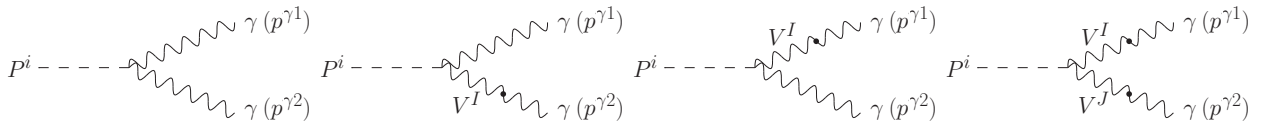


FIG. III.3. Diagrams contributing to the decay width of  $P^i \rightarrow 2\gamma$ .

in Eqs. (79, 103, 135), the transition amplitude of  $P^i \rightarrow 2\gamma$  is written as,

$$\mathcal{M}_{P^i \rightarrow 2\gamma} = R_i \epsilon^{\mu\nu\rho\sigma} p_\mu^{\gamma^1} p_\nu^{\gamma^2} \epsilon_\rho^{\gamma^1*} \epsilon_\sigma^{\gamma^2*}, \quad (137)$$

$$\begin{aligned} R_i &= -\frac{e^2}{f_\pi} \left[ 2h_i - \frac{1}{g} \left( 2 \sum_{I=1}^3 \chi_{iI} \eta_I - \sum_{I,J=1}^3 \bar{\theta}_{iIJ} \eta_I \eta_J \right) \right] \\ &= -\frac{e^2}{f_\pi} \left[ \frac{1}{4\pi^2} \left( O_{1i} + \frac{1}{\sqrt{3}} \sqrt{\frac{Z_2^\pi}{Z_1^\pi}} O_{2i} \right) - \frac{16}{3} c_{6-9-10} \sqrt{\frac{1}{Z_1^\pi}} O_{3i} \right]. \end{aligned} \quad (138)$$

where  $c_{6-9-10} = c_6^{\text{IP}}/g^2 + c_9^{\text{IP}} + 4c_{10}^{\text{IP}}$ . The partial decay width of  $P^i \rightarrow 2\gamma$  is given as,

$$\Gamma[P^i \rightarrow 2\gamma] = \frac{1}{64\pi} R_i^2 M_{P^i}^3. \quad (139)$$

#### 4. $P \rightarrow \gamma l^+ l^-$

In this subsection, a form factor for IP violating modes  $P^i \rightarrow \gamma l^+ l^-$  is obtained. The contributing diagrams are displayed in Fig. III.4. Following the notations used in experiments,

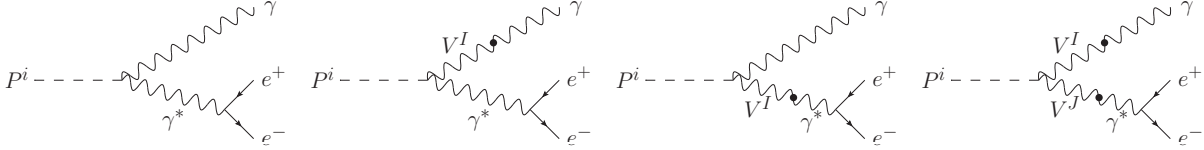


FIG. III.4. Diagrams contributing to the decay width of  $P^i \rightarrow \gamma l^+ l^-$ .

the differential decay width is written in terms of the TFF as,

$$\frac{d\Gamma(P^i \rightarrow \gamma l^+ l^-)}{ds d\cos\theta} = \frac{\alpha}{4\pi} \Gamma(P^i \rightarrow 2\gamma) \frac{\beta_l}{s} (2 - \beta_l^2 \sin^2\theta) \left(1 - \frac{s}{M_{P^i}^2}\right)^3 |F_{P^i}(s)|^2, \quad (140)$$

$$\frac{d\Gamma(P^i \rightarrow \gamma l^+ l^-)}{ds} = \frac{2\alpha}{3\pi} \Gamma(P^i \rightarrow 2\gamma) \frac{\beta_l}{s} \left(1 + \frac{2m_l^2}{s}\right) \left(1 - \frac{s}{M_{P^i}^2}\right)^3 |F_{P^i}(s)|^2, \quad (141)$$

$$\beta_l = \sqrt{1 - 4m_l^2/s}, \quad (142)$$

where  $s$  denotes the squared invariant mass in di-lepton system while  $\theta$  indicates an angle between  $P^i$  and  $l^+$  in the di-lepton rest frame. The model prediction for the TFF is,

$$|F_{P^i}(s)|^2 = \left| 1 + \frac{e^2 s}{g f_\pi R_i} \sum_{I=1}^3 \bar{\chi}_{iI} \eta_I \delta B_{VI} D_I(s) \right|^2. \quad (143)$$

5.  $V \rightarrow Pl^+l^-$

In this subsection, a form factor for IP violating electromagnetic decays for neutral vector mesons is analyzed. Contributing diagrams are exhibited in Fig. III.5. The differential decay

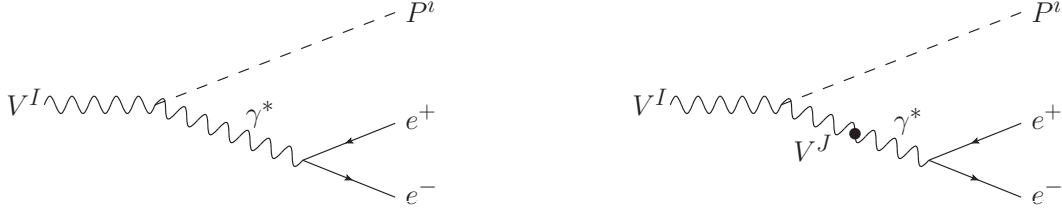


FIG. III.5. Diagrams contributing to the decay width of  $V^I \rightarrow P^i l^+ l^-$ .

width for  $V \rightarrow Pl^+l^-$  is written in terms of the TFF in the following form,

$$\frac{d^2\Gamma(V^I \rightarrow P^i l^+ l^-)}{ds d\cos\theta} = \frac{\alpha}{8\pi} \Gamma(V^I \rightarrow P^i \gamma) \frac{\beta_l}{s} (2 - \beta_l^2 \sin^2 \theta) \times \left[ \left( 1 + \frac{s}{m_I^2 - M_{P^i}^2} \right)^2 - \frac{4m_I^2 s}{(m_I^2 - M_{P^i}^2)^2} \right]^{\frac{3}{2}} |F_{V^I P^i}(s)|^2, \quad (144)$$

$$\frac{d\Gamma(V^I \rightarrow P^i l^+ l^-)}{ds} = \frac{\alpha}{3\pi} \Gamma(V^I \rightarrow P^i \gamma) \frac{\beta_l}{s} \left( 1 + \frac{2m_l^2}{s} \right) \times \left[ \left( 1 + \frac{s}{m_I^2 - M_{P^i}^2} \right)^2 - \frac{4m_I^2 s}{(m_I^2 - M_{P^i}^2)^2} \right]^{\frac{3}{2}} |F_{V^I P^i}(s)|^2, \quad (145)$$

where  $\theta$  is an angle between  $V^I$  and  $l^+$  in the di-lepton rest frame. As the model prediction, the TFF is obtained as,

$$|F_{V^I P^i}(s)|^2 = \left| 1 + \frac{s}{\bar{\chi}_{iI}} \sum_{J=1}^3 \bar{\theta}_{iIJ} \eta_J \delta B_{VJJ} D_J(s) \right|^2. \quad (146)$$

The TFF in the above equation are normalized as unity in the limit where virtual photon goes on-shell.

## 6. $V \rightarrow P\pi^+\pi^-$

In this subsection, partial decay widths for  $V \rightarrow P\pi^+\pi^-$  are analyzed. Interaction terms for the process are,

$$\mathcal{L}_{\text{IPV}}|_{V^I P^i \pi^+ \pi^-} = i \frac{J_{iI}}{f_\pi^3} \epsilon^{\mu\nu\rho\sigma} V_\mu^I \partial_\nu P^i \partial_\rho \pi^+ \partial_\sigma \pi^-, \quad (147)$$

$$\mathcal{L}_\chi|_{\rho^- P^i \pi^+ + \text{h.c.}} = i g_{\rho\pi\pi} O_{1i} \left[ \rho_\mu^- \left( P^i \overleftrightarrow{\partial}^\mu \pi^+ \right) - \rho_\mu^+ \left( P^i \overleftrightarrow{\partial}^\mu \pi^- \right) \right], \quad (148)$$

$$J_{iI} = \frac{g c_{123}}{\sqrt{3}} \left( 3 O_{1i} O_{V2I} + \sqrt{\frac{Z_2^\pi}{Z_1^\pi}} O_{2i} O_{V1I} \right) + 12 c_5^{\text{IP}} O_{1i} O_{V3I}, \quad (149)$$

where  $c_{123} = c_{12}^- + 2c_3^{\text{IP}}$ . The diagrams for the decay of  $V^I \rightarrow P^i \pi^+ \pi^-$  are given in Fig. III.6. Propagators for  $\rho^\pm$  are formulated in the following form as,

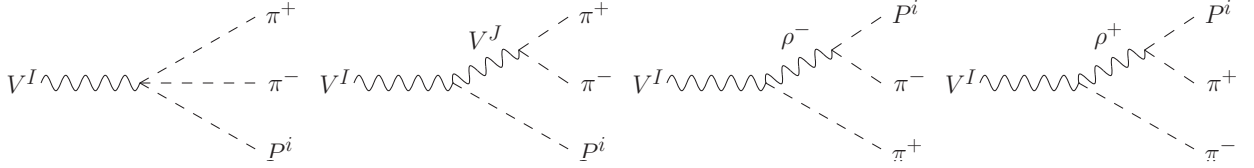


FIG. III.6. Diagrams contributing to the decay width of  $V^I \rightarrow P^i \pi^+ \pi^-$ .

$$i D_\pm^{\mu\nu}(Q) = i g^{\mu\nu} D_\pm(Q^2) + i Q^\mu Q^\nu D_{L\pm}(Q^2). \quad (150)$$

The transition amplitude is given as,

$$\mathcal{M} = Y_{iI} \epsilon^{\mu\nu\rho\sigma} \epsilon_\mu^V p_\nu^- p_\rho^+ p_\sigma^0, \quad (151)$$

$$Y_{iI} = \frac{\sqrt{Z_I}}{f_\pi^3} \left[ J_{iI} + \sum_{J=1}^3 \zeta_{iIJ} D^J(s_{+-}) + \kappa_{iI} (D_+(s_{+0}) + D_-(s_{-0})) \right], \quad (152)$$

$$\zeta_{iIJ} = M_V^2 \bar{\theta}_{iIJ} \Pi_J, \quad \kappa_{iI} = M_V^2 O_{1i} \gamma_I, \quad (153)$$

where  $s_{+0}$ ,  $s_{-0}$  and  $s_{+-}$  are squared invariant masses for the  $\pi^+ P^i$ ,  $\pi^- P^i$  and  $\pi^+ \pi^-$  system, respectively.  $s_{+-}$  is kinematically related with the other variables as  $s_{+-} = m_I^2 + 2M_{\pi^+}^2 + M_{P^i}^2 - s_{+0} - s_{-0}$ . The formula of the partial decay width is obtained as,

$$\Gamma[V^I \rightarrow P^i \pi^+ \pi^-] = \frac{1}{3072 \pi^3 m_I^3} \int \int_{(M_{\pi^+} + M_{P^i})^2}^{(m_I - M_{\pi^+})^2} |Y_{iI}|^2 H \theta(H) ds_{+0} ds_{-0}, \quad (154)$$

$$H = s_{+-} [s_{+0} s_{-0} + (m_I^2 - M_{\pi^+}^2)(M_{\pi^+}^2 - M_{P^i}^2)] - M_{\pi^+}^2 (m_I^2 - M_{P^i}^2)^2, \quad (155)$$

where  $\theta(H)$  denotes step function, and the integral regions are common for  $s_{+0}$  and  $s_{-0}$ .

7.  $P \rightarrow \pi^+ \pi^- \gamma$

In this subsection, differential decay widths for  $P \rightarrow \pi^+ \pi^- \gamma$  are calculated. The diagrams contributing to this process are given in Fig. III.7. The transition amplitude for the process

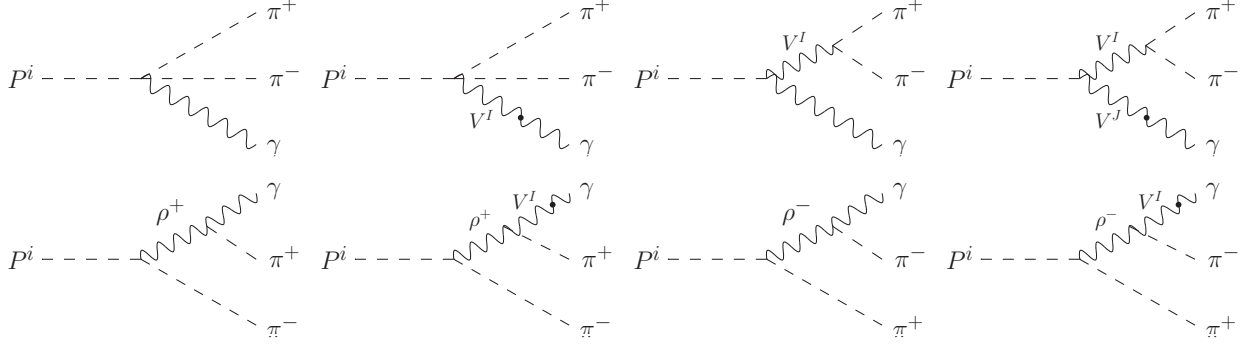


FIG. III.7. Diagrams contributing to the decay width for  $P^i \rightarrow \pi^+ \pi^- \gamma$ .

$P^i \rightarrow \pi^+ \pi^- \gamma$  ( $i = 2, 3$ ) is,

$$\mathcal{M}_{P^i \rightarrow \pi^+ \pi^- \gamma} = Y_i^\gamma \epsilon^{\mu\nu\rho\sigma} \epsilon_\mu^* p_\nu^- p_\rho^+ p_\sigma^\gamma, \quad (156)$$

$$Y_i^\gamma = -\frac{e}{f_\pi^3} [\bar{A}_i + \bar{B}_{iI} D^I(s) + \bar{C}_i (D_+(s_{+0}) + D_-(s_{-0}))], \quad (157)$$

$$\begin{aligned} \bar{A}_i &= \left( \frac{1}{4\pi^2} + 2c_{34}^+ \right) \left( O_{1i} + \frac{1}{\sqrt{3}} \sqrt{\frac{Z_2^\pi}{Z_1^\pi}} O_{2i} \right), \\ \bar{B}_{iI} &= -2g_{\rho\pi\pi} f_\pi^2 \bar{\chi}_{iI} \Pi^I, \quad \bar{C}_i = -\frac{4g_{\rho\pi\pi} f_\pi^2}{3} g c_{34}^+ O_{1i}. \end{aligned} \quad (158)$$

Using the above equations, one can obtain the differential decay width,

$$\frac{d^2\Gamma[P^i \rightarrow \pi^+ \pi^- \gamma]}{ds d\cos\theta} = \frac{1}{8192\pi^3 M_{P^i}^3} |Y_i^\gamma|^2 \sin^2\theta s^4 \beta_{\pi^+}^3 \left( 1 - \frac{M_{P^i}^2}{s} \right)^3, \quad (159)$$

where  $s$  denotes the squared invariant mass in  $\pi^+ \pi^-$  system and  $\theta$  implies the angle between  $\pi^+$  and  $\gamma$  in the rest frame of  $\pi^+ \pi^-$ .

#### IV. NUMERICAL ANALYSIS

In this section, phenomenological analysis is carried out in the model. In the following subsection, we perform  $\chi^2$  fittings in order to estimate the parameters in the model. As input data in the fittings, the following data are utilized: (1) the spectral function of  $\tau$  decay, (2) the masses of vector mesons and (3) the IP violating decay widths, the masses of

pseudoscalars and the TFFs of  $V \rightarrow Pl^+l^-$ . Subsequently, using the parameters estimated from the aforementioned observables, we give the prediction of the model. Specifically, the results are presented for Dalitz distributions and partial decay widths of IP violating modes.

In order to carry out the analysis, the following points are addressed:

- For the parameter  $c$  defined in Eq. (85), we take  $f = f_\pi$ .
- For  $\mu_P$  given in Eq. (31),  $f = f_\pi$  is also taken.
- In the expression of  $(g_{\rho\pi\pi})_{\text{tree}}$  in Eqs. (49, 50, 54-56, 58, 59), we use tree-level decay constant  $f$ , which is a free parameter.

### A. Parameter fit

#### 1. $\tau^- \rightarrow K_s \pi^- \nu$

In this subsection, we estimate parameters in the model with the decay distribution for  $\tau^- \rightarrow K_s \pi^- \nu$ . To evaluate the decay distribution, we use the procedure similar to the method in Ref. [6]. Throughout the analysis, we take isospin limit in the decay distribution.

The differential branching fraction for  $KP\nu$  ( $P = \pi, \eta$ ) is given as,

$$\begin{aligned} \frac{d\text{Br}[\tau \rightarrow KP\nu]}{d\sqrt{Q^2}} &= \frac{1}{\Gamma_\tau} \frac{G_F^2 |V_{us}|^2 (m_\tau^2 - Q^2)^2}{2^5 \pi^3} \frac{p_K^3}{m_\tau^3} p_K \\ &\times \left[ \left( \frac{2m_\tau^2}{3Q^2} + \frac{4}{3} \right) p_K^2 |F_V^{KP}(Q^2)|^2 + \frac{m_\tau^2}{2} |F_S^{KP}(Q^2)|^2 \right], \end{aligned} \quad (160)$$

where  $p_K$  is the momentum of  $K$  in the hadronic center of mass (CM) frame. The vector and scalar form factors are written in App. I. In order to compare the model prediction with the Belle data, we use the method in Ref. [6]. Including the overall normalization, the differential width in Eq. (160) is rewritten as,

$$\frac{N_{\text{tot}}}{\text{Br}^{\text{Belle}}[\tau^- \rightarrow K_s \pi^- \nu]} \times 11.5 \text{ MeV} \times \frac{d\text{Br}[\tau^- \rightarrow K_s \pi^- \nu]}{d\sqrt{Q^2}}, \quad (161)$$

where  $N_{\text{tot}}$  denotes the observed number of events for  $\tau$  decay while 11.5 MeV indicates the width of bins in the Belle experiment. We carry out the  $\chi^2$  fitting based on Eq. (161), which represents the expected number of events in the model.

In this paper, we take the tree-level pion decay constant,  $f$ , as a parameter. Since the effect of the  $K^*$  resonance is important in the decay mode, we choose the mass and the

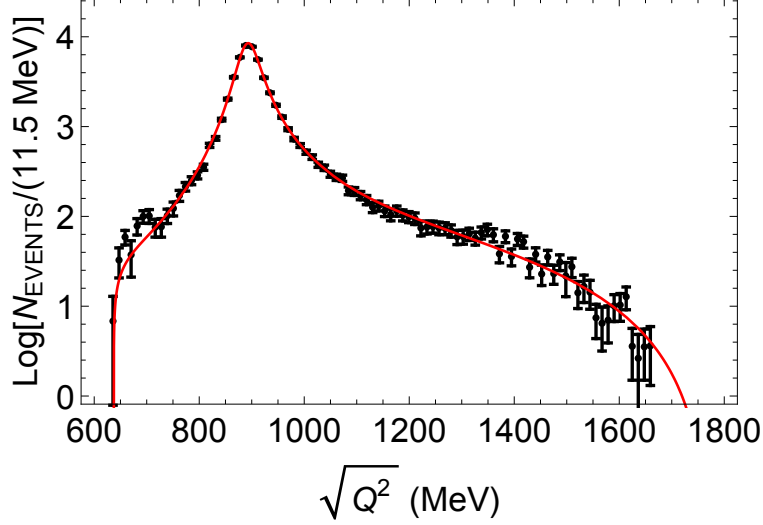


FIG. IV.1. The fitting result of the decay distribution for  $\tau^- \rightarrow K_s \pi^- \nu$ . The red line corresponds to the prediction of our model. The closed circles with the error bars are experimental data [11].

decay width of  $K^*$  meson as fitting parameters. Additionally, the octet vector meson mass and the finite parts of 1-loop ordered coefficients,  $K_1^r + K_2^r$  and  $L_9^r$ , are also free parameters. To summarize,  $(M_V, K_1^r + K_2^r, L_9^r, M_{K^*}, \Gamma_{K^*}, f)$  are the relevant fitting parameters in this mode. These six parameters are estimated from 90 bins of the data in the region  $M_K + M_\pi \leq \sqrt{Q^2} \leq 1665$  MeV. As a result of fitting, the parameters are determined as,

$$M_V = 851 \pm 100 \text{ MeV}, \quad K_1^r + K_2^r = 0.0268 \pm 0.0091, \quad L_9^r = (2.06 \pm 1.89) \times 10^{-3}, \quad (162)$$

$$M_{K^*} = 895.6 \pm 0.3 \text{ MeV}, \quad \Gamma_{K^*} = 48.4 \pm 0.6 \text{ MeV}, \quad f = 136 \pm 19 \text{ MeV},$$

where the obtained  $\chi^2_{\min}/\text{n.d.f.}$  is 147.1/84. The correlation matrix of  $(M_V, K_1^r + K_2^r, L_9^r, M_{K^*}, \Gamma_{K^*}, f)$  is,

$$\begin{pmatrix} 1 & 0.28 & 0.26 & 0.49 & 0.29 & -0.64 \\ * & 1 & 1.0 & -0.071 & 0.41 & -0.92 \\ * & * & 1 & -0.067 & 0.45 & -0.91 \\ * & * & * & 1 & 0.26 & -0.15 \\ * & * & * & * & 1 & -0.44 \\ * & * & * & * & * & 1 \end{pmatrix}. \quad (163)$$

The result of the decay distribution is shown in Fig. IV.1. In this plot, one can find that the resonance of  $K^*$  is seen around  $\sqrt{Q^2} \simeq 900$  MeV. The prediction for the branching fraction is  $0.403 \pm 0.069\%$  (the experimental value is  $(0.404 \pm 0.002 \pm 0.013)\%$  [11]).

TABLE I. Numerical values of the parameters in the model.

$g$	$6.68 \pm 1.56$	$C_2^r$	$-0.415 \pm 0.331$	$g_{\rho\pi\pi}$	$6.37 \pm 0.04$
$Z_V^r$	$0.819 \pm 0.002$	$C_3^r - 4C_4^r$	$-0.149_{-0.086}^{+0.080}$	$(g_{\rho\pi\pi})_{\text{tree}}$	$2.9_{-0.7}^{+1.1}$
$C_1^r$	$0.275 \pm 0.007$	$C_5^r$	$(9.92_{-8.88}^{+18.62}) \times 10^{-4}$	$c$	$-0.91_{-0.53}^{+0.37}$
$\sqrt{Z_1^\pi}$	$1.49_{-0.24}^{+0.27}$	$L_4^r$	$(-1.6_{-1.1}^{+1.0}) \times 10^{-3}$		
$\sqrt{Z_2^\pi}$	$0.96_{-0.14}^{+0.17}$	$L_5^r$	$(4.6_{-7.3}^{+2.1}) \times 10^{-3}$		

In Table I, we show other parameters which are also determined through Eqs. (162, 163). In the following, we clarify how the parameters in Table I are determined. In order to obtain the  $\rho\pi\pi$  coupling, we note that the decay width of  $K^*$  is given by the imaginary part of the self-energy [6],

$$\Gamma_{K^*} = \frac{1}{16\pi M_{K^*}} \frac{\nu_{K\pi}^3(M_{K^*}^2)}{M_{K^*}^4} \left( \frac{g_{\rho\pi\pi}}{2} \right)^2, \quad (164)$$

where  $\nu_{P\pi}(Q^2)$  is defined in Eq. (52). Solving Eq. (164) with respect to  $g_{\rho\pi\pi}$ , one can fix the  $\rho\pi\pi$  coupling since  $(M_V, f, M_K, \Gamma_K)$  are determined from the fitting. Moreover,  $g$  is also obtained from the definition of the  $\rho\pi\pi$  coupling in Eq. (17). In Table I we also give the value of  $(g_{\rho\pi\pi})_{\text{tree}}$  in Eq. (16). One can find that  $(g_{\rho\pi\pi})_{\text{tree}}$  and  $g_{\rho\pi\pi}$  are deviated from each other. This is because the tree-level decay constant denoted as  $f$  given in Eq. (162) is deviated from PDG value,  $f_\pi = 92.2$  MeV. In order to calculate  $L_4^r$  and  $L_5^r$ , we use the following pion and kaon decay constants [30] with obtained  $f$ ,

$$f_\pi = f \left\{ 1 - c(2\mu_\pi + \mu_K) + 4 \left( \frac{M_\pi^2 + 2M_K^2}{f^2} L_4^r + \frac{M_\pi^2}{f^2} L_5^r \right) \right\}, \quad (165)$$

$$f_K = f \left\{ 1 - \frac{3c}{4}(\mu_\pi + 2\mu_K + \mu_{\eta_8}) + 4 \left( \frac{M_\pi^2 + 2M_K^2}{f^2} L_4^r + \frac{M_K^2}{f^2} L_5^r \right) \right\}, \quad (166)$$

where in the above expressions,  $f$  represents the tree-level parameter given in Eq. (162). The coefficients of 1-loop ordered interaction,  $(Z_V^r, C_1^r, C_2^r, C_3^r - 4C_4^r, C_5^r)$ , are also determined from the procedure similar to one of Ref. [6]. Wavefunction renormalizations for  $\pi_3$  and  $\eta_8$  are calculated from Eq. (F9) and Eq. (F10), respectively. If one fixes the parameters as the best fit values in Eq. (162), the wavefunction renormalizations are,

$$\sqrt{Z_1^\pi} = 1.52, \quad \sqrt{Z_2^\pi} = 0.763. \quad (167)$$

Hereafter, the values in Eq. (167) are referred to as *best fit values* of the wavefunction renormalizations for pseudoscalars.



For the ratio of decay constants of pseudoscalars, we verify whether the model prediction of  $f_{K^-}/f_{\pi^-}$  is consistent with the experimental data if one uses  $f_\pi$  instead of the tree-level parameter in Eq. (84). The results in the model and the experimental data extracted from the PDG data [32] are,

$$f_{K^-}/f_{\pi^-} = \begin{cases} 1.40^{+0.18}_{-0.11} & (68.3\% \text{ C.L. in the model}) \\ 1.40^{+0.96}_{-0.24} & (99.7\% \text{ C.L. in the model}) \\ 1.197 \pm 0.006 & (1\sigma \text{ in the PDG}) \end{cases} . \quad (168)$$

In the above result, one can find that the model prediction is slightly deviated from the case of the tree-level  $\rho\pi\pi$  coupling in Eq. (84). This is because the estimated value of  $f$  is deviated from the experimental value of  $f_\pi$ . However, up to the 99.7% confidence interval of the model prediction, it is shown that the central value of the PDG data [32] is included.

## 2. Mass and width of vector mesons

In this subsection, we fix the parameters,  $g_{\rho\pi\pi}$ ,  $C_1^r$ ,  $Z_V^r$ ,  $\hat{g}_{1V}$  and  $M_{0V}$ , and evaluate the vector meson mass, the renormalization constant and the decay width.

At first, we consider the off-diagonal elements of  $V_\mu$ , *i.e.*,  $\rho^+$ ,  $K^{*+}$  and  $K^{*0}$  to obtain the parameters,  $g_{\rho\pi\pi}$ ,  $C_1^r$  and  $Z_V^r$ . We define the masses of  $\rho^+$  and  $K^{*+}$  mesons as the momentum-squared for which real parts of inverse propagators vanish,

$$M_V^2 + \text{Re}[\delta A_{\rho^+}(Q^2 = m_{\rho^+}^2; C_1^r, C_2^r)] = 0, \quad (169)$$

$$M_V^2 + \text{Re}[\delta A_{K^{*+}}(Q^2 = m_{K^{*+}}^2; C_1^r, C_2^r)] = 0, \quad (170)$$

where  $\delta A_{\rho^+}$  and  $\delta A_{K^{*+}}$  are shown in Eqs. (C15) and (C19), respectively. Solving the above equations, we have  $C_1^r$  and  $C_2^r$ ,

$$C_1^r = \frac{1}{\Delta_{K^{*+}\pi}} \{ Z_V^r \Delta_{K^{*+}\rho^+} - \text{Re}[\Delta A_{K^{*+}}(m_{K^{*+}}^2)] + \text{Re}[\Delta A_{\rho^+}(m_{\rho^+}^2)] \}, \quad (171)$$

$$C_2^r = -\frac{1}{2\bar{M}_K^2 + M_\pi^2} \{ M_V^2 - Z_V^r m_{K^{*+}}^2 + \text{Re}[\Delta A_{K^{*+}}(m_{K^{*+}}^2)] + C_1^r M_{K^+}^2 \}. \quad (172)$$

Imposing the condition for the residue of the vector meson propagator,  $\text{Res}D(Q^2 = m_{K^{*+}}^2) = 1$ , we have

$$Z_V^r = 1 + \left. \frac{d\text{Re}[\Delta A_{K^{*+}}(Q^2)]}{dQ^2} \right|_{Q^2=m_{K^{*+}}^2}. \quad (173)$$

Since  $\Delta A_V$  only depends on  $g_{\rho\pi\pi}$ ,  $C_1^r$  and  $Z_V^r$  can be fixed by  $g_{\rho\pi\pi}$ . On the other hand,  $C_2^r$  is related to two parameters,  $g_{\rho\pi\pi}$  and  $M_V$ .

To fix the value of  $g_{\rho\pi\pi}$ , we use the decay widths for  $\rho \rightarrow \pi\pi$  and  $K^{*\pm} \rightarrow (K\pi)^\pm$ . The decay widths are given by the imaginary part of the inverse propagators,

$$m_I \Gamma_I = -Z_I \text{Im}[\delta A_I(m_I^2)], \quad (174)$$

where  $I = \rho^+, K^{*+}, K^{*0}$ ,

$$(Z_I)^{-1} = Z_V^r - \frac{d\text{Re}[\Delta A_I(Q^2)]}{dQ^2} \Big|_{Q^2=m_I^2}, \quad (175)$$

where  $\Delta A_I$  is defined in Eqs. (C16, C18, C20).  $g_{\rho\pi\pi}$  is fixed to realize the minimum of  $\chi^2$  of the decay widths for  $V^I \rightarrow PP$ . The parameters  $C_1^r$  and  $Z_V^r$ , and the renormalization constants  $Z_i$  are estimated as follows,

$$\begin{aligned} g_{\rho\pi\pi} &= 6.37 \pm 0.04, \quad C_1^r = 0.275 \pm 0.007, \quad Z_V^r = 0.819 \pm 0.002, \\ Z_{\rho^+} &= 1.0461 \pm 0.0006, \quad Z_{K^{*0}} = 1.00244 \pm 0.00003. \end{aligned} \quad (176)$$

In the following, we determine the parameters  $\hat{g}_{1V}$  and  $M_{0V}$  with the  $\chi^2$  fitting of the neutral vector meson mass. The masses in Eq. (46) are written in terms of the mass eigenvalues of the mass matrix and the mixing angles of vector mesons. In Ref. [31], the authors introduced a method to express mixing angles and the eigenvalues in terms of the elements of the mass matrix. With varying the parameters in the elements of the mass matrix, one can conduct  $\chi^2$  fitting with respect to physical masses. The fitted results of the masses are shown in Table II, where the obtained  $\chi^2/\text{n.d.f}$  is 0.386/1. The parameters  $\hat{g}_{1V}$  and  $M_{0V}$  are fixed as,

$$\hat{g}_{1V} = 3.185 \pm 0.001, \quad M_{0V} = 871.8 \pm 0.1 \text{MeV}. \quad (177)$$

Using the above parameters, we have the orthogonal matrix  $O_V$  which diagonalizes vector meson mass matrix,

$$O_V = \begin{pmatrix} 0.9979 \pm 0.0001 & 0.0644 \pm 0.001 & -0.00375 \pm 0.00004 \\ -0.0447 \pm 0.0006 & 0.6475 \pm 0.0006 & -0.7608 \pm 0.0005 \\ -0.0466 \pm 0.0009 & 0.7594 \pm 0.0004 & 0.6490 \pm 0.0005 \end{pmatrix}, \quad (178)$$

where  $\omega - \phi$  mixing angle is  $(40.59 \pm 0.04)^\circ$ . The wave function renormalization of the neutral vector meson and the eigenvalues for the mass matrix are obtained as follows,

$$\begin{aligned} Z_{\rho^0} &= 1.0462 \pm 0.0005, \quad Z_\omega = 1.0281 \pm 0.0004, \quad Z_\phi = 0.9167 \pm 0.0008, \\ \mathcal{M}_1 &= 791.8 \pm 0.2 \text{MeV}, \quad \mathcal{M}_2 = 763.2 \pm 0.3 \text{MeV}, \quad \mathcal{M}_3 = 1001.9 \pm 0.2 \text{MeV}. \end{aligned} \quad (179)$$

TABLE II. The results of the neutral vector meson mass.

Mass	Theory(MeV)	PDG (MeV)
$m_{\rho^0}$	$775.42 \pm 0.01$	$775.26 \pm 0.25$
$m_{\omega}$	$782.65^{+0.18}_{-0.15}$	$782.65 \pm 0.12$
$m_{\phi}$	$1019.46 \pm 0.04$	$1019.461 \pm 0.019$

### 3. Intrinsic parity violating decays

In this subsection, we estimate model parameters by using the IP violating observables for light hadrons. As input data of  $\chi^2$  fittings, experimental data of decay widths and Dalitz distributions are used. We also utilize experimental values of masses for pseudoscalars to estimate parameters in the mass matrix.

The widths of radiative decays,  $\Gamma[\rho^+ \rightarrow \pi^+\gamma]$ ,  $\Gamma[K^{*0} \rightarrow K^0\gamma]$  and  $\Gamma[K^{*+} \rightarrow K^+\gamma]$ , are proportional to the IP violating parameter  $(gc_{34}^+)^2$ . In order to estimate this parameter, we consider the following statistic,

$$\chi^2 = \left( \frac{\Gamma[\rho^+ \rightarrow \pi^+\gamma] - \Gamma^{\text{PDG}}[\rho^+ \rightarrow \pi^+\gamma]}{\delta\Gamma^{\text{PDG}}[\rho^+ \rightarrow \pi^+\gamma]} \right)^2 + \left( \frac{\Gamma[K^{*0} \rightarrow K^0\gamma] - \Gamma^{\text{PDG}}[K^{*0} \rightarrow K^0\gamma]}{\delta\Gamma^{\text{PDG}}[K^{*0} \rightarrow K^0\gamma]} \right)^2, \quad (180)$$

where  $\delta\Gamma^{\text{PDG}}$  denotes experimental errors of the widths. As a result of the fitting, we find that the minimum of Eq. (180) is  $\chi^2_{\text{min}}/\text{d.o.f.} = 1.08/1$ , which results in the estimated parameter as,

$$g|c_{34}^+| = 0.102 \pm 0.05. \quad (181)$$

In this fitting, the sign of  $c_{34}^+$  is not fixed since the widths in Eqs. (126-128) depend on square of this parameter. In Table III, the widths calculated in the model are compared with the PDG values [32]. The model prediction for  $\Gamma[K^{*+} \rightarrow K^+\gamma]$  is also given in Table III. For the PDG value [32] of  $\Gamma[K^{*+} \rightarrow K^+\gamma]$ , we adopt the full width of  $K^{*+}$  obtained from tau decays. One finds  $3.4\sigma$  discrepancy between the model prediction and the experimental value of the width for  $K^{*+} \rightarrow K^+\gamma$ . Since the  $K^{*0}K^0\gamma$  coupling in Eq. (124) is two times larger than one for  $K^{*+}K^+\gamma$  in Eq. (123), the widths are related as  $\Gamma[K^{*0} \rightarrow K^0\gamma] \sim 4\Gamma[K^{*+} \rightarrow K^+\gamma]$ . However, this relation is not valid for the present PDG values [32] so that the deviation arises.

TABLE III. Partial widths of radiative decays. For  $\rho^+ \rightarrow \pi^+\gamma$  and  $K^{*0} \rightarrow K^0\gamma$ , the fitting result for  $\chi^2_{\min}/\text{d.o.f.} = 1.08/1$  is shown. The model prediction is given for  $K^{*+} \rightarrow K^+\gamma$ . For comparison, the PDG data [32] are also written.

Decay mode	Model [MeV]	PDG [MeV]
$\Gamma[\rho^+ \rightarrow \pi^+\gamma]$	$(7.3 \pm 0.7) \times 10^{-2}$	$(6.7 \pm 0.7) \times 10^{-2}$
$\Gamma[K^{*0} \rightarrow K^0\gamma]$	$0.11 \pm 0.01$	$0.12 \pm 0.01$
$\Gamma[K^{*+} \rightarrow K^+\gamma]$	$(2.8 \pm 0.3) \times 10^{-2}$	$(4.6 \pm 0.4) \times 10^{-2}$

For parameter estimation, we use observables for pseudoscalars. In particular, the PDG data [32] for masses of  $\pi^0, \eta'$  and decay widths of  $P \rightarrow 2\gamma$  ( $P = \pi^0, \eta, \eta'$ ) are adopted. In order to constrain parameters in the model, we consider the following system of equations,

$$M_{\pi^0}(\hat{g}_{2p}, \Delta_{\text{EM}}, M_{88}'^2, M_{80}'^2) = M_{\pi^0}^{\text{PDG}}, \quad (182)$$

$$M_{\eta'}(\hat{g}_{2p}, \Delta_{\text{EM}}, M_{88}'^2, M_{80}'^2) = M_{\eta'}^{\text{PDG}}, \quad (183)$$

$$\Gamma[\pi^0 \rightarrow 2\gamma](c_{6-9-10}, \hat{g}_{2p}, \Delta_{\text{EM}}, M_{88}'^2, M_{80}'^2) = \Gamma^{\text{PDG}}[\pi^0 \rightarrow 2\gamma], \quad (184)$$

$$\Gamma[\eta \rightarrow 2\gamma](c_{6-9-10}, \hat{g}_{2p}, \Delta_{\text{EM}}, M_{88}'^2, M_{80}'^2) = \Gamma^{\text{PDG}}[\eta \rightarrow 2\gamma], \quad (185)$$

$$\Gamma[\eta' \rightarrow 2\gamma](c_{6-9-10}, \hat{g}_{2p}, \Delta_{\text{EM}}, M_{88}'^2, M_{80}'^2) = \Gamma^{\text{PDG}}[\eta' \rightarrow 2\gamma], \quad (186)$$

where the left-handed sides in these equations denote the model expressions. Solution to Eqs. (182-186) leads to estimated values for the parameters given as  $(c_{6-9-10}, \hat{g}_{2p}, \Delta_{\text{EM}}, M_{88}'^2, M_{80}'^2)$ . This procedure of solving the equations is carried out in the following way: provided that the PDG data [32] obey Gaussian distributions, the right-handed sides in Eqs. (182-186) are generated as Gaussian data. For  $(\sqrt{Z_1^\pi}, \sqrt{Z_2^\pi})$ , we use the parameter list obtained from the fitting of tau decays, which is summarized in Table I. In order to determine model values of the masses in Eqs. (182-183), we use formalism in App. F which incorporates 1-loop correction to the mass matrix. One can numerically calculate the model values for pseudoscalar masses, which are eigenvalues of the mass matrix in Eq. (F21). For Eq. (184-186), the widths in the model are calculated on the basis of Eq. (139). Since  $\Gamma[P \rightarrow 2\gamma]$  depends on the pseudoscalar mixing matrix elements, we adopt a method [31] to write a mixing matrix in terms of mass matrix elements. Using  $10^4$  data samples, we solve the system of Eqs. (182-186) to obtain the parameters  $(c_{6-9-10}, \hat{g}_{2p}, \Delta_{\text{EM}}, M_{88}'^2, M_{80}'^2)$ . Confidence intervals of the parameters are estimated from a list of the solutions to Eqs. (182-186). In

Table IV, we show confidence intervals of the model parameters which are determined in this procedure. Since the parameters in the mass matrix are estimated, a mixing angle for pseudoscalars is also determined.  $\theta_1$  is obtained as  $\theta_1 = \arccos(O_{33})$ , where  $O_{33}$  is the mixing matrix element in Eq. (82). The numerical value of this angle is,

$$\theta_1 = \begin{cases} -28_{-5}^{+2}[\text{degree}] & (68.3\% \text{ C.L.}) \\ -28_{-43}^{+5}[\text{degree}] & (99.7\% \text{ C.L.}) \end{cases}. \quad (187)$$

TABLE IV. Confidence intervals of the model parameters estimated from the data [32] of widths and masses for pseudoscalars. See the text for a detailed explanation of parameter estimation.

Parameter	$c_{6-9-10} \times 10^2$	$\hat{g}_{2p}$	$\Delta_{\text{EM}} [\text{MeV}^2]$	$\sqrt{M_{88}'^2} [\text{MeV}]$	$\sqrt{ M_{80}'^2 } [\text{MeV}]$
68.3% C.L.	$1.1_{-0.2}^{+0.2}$	$-1.0_{-0.7}^{+0.7}$	$1220_{-60}^{+20}$	$660_{-20}^{+30}$	$510 \pm 20$
99.7% C.L.	$1.1_{-0.5}^{+0.7}$	$-1.0_{-2.3}^{+2.1}$	$1220_{-310}^{+30}$	$660_{-60}^{+260}$	$510 \pm 80$

In Eqs. (182-186), if one adopts the best fit model parameters in Eq. (162) on left-handed sides and central values of the PDG data [32] on right-handed sides, solution is obtained as,

$$c_{6-9-10} = 1.1 \times 10^{-2}, \quad \hat{g}_{2p} = -1.0, \\ \Delta_{\text{EM}} = 1220 [\text{MeV}^2], \quad M_{88}' = 662 [\text{MeV}], \quad M_{80}' = 507 [\text{MeV}]. \quad (188)$$

Using the above values, the mixing matrix and the wavefunction renormalizations of pseudoscalars are calculated as,

$$O = \begin{pmatrix} 0.99998 & -3.3 \times 10^{-4} & -6.8 \times 10^{-3} \\ 3.5 \times 10^{-3} & 0.88 & 0.47 \\ 5.8 \times 10^{-3} & -0.47 & 0.88 \end{pmatrix}, \quad (189)$$

In the following analysis, the parameter values in Eq. (189) are referred to as *best fit values* for the mixing matrix elements.

Here, we discuss a case in which singlet-induced contribution is absent. If one takes the limit  $c_{6-9-10} \rightarrow 0$ , the partial width of  $\eta'$  becomes  $\Gamma[\eta' \rightarrow 2\gamma] = 7 \times 10^{-5} \text{MeV}$ . This value is much smaller than the experimental data,  $\Gamma^{\text{PDG}}[\eta' \rightarrow 2\gamma] = (4.4 \pm 0.3) \times 10^{-3} \text{MeV}$ . Hence, one notices that the presence of singlet-induced IP violation is necessary in the framework of the singlet+octet scheme.

For parameter estimation of the IP violating parameters, the ratio of the effective coupling for  $VP\gamma$  to one for  $\rho^+\pi^+\gamma$  in Eq. (131) are compared with experimental values. Model parameters are estimated from the following statistic,

$$\chi^2 = \sum_{(i,I)}^{(1,2),(2,2),(3,2),(3,3)} \left( \frac{|X_{iI}/X_{\rho^+}| - |X_{iI}/X_{\rho^+}|^{\text{PDG}}}{\delta|X_{iI}/X_{\rho^+}|^{\text{PDG}}} \right)^2. \quad (190)$$

The experimental data used in the above  $\chi^2$  are extracted from PDG [32] through r.h.s in Eq. (130). In Eq. (131), the wavefunction renormalizations and the mixing matrices for mesons are set as the best fit values obtained in Eqs. (167, 189). (for vector meson mixing, Eq. number should be referred.) In the procedure to minimize the statistic in Eq. (190), one can vary model parameters,  $c_{69}/g^2c_{34}^+$  and  $c_8^{\text{IP}}/gc_{34}^+$ . The fitting results are shown in Table V. The parameter ranges estimated from this fitting are,

$$c_{69}/g^2c_{34}^+ = -0.91 \pm 0.04, \quad c_8^{\text{IP}}/gc_{34}^+ = 0.85 \pm 0.05, \quad (191)$$

where the correlation coefficient of these parameters is 0.12. Predictions for effective coupling ratios of  $\Gamma[V^I \rightarrow P^i\gamma]$  to  $\Gamma[\rho^+ \rightarrow \pi^+\gamma]$  for  $(i, I) = (1, 1), (1, 3), (2, 1), (2, 3)$  are given in Table V. Furthermore, the prediction for the decay widths of  $V^I \rightarrow P^i\gamma$  are shown in Table VI.

TABLE V. Fitting result and model prediction of the ratio of effective coupling for  $V^I \rightarrow P^i \gamma$  to one for  $\rho^+ \rightarrow \pi^+ \gamma$ . For  $(i, I) = (1, 2), (2, 2), (3, 2), (3, 3)$ , the fitting result for  $\chi^2_{\min}/\text{d.o.f.} = 1.12/2$  is shown while the model predictions are given for  $(i, I) = (1, 1), (1, 3), (2, 1), (2, 3)$ . For comparison, the experimental data extracted from the PDG data [32] are also shown. In the fourth column, the model prediction in the isospin limit is displayed with wave function renormalizations set as unity. Mixing angles for vector meson are defined as  $\cos \theta_V^{08} = O_{V22} \sim O_{V33}$  and  $\sin \theta_V^{08} = O_{V23} \sim -O_{V32}$ .

Ratio	Model	PDG	Model in the isospin limit
$ X_{12}/X_{\rho^+} $	$3.1 \pm 0.1$	$3.2 \pm 0.2$	$\sqrt{3}  \cos \theta_V^{08} - \frac{3c_8^{\text{IP}}}{gc_{34}^+} \sin \theta_V^{08} $
$ X_{22}/X_{\rho^+} $	$0.71^{+0.09}_{-0.08}$	$0.62 \pm 0.04$	$ \cos \theta_V^{08}   \cos \theta_1 + \sqrt{3}(\frac{c_{69}}{g^2 c_{34}}) \sin \theta_1 - \frac{\sqrt{3}c_8^{\text{IP}}}{gc_{34}^+} \cos \theta_1 \tan \theta_V^{08} $
$ X_{32}/X_{\rho^+} $	$0.53^{+0.16}_{-0.13}$	$0.60 \pm 0.04$	$ \cos \theta_V^{08}   \sin \theta_1 - \sqrt{3}(\frac{c_{69}}{g^2 c_{34}}) \cos \theta_1 - \frac{\sqrt{3}c_8^{\text{IP}}}{gc_{34}^+} \sin \theta_1 \cot \theta_V^{08} $
$ X_{33}/X_{\rho^+} $	$1.15^{+0.15}_{-0.13}$	$0.99 \pm 0.06$	$ \sin \theta_V^{08}   \sin \theta_1 - \sqrt{3}(\frac{c_{69}}{g^2 c_{34}}) \cos \theta_1 + \frac{\sqrt{3}c_8^{\text{IP}}}{gc_{34}^+} \sin \theta_1 \cot \theta_V^{08} $
$ X_{11}/X_{\rho^+} $	$0.80 \pm 0.02$	$1.15 \pm 0.10$	1
$ X_{13}/X_{\rho^+} $	$0.31 \pm 0.09$	$0.18 \pm 0.01$	$\sqrt{3}  \sin \theta_V^{08} + \frac{3c_8^{\text{IP}}}{gc_{34}^+} \cos \theta_V^{08} $
$ X_{21}/X_{\rho^+} $	$1.8 \pm 0.2$	$2.2 \pm 0.1$	$\sqrt{3}  \cos \theta_1 - (\frac{c_{69}}{g^2 c_{34}}) \tan \theta_1 $
$ X_{23}/X_{\rho^+} $	$0.6^{+0.1}_{-0.2}$	$0.96 \pm 0.05$	$ \sin \theta_V^{08}   \cos \theta_1 + \sqrt{3}(\frac{c_{69}}{g^2 c_{34}}) \sin \theta_1 + \frac{\sqrt{3}c_8^{\text{IP}}}{gc_{34}^+} \cos \theta_1 \cot \theta_V^{08} $

In the following, TFFs for Dalitz decay of vector mesons are analyzed. In particular, we fit  $|F_{V^I P^i}|^2$  for  $(i, I) = (1, 2), (1, 3)$  and  $(2, 3)$ , in each bin for di-lepton invariant mass. In order to minimize the statistic,

$$\chi^2 = \sum_{\text{Available data}} \sum_{(i,I)}^{(1,2),(1,3),(2,3)} \left( \frac{|F_{V^I P^i}|^2 - (|F_{V^I P^i}|^2)^{\text{Exp.}}}{\delta(|F_{V^I P^i}|^2)^{\text{Exp.}}} \right)^2, \quad (192)$$

we vary the IP violating parameters:  $(c_3^{\text{IP}}, c_5^{\text{IP}}, c_6^{\text{IP}}, c_7^{\text{IP}})$ . For the expression of  $|F_{V^I P^i}|^2$  in Eq. (146), the mixing matrices and wavefunction renormalizations of mesons are set as the best fit values in Eqs. (167, 178, 189). In Eq. (192) the experimental data extracted from Refs. [1, 33–38] are adopted for parameter estimation. In the fitting procedure, two cases:  $c_{34}^+ < 0$  and  $c_{34}^+ > 0$  are considered. For these cases, one can find that the goodness-of-fit is comparable with each other. We find that the minimum of Eq. (192) is  $\chi^2_{\min}/\text{d.o.f.} = 211.8/151$  (215.4/151) for  $c_{34}^+ < 0$  ( $> 0$ ). As an alternative analysis,

TABLE VI. Partial widths of the radiative decays for vector mesons. For comparison, the PDG data [32] are also shown.

	Model [MeV]	PDG [MeV]
$\Gamma[\omega \rightarrow \pi^0 \gamma]$	$0.71 \pm 0.09$	$0.70 \pm 0.02$
$\Gamma[\omega \rightarrow \eta \gamma]$	$(5.5^{+1.6}_{-1.3}) \times 10^{-3}$	$(3.9 \pm 0.3) \times 10^{-3}$
$\Gamma[\eta' \rightarrow \omega \gamma]$	$(4.6^{+3.3}_{-2.0}) \times 10^{-3}$	$(5.4 \pm 0.5) \times 10^{-3}$
$\Gamma[\phi \rightarrow \eta' \gamma]$	$(3.9^{+1.2}_{-0.9}) \times 10^{-4}$	$(2.67 \pm 0.09) \times 10^{-4}$
$\Gamma[\rho^0 \rightarrow \pi^0 \gamma]$	$(4.6 \pm 0.5) \times 10^{-2}$	$(9 \pm 1) \times 10^{-2}$
$\Gamma[\phi \rightarrow \pi^0 \gamma]$	$(17^{+12}_{-9}) \times 10^{-3}$	$(5.4 \pm 0.3) \times 10^{-3}$
$\Gamma[\rho \rightarrow \eta \gamma]$	$(3.3^{+0.8}_{-0.9}) \times 10^{-2}$	$(4.5 \pm 0.3) \times 10^{-2}$
$\Gamma[\phi \rightarrow \eta \gamma]$	$(2.2^{+0.9}_{-1.2}) \times 10^{-2}$	$(5.6 \pm 0.1) \times 10^{-2}$

we also fit  $\chi^2$  in the case without the Lepton-G data [34]. This fitting analysis leads to  $\chi^2_{\min}/\text{d.o.f.} = 170.1/144$  ( $173.7/144$ ) for  $c_{34}^+ < 0$  ( $> 0$ ), which is a slightly improved result. In this case, we find that the best fit values and the errors of  $(c_3^{\text{IP}}, c_5^{\text{IP}}, c_6^{\text{IP}}, c_7^{\text{IP}})$  are almost identical to ones in the case with the Lepton-G data. For each fitting,  $\chi^2_{\min}/\text{d.o.f.}$ , corresponding p-values and the estimated parameters are summarized in Table VII. As a result

TABLE VII. Fitting results of the TFFs for vector meson decays. For the four cases of fitting, the-goodness-of fit is shown. Estimated  $1\sigma$  ranges for the IP violating parameters are also given.

	$\chi^2_{\min}/\text{d.o.f.}$	p-value	$c_3^{\text{IP}} \times 10^2$	$c_5^{\text{IP}} \times 10^2$	$c_6^{\text{IP}}$	$c_7^{\text{IP}}$
$c_{34}^+ < 0$ without Lepton-G	170.1/144	0.068	$1.12 \pm 0.05$	$6.5 \pm 0.2$	$-1.3 \pm 0.7$	$-1.8 \pm 1.3$
$c_{34}^+ < 0$ with Lepton-G	211.8/151	$8.1 \times 10^{-4}$	$1.12 \pm 0.05$	$6.5 \pm 0.2$	$-1.3 \pm 0.7$	$-1.8 \pm 1.3$
$c_{34}^+ > 0$ without Lepton-G	173.7/144	0.046	$-1.12 \pm 0.05$	$-6.5 \pm 0.2$	$-0.3 \pm 0.8$	$-1.1 \pm 1.4$
$c_{34}^+ > 0$ with Lepton-G	215.4/151	$4.5 \times 10^{-4}$	$-1.12 \pm 0.05$	$-6.5 \pm 0.2$	$-0.3 \pm 0.8$	$-1.1 \pm 1.4$

of the fittings without the Lepton-G data, the correlation matrices for  $(c_3^{\text{IP}}, c_5^{\text{IP}}, c_6^{\text{IP}}, c_7^{\text{IP}})$  are,

$$\begin{pmatrix} 1 & 0.75 & -0.12 & -0.082 \\ * & 1 & -0.14 & -0.11 \\ * & * & 1 & 1.0 \\ * & * & * & 1 \end{pmatrix} (c_{34}^+ < 0), \quad \begin{pmatrix} 1 & 0.75 & -0.12 & -0.086 \\ * & 1 & -0.14 & -0.11 \\ * & * & 1 & 1.0 \\ * & * & * & 1 \end{pmatrix} (c_{34}^+ > 0). \quad (193)$$



In the following analysis in this paper, we adopt parameter sets which are estimated from the case without the Lepton-G data. The TFFs obtained in the model, which result from the case without the Lepton-G data, are shown in Fig. IV.2. One can see that best fit curves for  $c_{34}^+ < 0$  and  $c_{34}^+ > 0$  are slightly deviated from one another in  $\phi \rightarrow \eta l^+ l^-$  whereas the two predictions mostly overlap with each other for  $\omega \rightarrow \pi^0 l^+ l^-$  and  $\phi \rightarrow \pi^0 l^+ l^-$ .

We determine the IP violating parameters,  $(c_4^{\text{IP}}, c_8^{\text{IP}}, c_9^{\text{IP}}, c_{10}^{\text{IP}})$ , from Eqs. (181, 188, 191) and Table VII. The result is shown in Table VIII for two cases,  $c_{34}^+ < 0$  and  $c_{34}^+ > 0$ , separately.

TABLE VIII. Intrinsic parity violating parameters estimated in the fittings. For  $c_{34}^+ < 0$  and  $c_{34}^+ > 0$ , the confidence intervals are shown, respectively.

$(c_{34}^+ < 0)$	$c_4^{\text{IP}} \times 10^2$	$c_8^{\text{IP}} \times 10^2$	$c_9^{\text{IP}}$	$c_{10}^{\text{IP}}$
68.3% C.L.	$-2.7^{+0.3}_{-0.4}$	$-8.6^{+0.7}_{-0.7}$	$0.47^{+0.26}_{-0.22}$	$-0.11^{+0.05}_{-0.06}$
99.7% C.L.	$-2.7^{+0.7}_{-2.1}$	$-8.6^{+2.0}_{-2.2}$	$0.47^{+1.11}_{-0.66}$	$-0.11^{+0.15}_{-0.24}$
$(c_{34}^+ > 0)$	$c_4^{\text{IP}} \times 10^2$	$c_8^{\text{IP}} \times 10^2$	$c_9^{\text{IP}}$	$c_{10}^{\text{IP}}$
68.3% C.L.	$0.33^{+0.43}_{-0.31}$	$8.6^{+0.7}_{-0.7}$	$0.29^{+0.26}_{-0.22}$	$-0.06^{+0.05}_{-0.06}$
99.7% C.L.	$0.33^{+2.11}_{-0.74}$	$8.6^{+2.2}_{-2.0}$	$0.29^{+1.09}_{-0.67}$	$-0.06^{+0.15}_{-0.23}$

## B. Model prediction

In this subsection, predictions of the model are given for the TFFs of Dalitz decays, partial widths and differential decay widths of IP violating modes. We utilize the parameter set obtained in the previous subsection.

In Fig. IV.3, the model predictions for  $P^i \rightarrow \gamma l^+ l^-$  ( $i = 1, 2, 3$ ) are given. We show the result for the two cases,  $c_{34}^+ < 0$  and  $c_{34}^+ > 0$ , respectively. For  $c_{34}^+ > 0$ , one can find a discrepancy between the model prediction and the precise data obtained by the NA60 collaboration [1]. Thus, we do not give a further result of analysis for the case of  $c_{34}^+ > 0$  since this case is disfavored.

In Table IX, the model predictions for widths of IP violating decays are exhibited. Within 99.7% C.L. of the model predictions, one can find no disagreement with experimental data.

In Fig. IV.4, the differential decay widths for  $P^i \rightarrow \pi^+ \pi^- \gamma$  ( $i = 2, 3$ ) are displayed.

For comparison, the data measured by the WASA-at-COSY collaboration [39], which are originally given in arbitrary unit, are also shown for  $\eta \rightarrow \pi^+\pi^-\gamma$ . For  $\eta \rightarrow \pi^+\pi^-\gamma$  in (a) and (b), the widths are given in two units: one is physical unit, which is based on the calculation of decay width, while another is arbitrary unit. In order to compare the model values in physical unit with the experimental data, we multiplied WASA-at-COSY data (including central values and  $1\sigma$  errors) by (a)  $10^{-10}$  and (b)  $5 \times 10^{-9}$ , respectively. Likewise, in arbitrary unit, our data are rescaled by the same factors. We find that our numerical result agrees with the experimental data if one chooses the appropriate rescaling factors for comparison. In (c), one can find a resonance region around  $E_\gamma \sim 160\text{MeV}$ . This is because the photon energy in the rest frame of  $\eta'$  is related to  $\pi^+\pi^-$  invariant mass as  $E_\gamma = (M_{\eta'}^2 - s_{+-})/2M_{\eta'}$ , which indicates that  $E_\gamma = 164.9\text{MeV}(159.1\text{MeV})$  corresponds to the pole which arises from intermediate  $\rho$  ( $\omega$ ).

In Fig. IV.5, we present the numerical result for the Dalitz distributions of  $V^I \rightarrow P^i l^+ l^-$  for  $(i, I) = (1, 1), (2, 1), (2, 2), (3, 3)$ . Since these modes are not measured yet, it is expected that one can test the validity of the model via future experiments.

In Fig. IV.6, predictions for a branching ratio for  $\rho^0 \rightarrow \pi^0 \pi^+ \pi^-$  and decay widths of  $V^I \rightarrow \pi^0 \pi^+ \pi^-$  ( $I = 2, 3$ ) are shown. Varying the value of  $gc_{123}$ , we estimate error bands of the model prediction. For simplicity, we do not account uncertainty which arises from parameters in the vector meson propagators in Eq. (41). We find that if one fixes  $gc_{123} \sim 0.35$ , the predictions for  $V^I \rightarrow \pi^0 \pi^+ \pi^-$  ( $I = 1, 2, 3$ ) are consistent with the PDG data [32].

In the vicinity of the peak region, plots of the TFFs are exhibited for Dalitz decays in Fig. IV.7. The partial contributions from  $\rho, \omega$ , and interference between  $\rho$  and  $\omega$  are also indicated. In (a) and (c), the predictions in 68.3% C.L. are shown for TFFs of  $\phi \rightarrow \pi^0 l^+ l^-$  and  $\eta' \rightarrow \gamma l^+ l^-$ , respectively. In (b) and (d), the best fit predictions, in which the model parameters are fixed, are given for the two modes. For both  $\phi \rightarrow \pi^0 l^+ l^-$  and  $\eta' \rightarrow \gamma l^+ l^-$ , we find that the contribution from  $\omega$  pole is dominant around the region of resonance. It is shown that the partial contribution of interference between  $\rho$  and  $\omega$  is not negligible. In particular, for (b), one can see that the contribution of the interference is sizable.

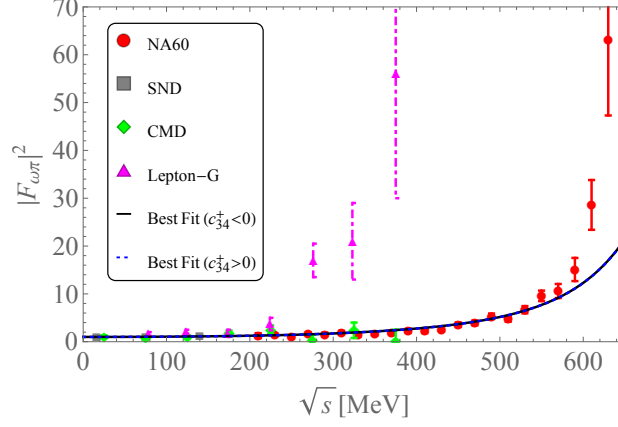
Using Eq. (67), we obtain the decay widths for  $\omega \rightarrow \pi\pi, \phi \rightarrow K^+ K^-$  and  $\phi \rightarrow K^0 \bar{K}^0$  which are shown in Table X. We should note that the leading contribution of the decay is a one-loop level and isospin breaking amplitude. About the  $\phi \rightarrow K^+ K^-$  and  $\phi \rightarrow K^0 \bar{K}^0$ , they are smaller than the experimental values. However the discrepancy depends on the

choice of  $f_\pi/f_K$  and its deviation from unity leads to two loop order effect. If the ratio is modified properly, one can obtain theoretical predictions which are in good agreement with the experimental results. We also note that the ratio of the decay widths of  $\phi \rightarrow K^+K^-$  and  $\phi \rightarrow K^0\bar{K}^0$  deviates from unity for both theoretical prediction and experimental result. This implies the presence of the isospin breaking contribution. We note the ratio of the two decay widths is in good agreement between theory and experiment:

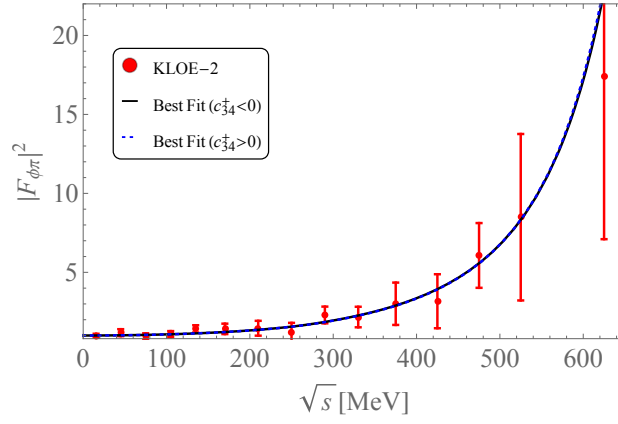
$$(\Gamma[\phi \rightarrow K^+K^-]/\Gamma[\phi \rightarrow K^0\bar{K}^0])_{\text{Th.}} = 1.53^{+0.22}_{-0.15}, \quad (194)$$

$$(\Gamma[\phi \rightarrow K^+K^-]/\Gamma[\phi \rightarrow K^0\bar{K}^0])_{\text{PDG}} = 1.430 \pm 0.026. \quad (195)$$

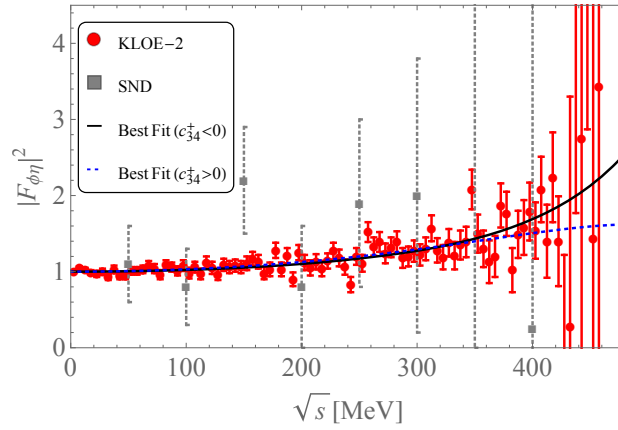
The fitted results of the widths for  $\rho \rightarrow \pi\pi$ ,  $K^{*\pm} \rightarrow (K\pi)^\pm$  are shown in Table XI.



(a)



(b)



(c)

FIG. IV.2. Transition form factors versus di-lepton invariant mass: (a)  $\omega \rightarrow \pi^0 l^+ l^-$ , (b)  $\phi \rightarrow \pi^0 l^+ l^-$  and (c)  $\phi \rightarrow \eta l^+ l^-$ . Black solid lines indicate best fit curves for  $c_{34}^+ < 0$  while blue dotted lines imply ones for  $c_{34}^+ > 0$ . For comparison, experimental data are shown for (a) NA60 [1], SND [33], Lepton-G [34] and CMD-2 [35], (b) KLOE-2 [36] and (c) SND [37] and KLOE-2 [38].

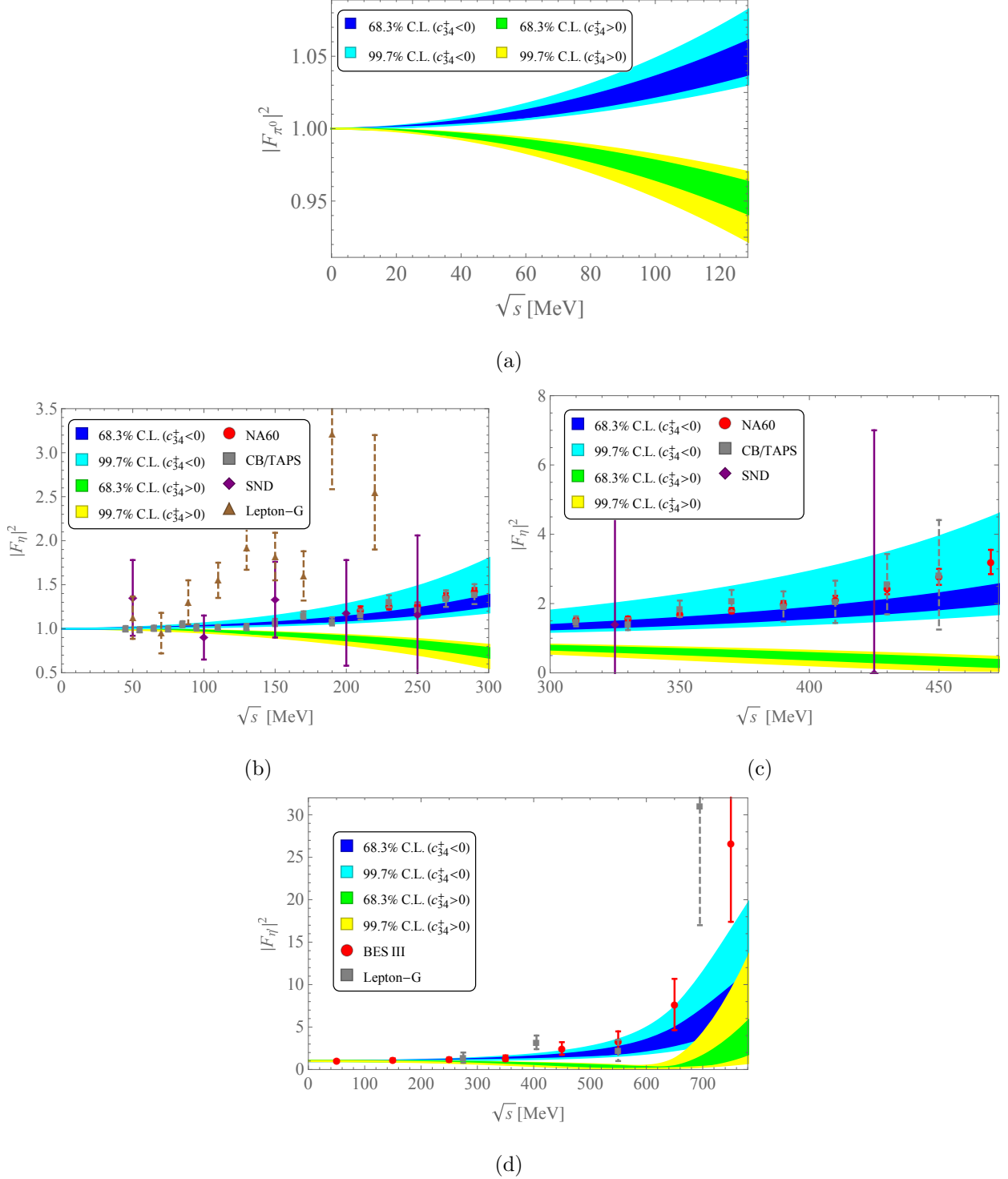


FIG. IV.3. Transition form factors versus di-lepton invariant mass: (a)  $\pi^0 \rightarrow \gamma l^+ l^-$ , (b)-(c)  $\eta \rightarrow \gamma l^+ l^-$  in the mass range for  $[2m_e, 300]$  MeV and for  $[300, 470]$  MeV respectively and (d)  $\eta' \rightarrow \gamma l^+ l^-$ . For  $c_{34}^+ < 0$ , blue (cyan) bands indicate theoretical predictions in 68.3% (99.7%) C.L. while for  $c_{34}^+ > 0$ , green (yellow) bands represent ones in 68.3% (99.7%) C.L. For comparison, the experimental data obtained by (b)-(c) NA60 [1], Lepton-G [40], CB/TAPS [41] and SND [37] and (d) BES III [2], Lepton-G [42] are shown.

TABLE IX. Partial decay widths of IPV decay modes. As model predictions, we give the estimated ranges of 68.3% C.L. and ones for 99.7% C.L., respectively. For comparison, the data obtained by the BES III collaboration [2] is shown for  $\Gamma[\eta' \rightarrow \gamma e^+ e^-]$  and the PDG data [32] are given for other decay modes. For  $\rho^0 \rightarrow \pi^0 e^+ e^-$  and  $\phi \rightarrow \eta \mu^+ \mu^-$ , the 90% C.L. upper bounds are written while  $1\sigma$  errors are shown for the other experimental values.

Decay mode	Model (68.3%C.L.) [MeV]	Model (99.7%C.L.) [MeV]	Exp. [MeV]
$\Gamma[\pi^0 \rightarrow \gamma e^+ e^-]$	$(9.05^{+0.01}_{-0.01}) \times 10^{-8}$	$(9.05^{+1.44}_{-0.48}) \times 10^{-8}$	$(9.1 \pm 0.3) \times 10^{-8}$
$\Gamma[\eta \rightarrow \gamma e^+ e^-]$	$(8.54^{+0.05}_{-0.04}) \times 10^{-6}$	$(8.54^{+0.41}_{-0.08}) \times 10^{-6}$	$(9.0 \pm 0.6) \times 10^{-6}$
$\Gamma[\eta \rightarrow \gamma \mu^+ \mu^-]$	$(3.7^{+0.3}_{-0.2}) \times 10^{-7}$	$(3.7^{+2.2}_{-0.4}) \times 10^{-7}$	$(4.1 \pm 0.6) \times 10^{-7}$
$\Gamma[\eta' \rightarrow \gamma e^+ e^-]$	$(8.7^{+0.5}_{-0.3}) \times 10^{-5}$	$(8.7^{+38.2}_{-0.8}) \times 10^{-5}$	$(9.28 \pm 0.95) \times 10^{-5}$
$\Gamma[\eta' \rightarrow \gamma \mu^+ \mu^-]$	$(1.6^{+0.5}_{-0.3}) \times 10^{-5}$	$(1.6^{+38.5}_{-0.7}) \times 10^{-5}$	$(2.1 \pm 0.6) \times 10^{-5}$
$\Gamma[\eta \rightarrow \pi^+ \pi^- \gamma]$	$(8.7^{+2.4}_{-2.2}) \times 10^{-5}$	$(8.7^{+8.4}_{-7.2}) \times 10^{-5}$	$(5.5 \pm 0.2) \times 10^{-5}$
$\Gamma[\eta' \rightarrow \pi^+ \pi^- \gamma]$	$(6.2^{+1.2}_{-1.0}) \times 10^{-2}$	$(6.2^{+4.3}_{-2.6}) \times 10^{-2}$	$(5.8 \pm 0.3) \times 10^{-2}$
$\Gamma[\phi \rightarrow \omega \pi^0]$	$(48^{+314}_{-44}) \times 10^{-4}$	$(48.3324^{+4845.9}_{-48.3319}) \times 10^{-4}$	$(2.0 \pm 0.2) \times 10^{-4}$
$\Gamma[\rho^0 \rightarrow \pi^0 e^+ e^-]$	$(0.43^{+0.05}_{-0.05}) \times 10^{-3}$	$(0.43^{+0.16}_{-0.13}) \times 10^{-3}$	$< 6.0 \times 10^{-3}$
$\Gamma[\rho^0 \rightarrow \pi^0 \mu^+ \mu^-]$	$(5.0^{+0.9}_{-0.7}) \times 10^{-5}$	$(5.0^{+3.3}_{-2.2}) \times 10^{-5}$	—
$\Gamma[\rho^0 \rightarrow \eta e^+ e^-]$	$(2.5^{+0.7}_{-0.5}) \times 10^{-4}$	$(2.5^{+2.4}_{-2.2}) \times 10^{-4}$	—
$\Gamma[\rho^0 \rightarrow \eta \mu^+ \mu^-]$	$(3.3^{+1.1}_{-0.8}) \times 10^{-8}$	$(3.3^{+4.4}_{-2.8}) \times 10^{-8}$	—
$\Gamma[\omega \rightarrow \pi^0 e^+ e^-]$	$(6.8^{+0.9}_{-0.8}) \times 10^{-3}$	$(6.8^{+3.3}_{-2.3}) \times 10^{-3}$	$(6.5 \pm 0.5) \times 10^{-3}$
$\Gamma[\omega \rightarrow \pi^0 \mu^+ \mu^-]$	$(0.89^{+0.15}_{-0.13}) \times 10^{-3}$	$(0.89^{+0.49}_{-0.30}) \times 10^{-3}$	$(1.1 \pm 0.3) \times 10^{-3}$
$\Gamma[\omega \rightarrow \eta e^+ e^-]$	$(4.2^{+1.3}_{-1.0}) \times 10^{-5}$	$(4.2^{+4.6}_{-3.4}) \times 10^{-5}$	—
$\Gamma[\omega \rightarrow \eta \mu^+ \mu^-]$	$(1.7^{+0.7}_{-0.5}) \times 10^{-8}$	$(1.7^{+4.3}_{-1.3}) \times 10^{-8}$	—
$\Gamma[\phi \rightarrow \pi^0 e^+ e^-]$	$(23^{+22}_{-13}) \times 10^{-5}$	$(23.4^{+424.3}_{-23.2}) \times 10^{-5}$	$(4.8 \pm 1.2) \times 10^{-5}$
$\Gamma[\phi \rightarrow \pi^0 \mu^+ \mu^-]$	$(6.7^{+16.7}_{-4.7}) \times 10^{-5}$	$(6.7^{+388.3}_{-6.6}) \times 10^{-5}$	—
$\Gamma[\phi \rightarrow \eta e^+ e^-]$	$(1.9^{+0.8}_{-1.0}) \times 10^{-4}$	$(1.886^{+70.95}_{-1.885}) \times 10^{-4}$	$(4.9 \pm 0.4) \times 10^{-4}$
$\Gamma[\phi \rightarrow \eta \mu^+ \mu^-]$	$(1.1^{+0.5}_{-0.6}) \times 10^{-5}$	$(1.0533^{+105.0}_{-1.0527}) \times 10^{-5}$	$< 4.0 \times 10^{-5}$
$\Gamma[\phi \rightarrow \eta' e^+ e^-]$	$(2.0^{+0.7}_{-0.5}) \times 10^{-6}$	$(2.0^{+2.5}_{-1.7}) \times 10^{-6}$	—

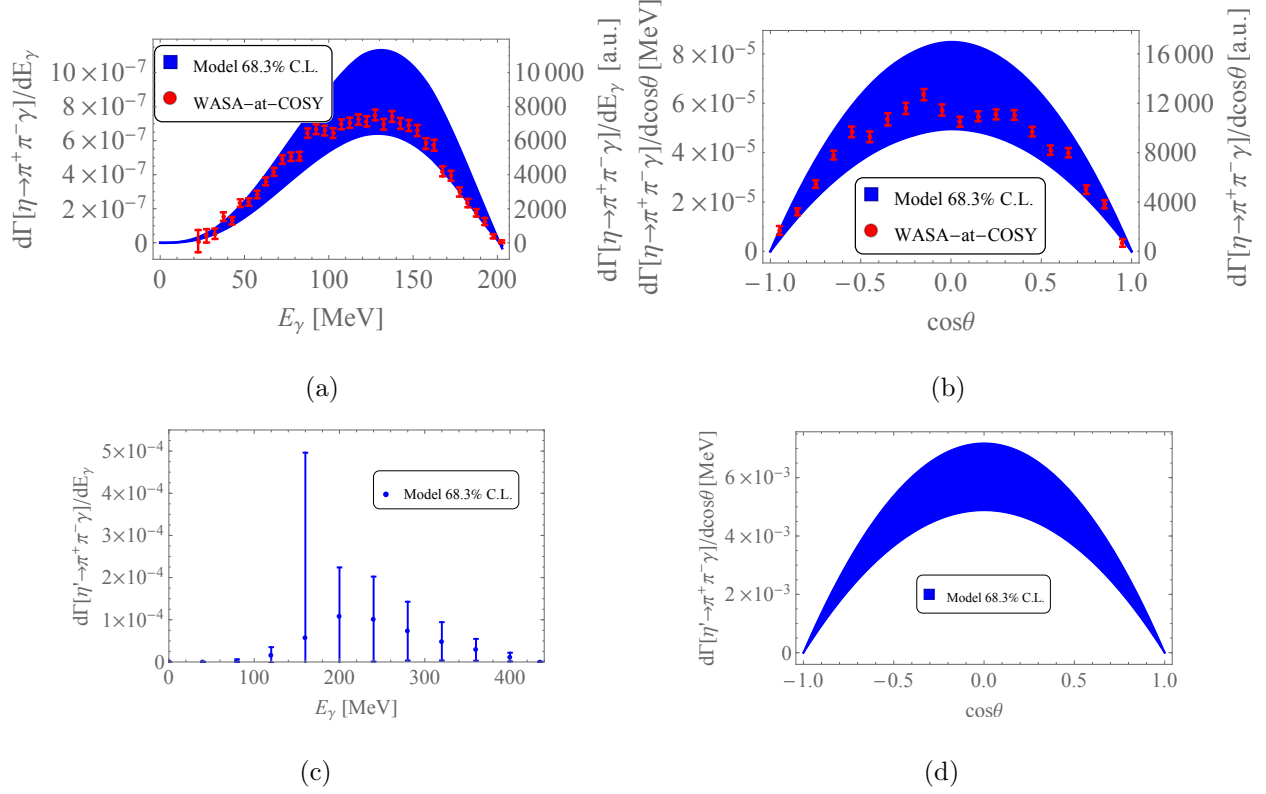


FIG. IV.4. Plots of differential decay width of  $P \rightarrow \pi^+\pi^-\gamma$ : (a), (c) the distributions of photon energy in the rest frame of  $\eta$  and  $\eta'$ , (b), (d) the distributions of cosine of the angle between  $\pi^+$  and  $\gamma$  in the rest frame of  $\pi^+\pi^-$  for decays of  $\eta$  and  $\eta'$ , respectively. For comparison, the data measured by the WASA-at-COSY collaboration [39] are shown as red circles in (a) and (b). For both (a) and (b), the vertical axis on the left side denotes the physical differential width while one on the right side shows arbitrary unit. See the text for a detailed explanation of units in which the differential widths of  $\eta \rightarrow \pi^+\pi^-\gamma$  are calculated.

TABLE X. The results of the decay widths for  $V \rightarrow PP$ .

Decay mode	Theory (MeV)	PDG (MeV)
$\Gamma[\omega \rightarrow \pi\pi]$	$0.114^{+0.03}_{-0.02}$	$0.130 \pm 0.016$
$\Gamma[\phi \rightarrow K^+K^-]$	$1.43^{+0.15}_{-0.10}$	$2.086 \pm 0.026$
$\Gamma[\phi \rightarrow K^0\bar{K}^0]$	$0.935^{+0.09}_{-0.06}$	$1.459 \pm 0.020$

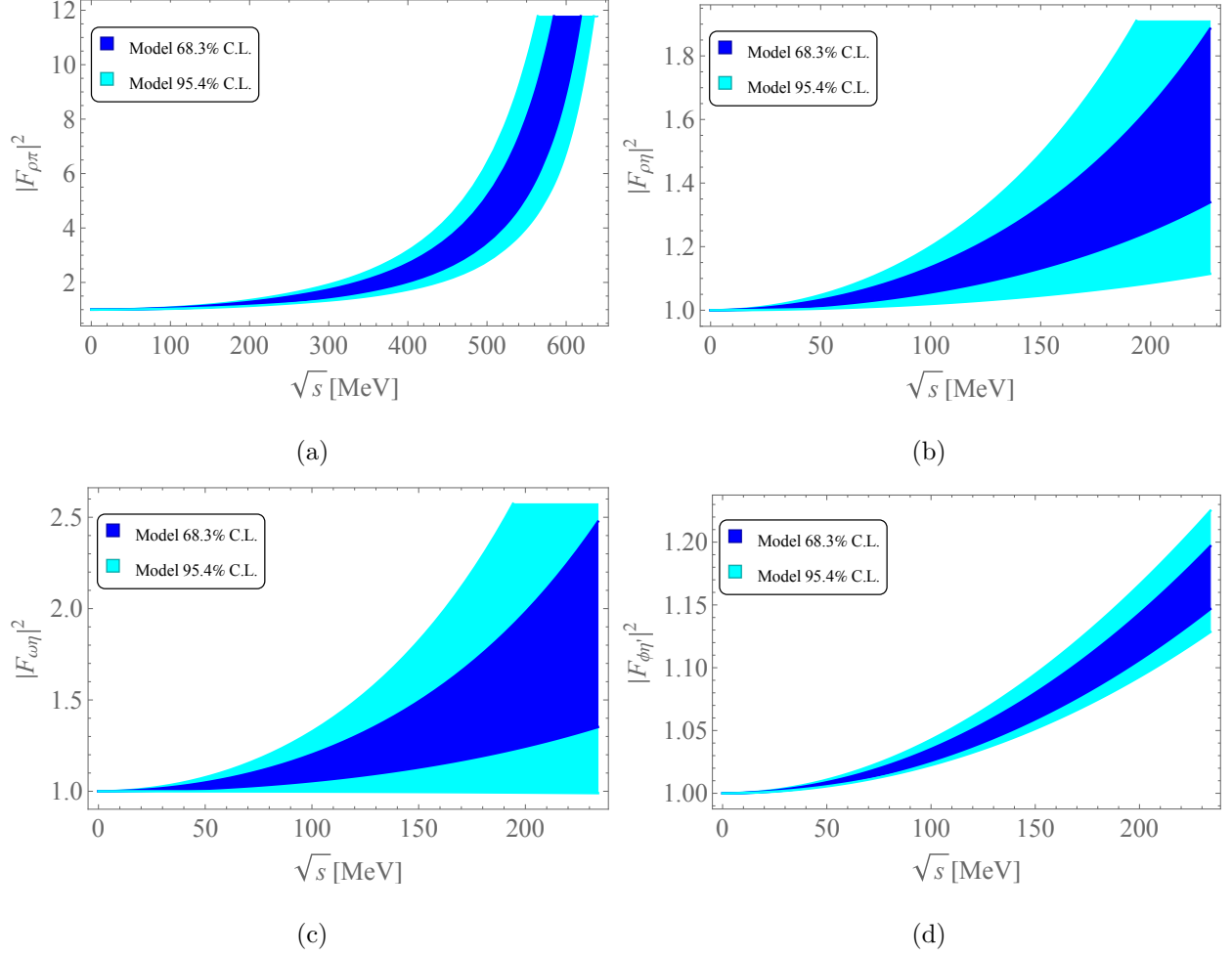
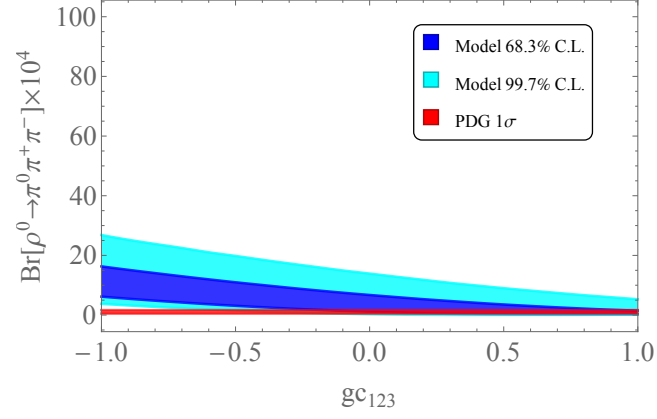


FIG. IV.5. Prediction of the model for TFFs: (a)  $\rho^0 \rightarrow \pi^0 l^+ l^-$ , (b)  $\rho^0 \rightarrow \eta l^+ l^-$ , (c)  $\omega \rightarrow \eta l^+ l^-$  and (d)  $\phi \rightarrow \eta' l^+ l^-$ . Blue (cyan) bands imply model prediction in 68.3% (95.4%) C.L.

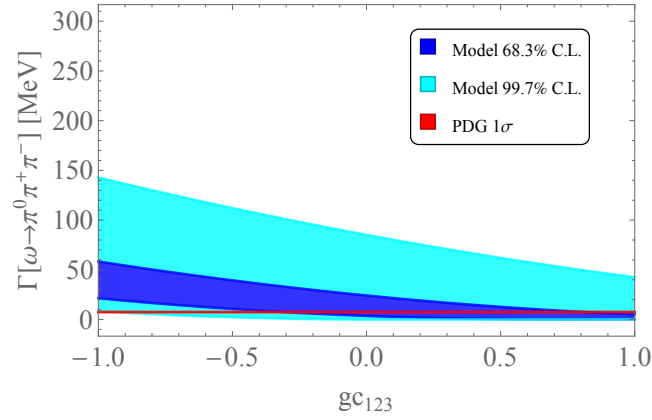
TABLE XI. The results of the decay widths for  $V \rightarrow PP$ .

Decay mode	Theory (MeV)	PDG (MeV)
$\Gamma[\rho \rightarrow \pi\pi]$	$157^{+66}_{-47}$	$149.1 \pm 0.8$
$\Gamma[K^{*\pm} \rightarrow (K\pi)^\pm]$	$45.4^{+20.6}_{-14.6}$	$46.2 \pm 1.3$

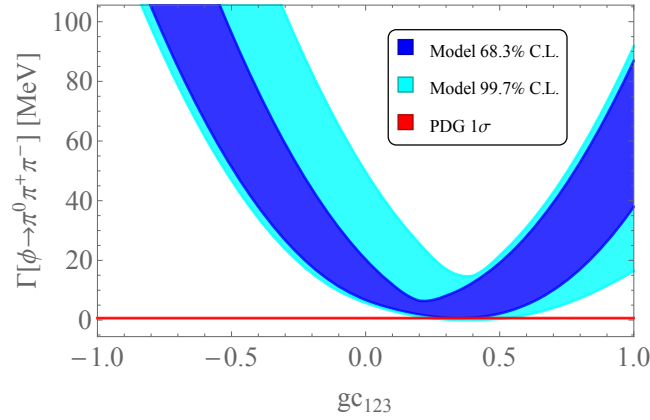




(a)



(b)



(c)

FIG. IV.6. Plots of model prediction: (a) branching ratio of  $\rho^+ \rightarrow \pi^0\pi^+\pi^-$ , (b) decay width of  $\rho^+ \rightarrow \pi^0\pi^+\pi^-$  and (c) decay width of  $\rho^+ \rightarrow \pi^0\pi^+\pi^-$ . In these plots, blue (cyan) bands represent 68.3% (99.7%) confidence intervals of the model predictions while red bands indicate  $1\sigma$  ranges of the PDG data [32].

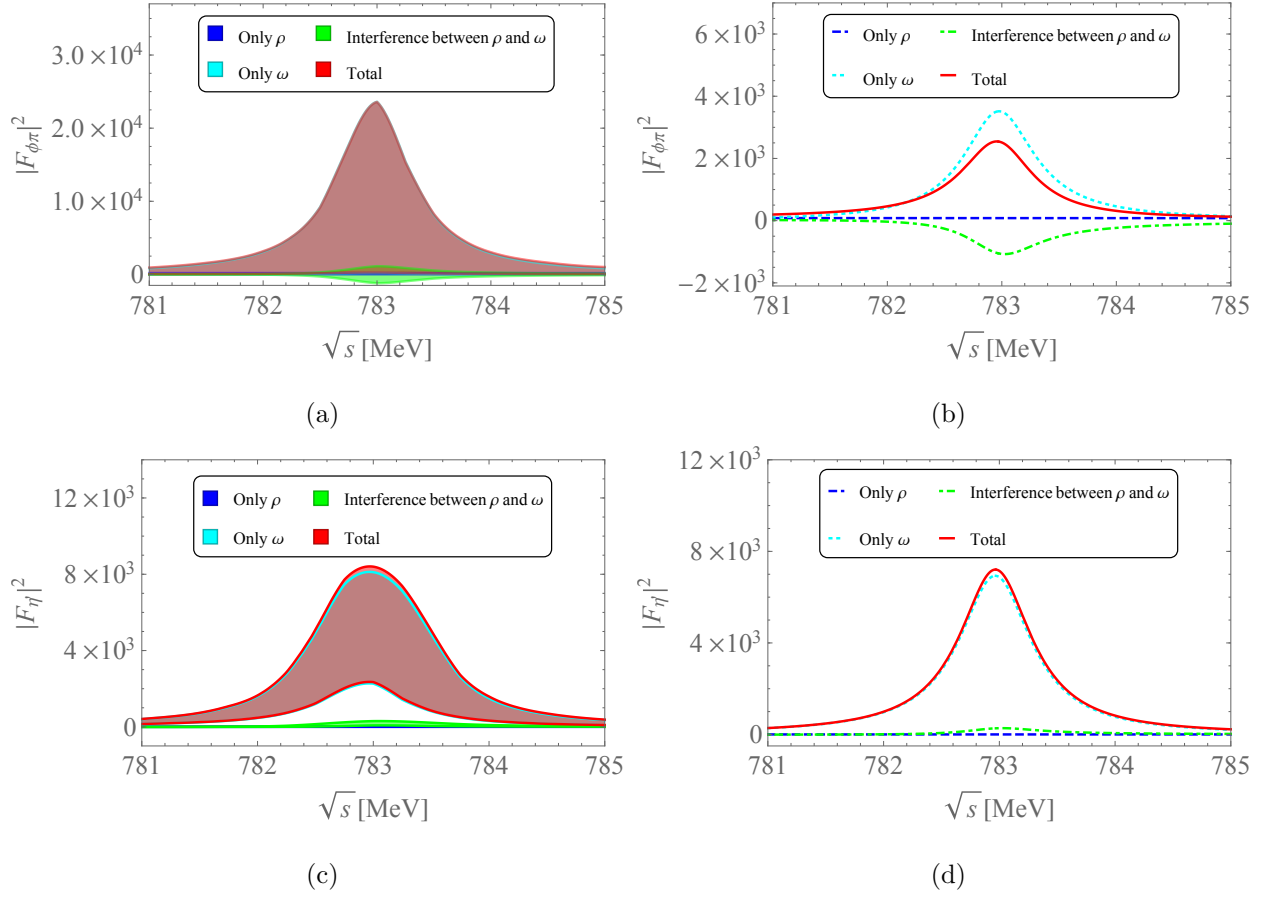


FIG. IV.7. Transition form factors versus di-lepton invariant mass in the vicinity of the resonance regions: (a)  $\phi \rightarrow \pi^0 l^+ l^-$  with 68.3% C.L. error bands, (b)  $\phi \rightarrow \pi^0 l^+ l^-$  for the best fit prediction, (c)  $\eta' \rightarrow \gamma l^+ l^-$  with 68.3% C.L. error bands and (d)  $\eta' \rightarrow \gamma l^+ l^-$  for the best fit prediction. For each figure, partial contributions from  $\rho^0$ ,  $\omega$  and interference between  $\rho^0$  and  $\omega$  are shown, respectively.

## V. SUMMARY AND DISCUSSION

The IP violating phenomena of light hadrons are investigated in the model of chiral Lagrangian including vector mesons. We introduced the suitable tree-level interaction terms which include singlet fields of vector meson and pseudoscalar. Power counting of superficial degree of divergence enables us to specify the 1-loop order interaction Lagrangian under the presence of the tree-level part. With introduced interactions, 1-loop correction to the self-energies of vector mesons is analyzed. Using the 1-loop corrected mass matrix, we obtained the expressions of physical masses and the mixing matrix of  $\rho, \omega$  and  $\phi$ . Including the kinetic mixing effect, the model expressions of the width for  $V \rightarrow PP$  decay are calculated. We also analyzed the mixing between photon and neutral vector mesons, which gives important contribution to processes such as  $V \rightarrow PV^* \rightarrow P\gamma$ .

For pseudoscalars, we took account of 1-loop correction to the mass matrix. The physical states of  $\pi^0, \eta, \eta'$  are written in terms of SU(3) eigenstates through wavefunction renormalizations and an orthogonal matrix which diagonalizes the 1-loop corrected mass matrix.

On the basis of the framework incorporating octet and singlet fields, the IP violating operators are introduced within SU(3) invariance. We constructed  $\mathcal{L}_i (i = 5 - 10)$ , which includes the SU(3) singlet fields of a pseudoscalar and a vector meson in addition to ones introduced in Refs. [18–20]. In order to realize the experimental data in the framework including the singlets and octets, we found that the singlet-induced operators play an important role; if  $\mathcal{L}_i (i = 5 - 10)$  were absent in the model,  $\Gamma[\eta' \rightarrow 2\gamma]$  would become much smaller than the observed value in the experiments.

Using the introduced IP violating operators, we obtained the analytic formulae for the IP violating (differential) decay widths. In particular, the widths of  $P \rightarrow V\gamma, V \rightarrow P\gamma, \phi \rightarrow \omega\gamma, P \rightarrow 2\gamma, V \rightarrow P\pi^+\pi^-$  are given. Moreover, the electromagnetic TFFs of  $P \rightarrow \gamma l^+l^-$  and  $V \rightarrow Pl^+l^-$  are also obtained. Additionally, the formula of the differential width for  $P \rightarrow \pi^+\pi^-\gamma$  is also shown.

For parameter estimation, we used precise data of spectrum function for  $\tau^- \rightarrow K_S\pi^-\nu$  measured by the Belle collaboration [11]. Furthermore, the PDG data [32] of physical masses of charged vector mesons,  $\rho^+$  and  $K^{*+}$  are used for parameter estimation of the coefficient of 1-loop order interaction terms. We also estimated the model parameters which appear in the mass matrix of neutral vector mesons by using the PDG data [32] of  $m_\rho, m_\omega$  and

$m_\phi$ . Since the masses of vector mesons are precisely measured in the experiment, the model parameters in the mass matrix are estimated with smaller uncertainty.

The numerical analyses of IP violating decay widths, the TFFs for electromagnetic decays, are carried out in the model. In order to estimate the IP violating parameters, we utilized the PDG data [32] of widths for radiative decays. Specifically, the experimental data of  $\Gamma[K^* \rightarrow K\gamma]$  and the effective coupling ratios of  $V^0 V^0 P^0$  to  $\rho^+ \pi^+ \gamma$  are used. We also considered constraints on a mass matrix and a mixing matrix of pseudoscalars. To obtain a parameter region which is consistent with the masses and  $\Gamma[P \rightarrow 2\gamma]$ , we solved the system of equations to realize the PDG data [32]. Furthermore,  $\chi^2$  fitting for the TFFs measured in the experiments [1, 33–38] is carried out. We found that the goodness-of-fit is improved if one does not use the input data measured by the Lepton-G experiment. Hence, we adopted the parameter set estimated without their data.

Using the estimated model parameters, we gave the model predictions for IP violating decays. In particular, we found that the electromagnetic TFFs of  $\eta \rightarrow \gamma l^+ l^-$ ,  $\eta' \rightarrow \gamma l^+ l^-$  are consistent with the experimental data for  $c_{34}^+ < 0$ . The partial widths of  $P \rightarrow \gamma l^+ l^-$ ,  $P \rightarrow \pi^+ \pi^- \gamma$ ,  $\phi \rightarrow \omega \pi^0$  and  $V \rightarrow P l^+ l^-$  are calculated, none of which result in significant deviation from the experimental data up to 99.7% C.L. For the differential widths of  $\eta \rightarrow \pi^+ \pi^- \gamma$  and  $\eta' \rightarrow \pi^+ \pi^- \gamma$ , the model predictions are given. The differential width of  $\eta \rightarrow \pi^+ \pi^- \gamma$  is compared with the data measured by the WASA-at-COSY collaboration [39]. Here, no significant deviation is found in this result. The predictions are also obtained for the TFFs of  $\rho \rightarrow \pi^0 l^+ l^-$ ,  $\rho \rightarrow \eta l^+ l^-$ ,  $\omega \rightarrow \eta l^+ l^-$  and  $\phi \rightarrow \eta' l^+ l^-$ , which are expected to be observed in future experiments. The model predictions for  $\text{Br}[\rho^0 \rightarrow \pi^0 \pi^+ \pi^-]$ ,  $\Gamma[\omega \rightarrow \pi^0 \pi^+ \pi^-]$  and  $\Gamma[\phi \rightarrow \pi^0 \pi^+ \pi^-]$  are also presented. We found that these IP violating observables are consistent with the PDG values [32]. In the vicinity of resonance region, the TFFs for  $\phi \rightarrow \pi^0 l^+ l^-$  and one for  $\eta' \rightarrow \gamma l^+ l^-$  are analyzed. It is shown that the  $\omega$  pole is dominant in the peak region for both TFFs. We also found that the contribution of the interference between  $\rho$  and  $\omega$  is non-negligible in the peak region. It is shown that the theoretical prediction for  $\Gamma[\phi \rightarrow K^+ K^-]/\Gamma[\phi \rightarrow K^0 \bar{K}^0]$  agrees with the experimental value, although  $\Gamma[\phi \rightarrow K^+ K^- (K^0 \bar{K}^0)]$  depends on two-loop ordered uncertainty.

Finally, we comment on some numerical results presented in this paper. One can find  $3.3\sigma$  deviation between the experimental data and the model prediction in the width of  $\rho^0 \rightarrow \pi^0 \gamma$ . This discrepancy arises due to the following fact: without isospin breaking,

$\Gamma[\rho^\pm \rightarrow \pi^\pm \gamma]$  and  $\Gamma[\rho^0 \rightarrow \pi^0 \gamma]$  become identical to each other. In order to explain the two widths simultaneously, one should include isospin breaking effects. However, in our work, isospin breaking is accounted only in the mixing matrices for mesons. In Ref. [20], the author introduced SU(3) violating IPV operators, and obtained  $\Gamma[\rho^0 \rightarrow \pi^0 \gamma] = 101 \pm 9[\text{keV}]$  and  $\Gamma[\rho^\pm \rightarrow \pi^\pm \gamma] = 68.1 \pm 7.1[\text{keV}]$ , both of which are consistent with the present PDG data [32]. Hence, it is expected that improvement will be presumably shown with such higher order correction of isospin breaking. Likewise, for  $K^{*+} \rightarrow K^+ \gamma$ ,  $3.4\sigma$  deviation between the width of the model prediction and one for the PDG data [32] is shown. The relation,  $\Gamma[K^{*0} \rightarrow K^0 \gamma] = 4\Gamma[K^{*+} \rightarrow K^+ \gamma]$ , is satisfied unless one accounts SU(3) breaking contributions. In our analysis, SU(3) breaking effect in the self-energy for vector mesons is considered. Nevertheless, we found that the relevant contribution vanishes in  $\Gamma[K^* \rightarrow K \gamma]$ . This is because the intermediate vector meson is changed into an on-shell photon as  $K^* \rightarrow KV^* \rightarrow K \gamma$ : The dependence on the eigenvalues of the vector mesons cancels out at  $q^2 = 0$ . Moreover, if one sums the contribution from the intermediate vector mesons,  $\rho, \omega$  and  $\phi$ , dependence on mixing angles vanishes due to orthogonality of the mixing matrix. Thus, in order to explain  $\Gamma[K^{*+} \rightarrow K^+ \gamma]$  and  $\Gamma[K^{*0} \rightarrow K^0 \gamma]$  simultaneously, SU(3) breaking in IP violating interaction is required.

## ACKNOWLEDGEMENT

This work is partially supported by Scientific Grants by the Ministry of Education, Culture, Sports, Science and Technology of Japan (Nos. 24540272 (HU), 26247038 (HU), 15H01037 (HU), 16H00871 (HU), 16H02189 (HU) and 17K05418 (TM)).

## Appendix A: Counter terms

The counter terms are computed with 1-loop correction of SU(3) singlet pseudoscalar in Ref. [6]. In this work, we only consider the corrections due to SU(3) octet pseudoscalars. The effect of SU(3)<sub>R</sub> external gauge boson is included. The counter terms in 1-loop order

are,

$$\begin{aligned}
\mathcal{L}_c = & L_1 (\text{Tr}(D_\mu U (D^\mu U)^\dagger))^2 + L_2 \text{Tr}(D_\mu U (D_\nu U)^\dagger) \text{Tr}(D^\mu U (D^\nu U)^\dagger) \\
& + L_3 \text{Tr}\{D^\mu U (D_\mu U)^\dagger D^\nu U (D_\nu U)^\dagger\} \\
& + \frac{4B}{f^2} L_4 \text{Tr}\{D_\mu U (D^\mu U)^\dagger\} \text{Tr}\{M(U + U^\dagger)\} \\
& + \frac{4B}{f^2} L_5 \text{Tr}\{D_\mu U (D^\mu U)^\dagger (UM + MU^\dagger)\} \\
& + \frac{16B^2}{f^4} L_6 \{\text{Tr}(M(U + U^\dagger))\}^2 \\
& + \frac{16B^2}{f^4} L_7 \{\text{Tr}(M(U - U^\dagger))\}^2 \\
& + \frac{16B^2}{f^4} L_8 \text{Tr}(MUMU + MU^\dagger MU^\dagger) \\
& + iL_9 \text{Tr}\{F_{L\mu\nu} (D^\mu U) (D^\nu U)^\dagger + F_{R\mu\nu} (D^\mu U)^\dagger D^\nu U\} \\
& + L_{10} \text{Tr}(F_{L\mu\nu} U F_R^{\mu\nu} U^\dagger) \\
& + H_1 \text{Tr}(F_{L\mu\nu} F_L^{\mu\nu} + F_{R\mu\nu} F_R^{\mu\nu}) \\
& + H_2 \left(\frac{4B}{f^2}\right)^2 \text{Tr}(M^2) \\
& + i\frac{K_1}{2} \text{Tr}(\xi^\dagger D^\mu U (D^\nu U)^\dagger \xi) (D_\mu v_\nu - D_\nu v_\mu + i[v_\mu, v_\nu]) \\
& - \frac{1}{2} (K_2 \text{Tr}(\xi^\dagger F_{L\mu\nu} \xi + \xi F_{R\mu\nu} \xi^\dagger) (D^\mu v^\nu - D^\nu v^\mu + i[v^\mu, v^\nu]) \\
& + K_3 \text{Tr}(D_\mu v_\nu - D_\nu v_\mu + i[v_\mu, v_\nu]) (D^\mu v^\nu - D^\nu v^\mu + i[v^\mu, v^\nu])) \\
& + \frac{4B}{f^2} (K_4 \text{Tr}\{(\xi M \xi + \xi^\dagger M \xi^\dagger) v^2\} + K_5 \text{Tr}\{M(U + U^\dagger)\} \text{Tr}(v^2)) \\
& + K_6 \text{Tr}(v_\rho \alpha_\perp^\mu) \text{Tr}(v^\rho \alpha_{\perp\mu}) + K_7 \text{Tr}(v^2 \alpha_{\perp\mu} \alpha_\perp^\mu) + K_8 \text{Tr}(\alpha_\perp^2) \text{Tr}(v^2) \\
& + K_9 \{\text{Tr}(v^2)\}^2 + K_{10} \text{Tr}(v^4) \\
& + i\frac{g_{2p}}{f^2} T_1 \eta_0 \text{Tr}\{(\xi M \xi - \xi^\dagger M \xi^\dagger) v^2\} \\
& + i\frac{g_{2p}}{f^2} T_2 \eta_0 \text{Tr}\{M(U - U^\dagger)\} \text{Tr}(v^2) \\
& + T_3 i\frac{g_{2p}}{f^2} \frac{4B}{f^2} \eta_0 \text{Tr}M(U + U^\dagger) \text{Tr}M(U - U^\dagger) \\
& + T_4 \left(\frac{g_{2p}}{f^2}\right)^2 \eta_0^2 (\text{Tr}M(U - U^\dagger))^2 + iT_5 \frac{4B}{f^2} \frac{g_{2p}}{f^2} \eta_0 \text{Tr}(MUMU - MU^\dagger MU^\dagger) \\
& + T_6 \left(\frac{g_{2p}}{f^2}\right)^2 \eta_0^2 \text{Tr}(MUMU + MU^\dagger MU^\dagger - 2M^2) \\
& + i\frac{g_{2p}}{f^2} \eta_0 [T_7 \text{Tr}\{M(D_\mu U (D^\mu U)^\dagger U - U^\dagger D_\mu U (D^\mu U)^\dagger)\} \\
& + T_8 \text{Tr}(M(U - U^\dagger)) \text{Tr}(D_\mu U (D^\mu U)^\dagger)], \tag{A1}
\end{aligned}$$

$$v_\mu = g_{\rho\pi\pi} \left( V_\mu - \frac{\alpha_\mu}{g} \right), \quad (\text{A2})$$

$$L_i = \lambda \Gamma_i + L_i^r (i = 1 - 10), \quad (\text{A3})$$

$$K_i = \lambda k_i + K_i^r (i = 1 - 10), \quad (\text{A4})$$

$$H_i = \lambda \Delta_i + H_i^r (i = 1 - 2), \quad (\text{A5})$$

$$T_i = \lambda t_i + T_i^r (i = 1 - 8), \quad (\text{A6})$$

$$\lambda = -\frac{1}{32\pi^2} (1 + C_{UV} - \ln \mu^2), \quad (\text{A7})$$

$$C_{UV} = \frac{1}{2 - \frac{d}{2}} - \gamma + \ln 4\pi. \quad (\text{A8})$$

In Eq. (A1), the contribution from singlet pseudoscalar is omitted in the coefficients of  $\Gamma_6, \Gamma_8$  and  $\Delta_2$ . We have also corrected the sign of  $k_9$  and  $k_{10}$  in Ref. [6].

TABLE XII. The coefficients of the counter terms:  $k_i, \Gamma_i$  and  $\Delta_i$ .

$k_1 = 1$	$t_1 = -6$	$\Gamma_1 = \frac{2c^2+1}{32}$	$\Delta_1 = -\frac{1}{8}$
$k_2 = 1$	$t_2 = -2$	$\Gamma_2 = \frac{1+2c^2}{16}$	$\Delta_2 = \frac{5}{24}$
$k_3 = 1$	$t_3 = -\frac{11}{18}$	$\Gamma_3 = \frac{3(c^2-1)}{16}$	
$k_4 = \frac{3}{2}$	$t_4 = -\frac{11}{9}$	$\Gamma_4 = \frac{c}{8}$	
$k_5 = \frac{1}{2}$	$t_5 = -\frac{5}{6}$	$\Gamma_5 = \frac{3c}{8}$	
$k_6 = 4c$	$t_6 = -\frac{5}{3}$	$\Gamma_6 = \frac{11}{144}$	
$k_7 = 6c$	$t_7 = -\frac{3c}{2}$	$\Gamma_7 = 0$	
$k_8 = 2c$	$t_8 = -\frac{c}{2}$	$\Gamma_8 = \frac{5}{48}$	
$k_9 = 3$		$\Gamma_9 = \frac{1}{4}$	
$k_{10} = 3$		$\Gamma_{10} = -\frac{1}{4}$	

## Appendix B: Power counting with SU(3) breaking and singlets

In this appendix, we show the power counting rule which is used to classify the interaction Lagrangian in Eq. (1) and counter terms in Eq. (A1). Since we treat the electromagnetic correction due to the term proportional to  $C$  in Eq. (1) only within tree level, in the following power counting, we do not take this term into account. Since we employ the loop expansion

due to pseudoscalar octet, the Lagrangian is organized as follows,

$$\sum_{n=0}^{\infty} \mathcal{L}^{(n)} \hbar^{n-1}, \quad (\text{B1})$$

where we denote  $\mathcal{L}^{(n)}$  as  $n$  loop contribution. We first evaluate the superficial degree of divergence of the  $n$  loop diagram of Nambu-Goldstone bosons using the interaction part of the tree level Lagrangian,

$$\begin{aligned} \mathcal{L}_{\text{int}}^{(0)} = & \frac{f^2}{4} \text{Tr}(D_\mu U D^\mu U^\dagger) + \frac{M_V^2}{g^2} \text{Tr}(\alpha_\mu \alpha^\mu) - \frac{2M_V^2}{g} \text{Tr}(V_\mu \alpha^\mu) \\ & + B \text{Tr}[M(U + U^\dagger)] - i g_{2p} \eta_0 \text{Tr}[M(U - U^\dagger)]. \end{aligned} \quad (\text{B2})$$

The first two terms of Eq.(B2) denote the interaction with the second derivatives among the Nambu-Goldstone bosons. The third term with the first derivative is the interaction between SU(3) octet vector mesons and SU(3) octet pseudoscalars. The other terms are the chiral breaking term which is proportional to the coefficient  $B$  and the interaction term between SU(3) singlet  $\eta_0$  and SU(3) octets. We compute the superficial degree of divergence  $\omega$  for  $N_L$  loop with  $N_\chi$  insertions of the chiral breaking term and with  $N_{\eta^0}$  ( $N_{V_8}$ ) external pseudoscalar singlets (vector meson octets) lines. It is given as follows,

$$\omega = 4N_L + 2N_2 + N_{V_8} - 2N_I, \quad (\text{B3})$$

where  $N_2$  is the number of the vertex with second derivatives and  $N_I$  denotes the numbers of the propagators of pseudoscalar octets in the internal line. It is related to the total number of the vertex ( $N_v$ ) and the number of loop ( $N_L$ ) as follows,

$$N_I = N_L + (N_v - 1), \quad (\text{B4})$$

where  $N_v$  is

$$N_v = N_{\eta^0} + N_\chi + N_{V_8} + N_2. \quad (\text{B5})$$

Substituting Eq.(B4) with Eq.(B5) into Eq. (B3), one obtains the following formula,

$$\omega = 2N_L + 2 - N_{V_8} - 2(N_{\eta^0} + N_\chi). \quad (\text{B6})$$

The ultraviolet divergence can occur when  $\omega \geq 0$  and we obtain the following condition which the divergent diagrams satisfy,

$$2N_L + 2 \geq N_{V_8} + 2(N_{\eta^0} + N_\chi). \quad (\text{B7})$$



The counter terms which subtract the divergence also satisfy the above condition on the number of the external lines ( $N_{\eta^0}, N_{V_8}$ ) and the powers of  $B$  which correspond to  $N_\chi$ . Let us examine the types of the counter terms which are required within one-loop calculation by setting  $N_L = 1$ . Then the superficial degree of divergence is

$$\omega = 4 - N_{V_8} - 2(N_{\eta^0} + N_\chi). \quad (\text{B8})$$

Note that the  $\omega$  is equal to the number of the derivatives  $\omega_0$  included in the counter terms. In Table XIII, we show  $\omega_0(\geq 0)$ ,  $N_\chi$ ; the powers of  $B$ ,  $N_{\eta^0}$  and  $N_{V_8}$  in each 1-loop counter term. We classify each counter term in Eq. (A1) according to these numbers and show their coefficients.

Next we study the power counting of the interaction terms for singlet vector meson. In contrast to the octet vector mesons, the chiral invariant interaction of the singlet vector meson to the octet pseudoscalars with the first derivative vanishes,

$$\phi^{0\mu} \text{Tr} \left( V_\mu - \frac{\alpha_\mu}{g} \right) = 0. \quad (\text{B9})$$

Therefore there is no tree level interaction for the singlet vector meson. The interaction of the singlet vector meson with chiral breaking term

$$g_{1V} \phi^{\mu 0} \text{Tr} (\xi M \xi + \xi^\dagger M \xi^\dagger) \left( V_\mu - \frac{\alpha_\mu}{g} \right), \quad (\text{B10})$$

is classified as the one loop level interaction since this term also includes a vector meson with the first derivative and the chiral breaking  $M$ , which has a structure similar to the one loop effective counter terms in Eq. (B11) for vector meson octets given below,

$$\begin{aligned} & C_1 \frac{2B}{f^2} \text{Tr} \left\{ (\xi M \xi + \xi^\dagger M \xi^\dagger) \left( V_\mu - \frac{\alpha_\mu}{g} \right) \left( V^\mu - \frac{\alpha^\mu}{g} \right) \right\} \\ & + C_2 \frac{2B}{f^2} \text{Tr} (\xi M \xi + \xi^\dagger M \xi^\dagger) \text{Tr} \left\{ \left( V_\mu - \frac{\alpha_\mu}{g} \right) \left( V^\mu - \frac{\alpha^\mu}{g} \right) \right\}. \end{aligned} \quad (\text{B11})$$

TABLE XIII.  $(\omega_0, N_\chi, N_{\eta_0}, N_{V_8})$  for 1-loop counter terms.

$\omega_0$	$N_\chi$	$N_{\eta_0}$	$N_{V_8}$	The coefficients of the counter terms
4	0	0	0	$L_1, L_2, L_3, L_9, L_{10}, H_1, K_1, K_2, K_3, K_6, K_7, K_8, K_9, K_{10}$
3	0	0	1	$K_1, K_2, K_3, K_6, K_7, K_8, K_9, K_{10}$
2	1	0	0	$L_4, L_5, K_4, K_5$
0	2	0	0	$L_6, L_7, L_8, H_2$
2	0	0	2	$K_1, K_2, K_3, K_6, K_7, K_8, K_9, K_{10}$
2	0	1	0	$T_1, T_2, T_7, T_8$
1	0	1	1	$T_1, T_2$
0	0	1	2	$T_1, T_2$
0	1	1	0	$T_3, T_5$
0	0	2	0	$T_4, T_6$
0	1	0	2	$K_4, K_5$
1	1	0	1	$K_4, K_5$
1	0	0	3	$K_3, K_9, K_{10}$
0	0	0	4	$K_3, K_9, K_{10}$

### Appendix C: 1-loop correction to self-energy for $K^{*+}, K^{*0}$ and $\rho^+$

In this appendix, we study self-energy corrections to  $K^{*+0}$  mesons and charged  $\rho$  meson taking SU(3) breaking into account. The interaction Lagrangian for  $V \rightarrow PP$  is given as,

$$\begin{aligned}
 \mathcal{L}^{VPP} &= -\frac{2g_{\rho\pi\pi}}{i} \text{Tr}(V_\mu[\Delta, \partial^\mu \Delta]) \\
 &= i\frac{g_{\rho\pi\pi}}{2} \left[ K^{*+\mu} \left( \hat{K}^- \overset{\leftrightarrow}{\partial}_\mu \hat{\pi}_3 + \sqrt{3} \hat{K}^- \overset{\leftrightarrow}{\partial}_\mu \hat{\eta}_8 + \sqrt{2} \hat{K}^0 \overset{\leftrightarrow}{\partial}_\mu \hat{\pi}^- \right) \right. \\
 &\quad + K^{*0\mu} \left( -\hat{K}^0 \overset{\leftrightarrow}{\partial}_\mu \hat{\pi}_3 + \sqrt{3} \hat{K}^0 \overset{\leftrightarrow}{\partial}_\mu \hat{\eta}_8 + \sqrt{2} \hat{K}^- \overset{\leftrightarrow}{\partial}_\mu \hat{\pi}^- \right) \\
 &\quad \left. + \rho^{+\mu} \left( 2\hat{\pi}^- \overset{\leftrightarrow}{\partial}_\mu \hat{\pi}_3 + \sqrt{2} \hat{K}^0 \overset{\leftrightarrow}{\partial}_\mu \hat{K}^- \right) \right] + h.c., \tag{C1}
 \end{aligned}$$

$$\Delta = \frac{1}{2} \begin{pmatrix} \hat{\pi}_3 + \frac{\hat{\eta}_8}{\sqrt{3}} & \sqrt{2}\hat{\pi}^+ & \sqrt{2}\hat{K}^+ \\ \sqrt{2}\hat{\pi}^- & -\hat{\pi}_3 + \frac{\hat{\eta}_8}{\sqrt{3}} & \sqrt{2}\hat{K}^0 \\ \sqrt{2}\hat{K}^+ & \sqrt{2}\hat{K}^0 & -2\frac{\hat{\eta}_8}{\sqrt{3}} \end{pmatrix}, \tag{C2}$$

where  $\Delta$  denotes the quantum fluctuation for the pseudoscalar octet in the background field method [6]. The isospin breaking leads to  $\pi_3 - \eta_8$  mixing and the Feynman diagrams of the self-energy for  $K^{*+0}$  are shown in Fig. C.1.  $\pi_3 - \eta_8$  mixing obtained from the chiral breaking

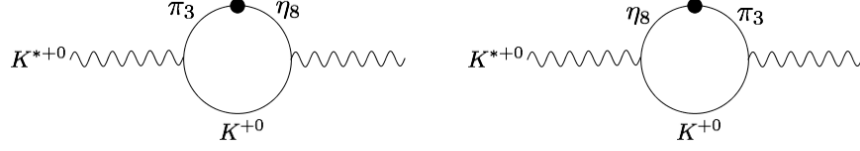


FIG. C.1. Self-energy corrections to  $K^{*+0}$ . The diagrams include the  $\pi_3 - \eta_8$  mixing due to the isospin breaking effect.

term is given by the following Lagrangian,

$$\mathcal{L} = -M_{38}^2 \hat{\pi}_3 \hat{\eta}_8, \quad (\text{C3})$$

$$M_{38}^2 = \frac{1}{\sqrt{3}}(M_{K^+}^2 - M_{K^0}^2). \quad (\text{C4})$$

We treat the mixing in Eq. (C3) as perturbation. The mixing insertion is denoted with black circles in Fig. C.1. Below, the amplitude corresponding to the diagrams in Fig. C.1 is shown,

$$\begin{aligned} & \frac{g_{\rho\pi\pi}^2}{4} \int \frac{d^d k}{(2\pi)^{d_i}} \frac{(Q-2k)_\mu (Q-2k)_\nu}{((Q-k)^2 - M_\pi^2)((Q-k)^2 - M_{\eta_8}^2)(k^2 - M_K^2)} 2\sqrt{3}M_{38}^2 \\ &= \frac{g_{\rho\pi\pi}^2}{2} \frac{M_{K^+}^2 - M_{K^0}^2}{M_{\eta_8}^2 - M_\pi^2} (J_{\mu\nu}^{\eta_8 K} - J_{\mu\nu}^{\pi^0 K}) \\ &= 2g_{\rho\pi\pi}^2 \frac{M_{K^+}^2 - M_{K^0}^2}{M_{\eta_8}^2 - M_\pi^2} Q_{\mu\nu} (M_{K\eta_8}^r - M_{K\pi}^r) \\ & \quad + g_{\rho\pi\pi}^2 (M_{K^+}^2 - M_{K^0}^2) g_{\mu\nu} \left( 2 \frac{L_{K\eta_8} - L_{K\pi}}{M_{\eta_8}^2 - M_\pi^2} - \lambda - \frac{\mu_{\eta_8} - \mu_\pi}{M_{\eta_8}^2 - M_\pi^2} \right), \end{aligned} \quad (\text{C5})$$

where  $Q_{\mu\nu}$  is defined in Eq. (21) and  $M_K$  denotes  $M_{K^+}$  or  $M_{K^0}$  and one uses the following 1-loop function,

$$\begin{aligned} J_{\mu\nu}^{QP} &= \int \frac{d^d k}{(2\pi)^{d_i}} \frac{(Q-2k)_\mu (Q-2k)_\nu}{((Q-k)^2 - M_Q^2)(k^2 - M_P^2)} \\ &= Q_{\mu\nu} \left( 4M_{PQ}^r - \frac{2}{3}\lambda \right) + g_{\mu\nu} (4L_{PQ} - 2\lambda\Sigma_{PQ} - 2(\mu_Q + \mu_P)), \end{aligned} \quad (\text{C6})$$

$$\Sigma_{PQ} = M_P^2 + M_Q^2. \quad (\text{C7})$$

In Eqs. (C5, C6),  $\lambda$  denotes the ultraviolet divergence defined in Eq. (A7). In Eq. (C6),  $L_{PQ}$  and  $M_{PQ}^r$  are functions given below,

$$M_{PQ}^r = \frac{1}{12Q^2} (Q^2 - 2\Sigma_{PQ}) \bar{J}_{PQ} + \frac{\Delta_{PQ}^2}{3Q^4} \left[ \bar{J}_{PQ} - Q^2 \frac{1}{32\pi^2} \left( \frac{\Sigma_{PQ}}{\Delta_{PQ}^2} + 2 \frac{M_P^2 M_Q^2}{\Delta_{PQ}^3} \ln \frac{M_Q^2}{M_P^2} \right) \right] - \frac{k_{PQ}}{6} + \frac{1}{288\pi^2}, \quad (\text{C8})$$

$$L_{PQ} = \frac{\Delta_{PQ}^2}{4s} \bar{J}_{PQ}, \quad (\text{C9})$$

$$k_{PQ} = \frac{(\mu_P - \mu_Q) f^2}{\Delta_{PQ}}. \quad (\text{C10})$$

In Eqs. (C8, C9),  $\bar{J}_{PQ}$  is a 1-loop scalar function of pseudoscalar mesons with masses  $M_P$  and  $M_Q$ . Above the threshold  $Q^2 \geq (M_P + M_Q)^2$ , it is given by,

$$\bar{J}_{PQ}(Q^2) = \frac{1}{32\pi^2} \left[ 2 + \frac{\Delta_{PQ}}{Q^2} \ln \frac{M_Q^2}{M_P^2} - \frac{\Sigma_{PQ}}{\Delta_{PQ}} \ln \frac{M_Q^2}{M_P^2} - \frac{\nu_{PQ}}{Q^2} \ln \frac{(Q^2 + \nu_{PQ})^2 - \Delta_{PQ}^2}{(Q^2 - \nu_{PQ})^2 - \Delta_{PQ}^2} \right] + \frac{i}{16\pi} \frac{\nu_{PQ}}{Q^2}, \quad (\text{C11})$$

$$\nu_{PQ}^2 = Q^4 - 2Q^2 \Sigma_{PQ} + \Delta_{PQ}^2, \quad (\text{C12})$$

while below the threshold  $(M_P - M_Q)^2 \leq Q^2 \leq (M_P + M_Q)^2$ ,

$$\bar{J}_{PQ}(Q^2) = \frac{1}{32\pi^2} \left[ 2 + \frac{\Delta_{PQ}}{Q^2} \ln \frac{M_Q^2}{M_P^2} - \frac{\Sigma_{PQ}}{\Delta_{PQ}} \ln \frac{M_Q^2}{M_P^2} - 2 \frac{\sqrt{-\nu_{PQ}^2}}{Q^2} \left( \arctan \frac{Q^2 - \Delta_{PQ}}{\sqrt{-\nu_{PQ}^2}} + \arctan \frac{Q^2 + \Delta_{PQ}}{\sqrt{-\nu_{PQ}^2}} \right) \right]. \quad (\text{C13})$$

We write inverse propagators of vector mesons as,

$$D_{V\mu\nu}^{-1} = (M_V^2 + \delta A_V) g_{\mu\nu} + \delta \tilde{B}_V Q_\mu Q_\nu, \quad (\text{C14})$$

where the metric part of the inverse propagator consists of the sum of tree-level mass  $M_V$  and loop correction  $\delta A_V$ . Using loop functions defined, we add the isospin breaking corrections in Fig. C.1 to the calculation given in Ref. [6]. We also take account of the mass differences of  $K^+ - K^0$  and  $\pi^+ - \pi^0$ , which were not considered in the previous study. The self-energy

corrections to  $K^{*+0}$  and  $\rho^+$  mesons are obtained as,

$$\begin{aligned}\delta\tilde{B}_{K^{*+}} &= Z_V^r(\mu) + g_{\rho\pi\pi}^2 \left[ 2M_{K^0\pi^+}^r + M_{K^+\pi^0}^r + 3M_{K^+\eta_8}^r + 2\frac{M_{K^+}^2 - M_{K^0}^2}{M_{\eta_8}^2 - M_\pi^2} (M_{K^+\eta_8}^r - M_{K^+\pi^0}^r) \right], \\ \delta A_{K^{*+}} &= \Delta A_{K^{*+}} + C_1^r(\mu)M_{K^+}^2 + C_2^r(\mu)(2\bar{M}_K^2 + M_\pi^2) - Q^2 Z_V^r(\mu),\end{aligned}\quad (C15)$$

$$\begin{aligned}\Delta A_{K^{*+}} &= -Q^2 g_{\rho\pi\pi}^2 \left[ 2M_{K^0\pi^+}^r + M_{K^+\pi^0}^r + 3M_{K^+\eta_8}^r + 2\frac{M_{K^+}^2 - M_{K^0}^2}{M_{\eta_8}^2 - M_\pi^2} (M_{K^+\eta_8}^r - M_{K^+\pi^0}^r) \right] \\ &+ g_{\rho\pi\pi}^2 \left[ 2 \left( \frac{M_{K^+}^2 - M_{K^0}^2}{M_{\eta_8}^2 - M_\pi^2} \right) \left( L_{K^+\eta_8} - L_{K^+\pi^0} - \frac{f^2}{2}(\mu_{\eta_8} - \mu_\pi) \right) + 2L_{K^0\pi^+} + L_{K^+\pi^0} \right. \\ &\left. + 3L_{K^+\eta_8} - \frac{f^2}{2} \{ 2(\mu_{K^0} + \mu_\pi) + \mu_{K^+} + \mu_\pi + 3(\mu_{K^+} + \mu_{\eta_8}) \} \right],\end{aligned}\quad (C16)$$

$$\begin{aligned}\delta\tilde{B}_{K^{*0}} &= Z_V^r(\mu) + g_{\rho\pi\pi}^2 \left[ 2M_{K^+\pi^-}^r + M_{K^0\pi^0}^r + 3M_{K^0\eta_8}^r - 2\frac{M_{K^+}^2 - M_{K^0}^2}{M_{\eta_8}^2 - M_\pi^2} (M_{K^0\eta_8}^r - M_{K^0\pi^0}^r) \right], \\ \delta A_{K^{*0}} &= \Delta A_{K^{*0}} + C_1^r(\mu)M_{K^0}^2 + C_2^r(\mu)(2\bar{M}_K^2 + M_\pi^2) - Q^2 Z_V^r(\mu),\end{aligned}\quad (C17)$$

$$\begin{aligned}\Delta A_{K^{*0}} &= -Q^2 g_{\rho\pi\pi}^2 \left[ 2M_{K^+\pi^-}^r + M_{K^0\pi^0}^r + 3M_{K^0\eta_8}^r - 2\frac{M_{K^+}^2 - M_{K^0}^2}{M_{\eta_8}^2 - M_\pi^2} (M_{K^0\eta_8}^r - M_{K^0\pi^0}^r) \right] \\ &+ g_{\rho\pi\pi}^2 \left[ -2 \left( \frac{M_{K^+}^2 - M_{K^0}^2}{M_{\eta_8}^2 - M_\pi^2} \right) \left( L_{K^0\eta_8} - L_{K^0\pi^0} - \frac{f^2}{2}(\mu_{\eta_8} - \mu_\pi) \right) \right. \\ &\left. + 2L_{K^+\pi^-} + L_{K^0\pi^0} + 3L_{K^0\eta_8} - \frac{f^2}{2} \{ 2(\mu_{K^+} + \mu_\pi) + \mu_{K^0} + \mu_\pi + 3(\mu_{K^0} + \mu_{\eta_8}) \} \right],\end{aligned}\quad (C18)$$

$$\begin{aligned}\delta\tilde{B}_{\rho^+} &= Z_V^r(\mu) + g_{\rho\pi\pi}^2 (4M_{\pi^+\pi^0}^r + 2M_{K^+\bar{K}^0}^r), \\ \delta A_{\rho^+} &= \Delta A_{\rho^+} + C_1^r(\mu)M_\pi^2 + C_2^r(\mu)(2\bar{M}_K^2 + M_\pi^2) - Q^2 Z_V^r(\mu),\end{aligned}\quad (C19)$$

$$\begin{aligned}\Delta A_{\rho^+} &= -Q^2 g_{\rho\pi\pi}^2 (4M_{\pi^+\pi^0}^r + 2M_{K^+\bar{K}^0}^r) \\ &+ 2g_{\rho\pi\pi}^2 \left( 2L_{\pi^+\pi^0} + L_{K^+\bar{K}^0} - \frac{f^2}{2} (4\mu_\pi + \mu_{K^+} + \mu_{K^0}) \right).\end{aligned}\quad (C20)$$

#### Appendix D: Proof of the relation for $V - A$ mixing vertex

In this section, we show that the metric tensor part of the two-point functions for the  $V - A$  mixing satisfies the relation in Eq. (78). Multiplying Eq. (77) by  $O_V^T$ , one can find,

$$\begin{aligned}\Pi^{VA} &= O_V^T \Pi^{V^0A} \\ &= -\frac{1}{g} \begin{pmatrix} M_\rho^2 O_{V11} + M_{V\rho 8}^2 O_{V21} + M_{V0\rho}^2 O_{V31} + \frac{M_{V\rho 8}^2 O_{V11} + M_{V88}^2 O_{V21} + M_{V08}^2 O_{V31}}{\sqrt{3}} \\ M_\rho^2 O_{V12} + M_{V\rho 8}^2 O_{V22} + M_{V0\rho}^2 O_{V32} + \frac{M_{V\rho 8}^2 O_{V12} + M_{V88}^2 O_{V22} + M_{V08}^2 O_{V32}}{\sqrt{3}} \\ M_\rho^2 O_{V13} + M_{V\rho 8}^2 O_{V23} + M_{V0\rho}^2 O_{V33} + \frac{M_{V\rho 8}^2 O_{V13} + M_{V88}^2 O_{V23} + M_{V08}^2 O_{V33}}{\sqrt{3}} \end{pmatrix}.\end{aligned}\quad (D1)$$

Meanwhile, the diagonalization of the mass matrix leads to,

$$\begin{pmatrix} M_\rho^2 & M_{V\rho 8}^2 & M_{V0\rho}^2 \\ M_{V\rho 8}^2 & M_{V88}^2 & M_{V08}^2 \\ M_{V0\rho}^2 & M_{V08}^2 & M_{0V}^2 \end{pmatrix} O_V = O_V \begin{pmatrix} \mathcal{M}_1^2 & 0 & 0 \\ 0 & \mathcal{M}_2^2 & 0 \\ 0 & 0 & \mathcal{M}_3^2 \end{pmatrix}. \quad (\text{D2})$$

In the above equation, the matrix elements for  $(i, j) = (1, I), (2, I)$  indicate the following relations,

$$M_\rho^2 O_{V1I} + M_{V\rho 8}^2 O_{V2I} + M_{V0\rho}^2 O_{V3I} = \mathcal{M}_I^2 O_{V1I}, \quad (\text{D3})$$

$$M_{V\rho 8}^2 O_{V1I} + M_{V88}^2 O_{V2I} + M_{V08}^2 O_{V3I} = \mathcal{M}_I^2 O_{V2I}. \quad (\text{D4})$$

Plugging Eqs. (D3, D4) into Eq. (D1), one can find that the relation in Eq. (78) is satisfied.

### Appendix E: 1-loop correction to self-energy for $\pi^+, K^+$ and $K^0$

In this appendix, the radiative correction to charged pseudoscalar masses is discussed. Background field method is used to evaluate the chiral loop correction[44, 45]. Kinetic terms and 1-loop corrected masses in effective Lagrangian are given as,

$$\mathcal{L}_{\text{eff}} = \sum_P^{\pi^+, K^+, K^0} \left( \frac{1}{Z_P} \partial_\mu P_f \partial^\mu \bar{P}_f - M_P^2 P_f \bar{P}_f \right) \quad (\text{E1})$$

$$= \sum_P^{\pi^+, K^+, K^0} (\partial_\mu P \partial^\mu \bar{P} - M_P^2 P \bar{P}). \quad (\text{E2})$$

In Eq. (E1), we denote  $P_f$  as the pseudoscalar in original flavor basis and the coefficient of the kinetic term is,

$$\frac{1}{Z_P} = 1 - Z_{P(1)}, \quad (\text{E3})$$

$$Z_{\pi^+(1)} \sim -8 \left( \frac{M_{\pi^+}^2 + 2\bar{M}_K^2}{f^2} L_4^r + \frac{M_{\pi^+}^2}{f^2} L_5^r \right) + 2c(2\mu_{\pi^+} + \bar{\mu}_K), \quad (\text{E4})$$

$$Z_{K^+(1)} \simeq Z_{K^0(1)} \sim -8 \left( \frac{M_{\pi^+}^2 + 2\bar{M}_K^2}{f^2} L_4^r + \frac{\bar{M}_K^2}{f^2} L_5^r \right) + c \left( \frac{3}{2}\mu_{\pi^+} + \frac{3}{2}\mu_{88} + 3\bar{\mu}_K \right). \quad (\text{E5})$$

In Eq. (E1), normalization of the kinetic term is slightly deviated from unity due to 1-loop correction. In order to canonically normalize  $Z_P$  in Eq. (E1), one should implement the transformation in the following form as,

$$P_f^{(-)} = \sqrt{Z_P} P^{(-)}, \quad (\text{E6})$$

$$\sqrt{Z_P} \sim 1 + \frac{Z_{P(1)}}{2}. \quad (\text{E7})$$

Using transformation in Eq. (E6), one obtains Lagrangian in Eq. (E2). We keep linear order of the small quantities (we neglect quadratic terms with respect to isospin breaking and 1-loop correction multiplied by isospin violation). The masses in Eq. (E2) are,

$$M_{\pi^+}^{\prime 2} \simeq (M_{\pi^+}^2)_{\text{tr}} \left[ 1 + (4c - 3)\mu_{\pi^+} - \frac{1}{3}\mu_{88} + 2(c - 1)\bar{\mu}_K \right. \\ \left. - 8\frac{M_{\pi^+}^2 + 2\bar{M}_K^2}{f^2}L_{46}^r - 8\frac{M_{\pi^+}^2}{f^2}L_{58}^r \right] + \Delta_{\text{EM}}, \quad (\text{E8})$$

$$M_{K^+}^{\prime 2} \simeq (M_{K^+}^2)_{\text{tr}} \left[ 1 + \frac{3}{2}(c - 1)\mu_{\pi^+} + \frac{1}{6}(9c - 5)\mu_{88} + 3(c - 1)\bar{\mu}_K \right. \\ \left. - 8\frac{M_{\pi^+}^2 + 2\bar{M}_K^2}{f^2}L_{46}^r - 8\frac{\bar{M}_K^2}{f^2}L_{58}^r \right] + \Delta_{\text{EM}}, \quad (\text{E9})$$

$$M_{K^0}^{\prime 2} \simeq (M_{K^0}^2)_{\text{tr}} \left[ 1 + \frac{3}{2}(c - 1)\mu_{\pi^+} + \frac{1}{6}(9c - 5)\mu_{88} + 3(c - 1)\bar{\mu}_K \right. \\ \left. - 8\frac{M_{\pi^+}^2 + 2\bar{M}_K^2}{f^2}L_{46}^r - 8\frac{\bar{M}_K^2}{f^2}L_{58}^r \right], \quad (\text{E10})$$

where low energy constants are denoted as,

$$L_{46}^r = L_4^r - 2L_6^r, \quad L_{58}^r = L_5^r - 2L_8^r, \quad \Delta_{\text{EM}} = \frac{2C}{9f^2}. \quad (\text{E11})$$

In Eqs. (E8-E10),  $(M_P^2)_{\text{tr}}$  denotes the tree-level mass parameters, and in the loop corrections, pseudoscalar masses are identified with physical masses expressed as  $M_{\pi^+}^2$  and  $\bar{M}_K^2$  defined in Eq. (32) since their difference gives rise to minor correction in Eqs. (E8-E10). The tree-level mass parameters in r.h.s. of Eqs. (E8-E10) are given as Gell-Mann-Oakes-Renner (GMOR) relation,

$$(M_{\pi^+}^2)_{\text{tr}} = \frac{2B(m_u + m_d)}{f^2}, \quad (M_{K^+}^2)_{\text{tr}} = \frac{2B(m_u + m_s)}{f^2}, \quad (M_{K^0}^2)_{\text{tr}} = \frac{2B(m_d + m_s)}{f^2}. \quad (\text{E12})$$

One can clarify that the 1-loop masses are renormalization scale invariant. Therefore, we find that the following equation is satisfied,

$$\frac{\partial M_{\pi^+}^{\prime 2}}{\partial \ln \mu} = \frac{\partial M_{K^+}^{\prime 2}}{\partial \ln \mu} = \frac{\partial M_{K^0}^{\prime 2}}{\partial \ln \mu} = 0. \quad (\text{E13})$$

## Appendix F: 1-loop correction to self-energy for neutral pseudoscalars

In this appendix, the radiative correction to pseudoscalar masses is evaluated for neutral particles. As analogous to the previous section, the background field method is used to

evaluate the quantum correction. We consider the framework in which chiral octet loop correction is taken into account. Masses and kinetic terms of pseudoscalars in 1-loop corrected effective Lagrangian are written as,

$$\mathcal{L}_{\text{eff}} = \frac{1}{2}(\partial_\mu \pi_3, \partial_\mu \eta_8, \partial_\mu \eta_0) \frac{1}{Z} (\partial^\mu \pi_3, \partial^\mu \eta_8, \partial^\mu \eta_0)^T - \frac{1}{2}(\pi_3, \eta_8, \eta_0) M^2 (\pi_3, \eta_8, \eta_0)^T \quad (\text{F1})$$

(SU(3) eigenstate)

$$= \frac{1}{2} \partial_\mu \pi_3^R \partial^\mu \pi_3^R + \frac{1}{2} \partial_\mu \eta_8^R \partial^\mu \eta_8^R + \frac{1}{2} \partial_\mu \eta_0^R \partial^\mu \eta_0^R - \frac{1}{2} (\pi_3^R, \eta_8^R, \eta_0^R) M'^2 (\pi_3^R, \eta_8^R, \eta_0^R)^T \quad (\text{F2})$$

(kinetic terms rescaled)

$$= \frac{1}{2} \partial_\mu \pi^0 \partial^\mu \pi^0 + \frac{1}{2} \partial_\mu \eta \partial^\mu \eta + \frac{1}{2} \partial_\mu \eta' \partial^\mu \eta' - \frac{1}{2} (\pi^0, \eta, \eta') \text{diag}(M_{\pi^0}^{\prime 2}, M_\eta^{\prime 2}, M_{\eta'}^{\prime 2}) (\pi^0, \eta, \eta')^T. \quad (\text{F3})$$

(mass eigenstate)

In Eq. (F1), the coefficient of kinetic terms is given as a  $3 \times 3$  matrix,

$$\frac{1}{Z} \simeq \begin{pmatrix} 1 - Z_{33(1)} & 0 & 0 \\ 0 & 1 - Z_{88(1)} & 0 \\ 0 & 0 & 1 \end{pmatrix}, \quad (\text{F4})$$

$$Z_{33(1)} \sim Z_{\pi^+(1)}, \quad (\text{F5})$$

$$Z_{88(1)} = -8 \left( \frac{M_{\pi^+}^2 + 2\bar{M}_K^2}{f^2} L_4^r + \frac{M_{88}^2}{f^2} L_5^r \right) + 6c\mu_{\bar{K}}, \quad (\text{F6})$$

$$M_{88}^2 = \frac{2(M_{K^+}^2)_{\text{tr}} + 2(M_{K^0}^2)_{\text{tr}} - (M_{\pi^+}^2)_{\text{tr}}}{3}. \quad (\text{F7})$$

The matrix in Eq. (F4) implies that the kinetic terms in Eq. (F1) are slightly deviated from unity with 1-loop correction. The mass matrix denoted as  $M^2$  in Eq. (F1) indicates the 1-loop corrected mixing mass matrix in the SU(3) basis. To normalize the kinetic terms in Eq. (F1) canonically, one should implement basis transformation,

$$\begin{pmatrix} \pi_3 \\ \eta_8 \\ \eta_0 \end{pmatrix} = \sqrt{Z} \begin{pmatrix} \pi_3^R \\ \eta_8^R \\ \eta_0^R \end{pmatrix}, \quad \sqrt{Z} \sim \begin{pmatrix} \sqrt{Z_1^\pi} & 0 & 0 \\ 0 & \sqrt{Z_2^\pi} & 0 \\ 0 & 0 & 1 \end{pmatrix}, \quad (\text{F8})$$

$$\sqrt{Z_1^\pi} = 1 + \frac{Z_{33(1)}}{2} \sim \sqrt{Z_{\pi^+}}, \quad (\text{F9})$$

$$\sqrt{Z_2^\pi} = 1 + \frac{Z_{88(1)}}{2}. \quad (\text{F10})$$

The transformation in Eq. (F8) relates the basis in Eq. (F1) to one given in Eq. (F2). Thus, the kinetic terms are canonically normalized in Eqs. (F2-F3). One diagonalizes the mass



matrix in Eq. (F2) and obtains Lagrangian with mass eigenstates in Eq. (F3). The mass matrix given in Eq. (F2) is expressed as,

$$M'^2 = \begin{pmatrix} M'_{33}{}^2 & M'_{38}{}^2 & M'_{30}{}^2 \\ * & M'_{88}{}^2 & M'_{80}{}^2 \\ * & * & M'_{00}{}^2 \end{pmatrix}. \quad (\text{F11})$$

In the above mass matrix, the 1-loop corrected masses are denoted with primes. We ignore quadratic terms with respect to the small quantities so that the 1-loop corrected masses in Eq. (F11) are simplified as,

$$M'_{33}{}^2 \simeq (M_{\pi^+}^2)_{\text{tr}} \left[ 1 + (4c - 3)\mu_{\pi^+} - \frac{1}{3}\mu_{88} + 2(c - 1)\bar{\mu}_K \right. \\ \left. - 8\frac{M_{\pi^+}^2 + 2\bar{M}_K^2}{f^2}L_{46}^r - 8\frac{M_{\pi^+}^2}{f^2}L_{58}^r \right], \quad (\text{F12})$$

$$M'_{38}{}^2 \simeq M_{38}^2 = \frac{(M_{K^+}^2)_{\text{tr}} - (M_{K^0}^2)_{\text{tr}}}{\sqrt{3}}, \quad (\text{F13})$$

$$M'_{88}{}^2 \simeq M_{88}^2 - M_{\pi^+}^2\mu_{\pi^+} - \left( \frac{16\bar{M}_K^2 - 7M_{\pi^+}^2}{9} \right) \mu_{88} + \frac{2}{3} (9cM_{88}^2 + 3M_{\pi^+}^2 - 8\bar{M}_K^2) \bar{\mu}_K \\ - \frac{8M_{88}^2}{f^2} (M_{\pi^+}^2 + 2\bar{M}_K^2) L_{46}^r - \frac{8}{f^2} M_{88}^4 L_5^r + \frac{16}{3f^2} [8(M_{\pi^+}^2 - \bar{M}_K^2)^2 L_7^r \\ + (M_{\pi^+}^4 + 2(M_{\pi^+}^2 - 2\bar{M}_K^2)^2) L_8^r], \quad (\text{F14})$$

$$M'_{30}{}^2 \simeq M_{30}^2 = -\hat{g}_{2p} [(M_{K^+}^2)_{\text{tr}} - (M_{K^0}^2)_{\text{tr}}], \quad (\text{F15})$$

$$M'_{80}{}^2 \simeq M_{80}^2 + \frac{\hat{g}_{2p}}{\sqrt{3}} \left[ 3M_{\pi^+}^2\mu_{\pi^+} + \frac{1}{3} (5M_{\pi^+}^2 - 8\bar{M}_K^2) \mu_{88} + 2 \{ 3c(M_{\pi^+}^2 - \bar{M}_K^2) \right. \\ \left. + (3M_{\pi^+}^2 - 4\bar{M}_K^2) \} \bar{\mu}_K \right] - 2M_{80}^2 \left[ \frac{M_{\pi^+}^2 + 2\bar{M}_K^2}{f^2} T_{34}^r - \frac{2\bar{M}_K^2}{f^2} T_5^r + \frac{2M_{88}^2}{f^2} L_5^r \right], \quad (\text{F16})$$

where  $T_{34}^r = 2L_4^r - T_3^r$  and  $\hat{g}_{2p} = fg_{2p}/B$ . Since 1-loop corrected masses in Eqs. (F12-F16) are invariant under renormalization, one can confirm that they satisfy the following relation,

$$\frac{\partial M'_{33}{}^2}{\partial \ln \mu} = \frac{\partial M'_{38}{}^2}{\partial \ln \mu} = \frac{\partial M'_{88}{}^2}{\partial \ln \mu} = \frac{\partial M'_{30}{}^2}{\partial \ln \mu} = \frac{\partial M'_{80}{}^2}{\partial \ln \mu} = 0. \quad (\text{F17})$$

Comparing Eqs. (E8-E10) with Eqs. (F12, F13, F15), we find that the neutral mass matrix elements are related to charged ones as,

$$M'_{33}{}^2 \sim M_{\pi^+}^2 - \Delta_{\text{EM}}, \quad (\text{F18})$$

$$M'_{38}{}^2 \sim \frac{1}{\sqrt{3}} (M_{K^+}^2 - M_{K^0}^2 - \Delta_{\text{EM}}), \quad (\text{F19})$$

$$M'_{30}{}^2 \sim -\hat{g}_{2p} (M_{K^+}^2 - M_{K^0}^2 - \Delta_{\text{EM}}). \quad (\text{F20})$$

Using Eqs. (F18-F20), one can write the mass matrix in Eq. (F11) as,

$$M'^2 = \begin{pmatrix} M'_{\pi^+} - \Delta_{\text{EM}} & \frac{1}{\sqrt{3}}(M'_{K^+} - M'_{K^0} - \Delta_{\text{EM}}) & -\hat{g}_{2p}(M'_{K^+} - M'_{K^0} - \Delta_{\text{EM}}) \\ * & M'_{88} & M'_{80} \\ * & * & M'_{\pi^0} + M'_{\eta} + M'_{\eta'} - M'_{\pi^+} - \Delta_{\text{EM}} - M'_{88} \end{pmatrix}, \quad (\text{F21})$$

where we utilized the relation of trace for the mass matrix,

$$M_{00}^2 = M_{\pi^0}^2 + M_{\eta}^2 + M_{\eta'}^2 - M_{33}^2 - M_{88}^2. \quad (\text{F22})$$

Provided that physical masses,  $M_{\pi^+}^2$ ,  $M_{K^+}^2$ ,  $M_{K^0}^2$ ,  $M_{\pi^0}^2$ ,  $M_{\eta}^2$  and  $M_{\eta'}^2$  are given as experimental values, the mass matrix in Eq. (F21) is written in terms of four model parameters:  $(\hat{g}_{2p}, \Delta_{\text{EM}}, M_{88}^2, M_{80}^2)$ . The mixing matrix should be determined to diagonalize the mass matrix in Eq. (F21) as,

$$O^T M'^2 O = \text{diag}(M_{\pi^0}^2, M_{\eta}^2, M_{\eta'}^2). \quad (\text{F23})$$

### Appendix G: 1-loop correction to decay constants of $\pi^+$ and $K^+$

In this appendix, 1-loop corrected decay constants are analyzed for charged pseudoscalars. The decay constants are defined with parameterizing matrix elements as,

$$\langle \pi^+(p) | \bar{u} \gamma_{\mu} \gamma_5 d | 0 \rangle |_{1\text{-loop order}} = i\sqrt{2} f_{\pi^+} p_{\mu}, \quad (\text{G1})$$

$$\langle K^+(p) | \bar{u} \gamma_{\mu} \gamma_5 s | 0 \rangle |_{1\text{-loop order}} = i\sqrt{2} f_{K^+} p_{\mu}. \quad (\text{G2})$$

One can find that 1-loop corrected decay constants are related with wave function renormalization in Eq. (E6) in the following as,

$$f_{\pi^+} = \frac{f}{\sqrt{Z_{\pi^+}}}, \quad f_{K^+} = \frac{f}{\sqrt{Z_{K^+}}}, \quad (\text{G3})$$

where one can show that the quantities in Eq. (G3) are renormalization scale invariant, *i.e.*,

$$\frac{\partial}{\partial \ln \mu} f_{\pi^+} = \frac{\partial}{\partial \ln \mu} f_{K^+} = 0. \quad (\text{G4})$$

Equation (G3) leads to the relation between the decay constants of pion and one for kaon in Eq. (84).

## Appendix H: Wess-Zumino-Witten term

In this appendix, we give the expression for the WZW term. As suggested in Ref. [16], one can obtain the WZW term by integrating the Bardeen form anomaly. Following Ref. [46], we can write the expression for the WZW term,

$$\begin{aligned} \mathcal{L}_{\text{WZ}} = & -\frac{N_c}{16\pi^2} \epsilon^{\mu\nu\rho\sigma} \int_0^1 dt \text{tr} \frac{\pi}{f} \left[ V_{\mu\nu}(t) V_{\rho\sigma}(t) + \frac{1}{3} A_{\mu\nu}(t) A_{\rho\sigma}(t) \right. \\ & - \frac{8i}{3} (V_{\mu\nu}(t) A_\rho(t) A_\sigma(t) + A_\mu(t) V_{\nu\rho}(t) A_\sigma(t) + A_\mu(t) A_\nu(t) V_{\rho\sigma}(t)) \\ & \left. - \frac{32}{3} A_\mu(t) A_\nu(t) A_\rho(s) A_\sigma(t) \right], \end{aligned} \quad (\text{H1})$$

where  $N_c = 3$  indicates the color factor. The notations in Eq. (H1) are defined as,

$$\begin{aligned} V_\mu(t) = & \frac{1}{2} (\xi(t) V_\mu \xi(-t) + \xi(-t) V_\mu \xi(t) + \xi(t) A_\mu \xi(-t) - \xi(-t) A_\mu \xi(t) \\ & - i\xi(t) \partial_\mu \xi(-t) - i\xi(-t) \partial_\mu \xi(t)), \end{aligned} \quad (\text{H2})$$

$$\begin{aligned} A_\mu(t) = & \frac{1}{2} (\xi(t) V_\mu \xi(-t) - \xi(-t) V_\mu \xi(t) + \xi(t) A_\mu \xi(-t) + \xi(-t) A_\mu \xi(t) \\ & - i\xi(t) \partial_\mu \xi(-t) + i\xi(-t) \partial_\mu \xi(t)), \end{aligned} \quad (\text{H3})$$

$$V_{\mu\nu}(t) = \partial_\mu V_\nu(t) - \partial_\nu V_\mu(t) + i[V_\mu(t), V_\nu(t)] + i[A_\mu(t), A_\nu(t)], \quad (\text{H4})$$

$$A_{\mu\nu}(t) = \partial_\mu A_\nu(t) - \partial_\nu A_\mu(t) + i[V_\mu(t), A_\nu(t)] + i[A_\mu(t), V_\nu(t)], \quad (\text{H5})$$

$$\xi(t) = e^{-i(1-t)\pi/f}. \quad (\text{H6})$$

The expressions given in Eqs. (H1-H6) are all defined in Minkowski space-time.

## Appendix I: Form factors at $O(p^4)$ for $\tau^- \rightarrow K_s \pi^- \nu$ decay

The vector form factors for  $\tau^- \rightarrow K_s \pi^- \nu$  decays including  $\eta^0$  meson loop were computed in Ref. [6]. In the present work, we do not include the loop contribution of the singlet meson. Below, we show the expression for form factors without the singlet meson loop contribution, which is used to calculate the decay spectrum of  $\tau^- \rightarrow K_s \pi^- \nu$ . The expression in this appendix can be obtained from Eqs. (40-54) in [6], by simply setting the mixing angle ( $\theta_{08}$ ) between the singlet meson and the octet meson to be zero. In the formulas shown below, the isospin breaking effect and the mixing induced CP violation of the neutral kaon system is also neglected. By ignoring CP violation due to the mixing,  $K_s$  is CP even state,

$$|K_s\rangle = \frac{1}{\sqrt{2}} (|K^0\rangle - |\bar{K}^0\rangle), \quad (\text{I1})$$

where  $|\bar{K}^0\rangle = -CP|K^0\rangle$ . Since  $\Delta S = \Delta Q = -1$  rule holds, one finds the following relation,

$$\langle K_s\pi^-|\bar{s}\gamma_\mu u|0\rangle = -\frac{1}{\sqrt{2}}\langle\bar{K}^0\pi^-|\bar{s}\gamma_\mu u|0\rangle. \quad (I2)$$

One defines the vector form factors for  $\bar{K}^0\pi^-(K^-\pi^0)$  and its CP conjugate states,

$$\begin{aligned} \langle\bar{K}^0\pi^-|\bar{s}\gamma_\mu u|0\rangle &= F_V^{\bar{K}^0\pi^-}(q_\mu - Q_\mu\frac{\Delta_{K\pi}}{Q^2}) + F_S^{\bar{K}^0\pi^-}\frac{Q_\mu}{Q^2}, \\ \langle K^0\pi^+|\bar{u}\gamma_\mu s|0\rangle &= F_V^{K^0\pi^+}(q_\mu - Q_\mu\frac{\Delta_{K\pi}}{Q^2}) + F_S^{K^0\pi^+}\frac{Q_\mu}{Q^2}, \\ \langle K^-\pi^0|\bar{s}\gamma_\mu u|0\rangle &= F_V^{K^-\pi^0}(q_\mu - Q_\mu\frac{\Delta_{K\pi}}{Q^2}) + F_S^{K^-\pi^0}\frac{Q_\mu}{Q^2}, \\ \langle K^+\pi^0|\bar{u}\gamma_\mu s|0\rangle &= F_V^{K^+\pi^0}(q_\mu - Q_\mu\frac{\Delta_{K\pi}}{Q^2}) + F_S^{K^+\pi^0}\frac{Q_\mu}{Q^2}. \end{aligned} \quad (I3)$$

Since under CP transformation, the charged currents are related to each other as follows,

$$CP(\bar{s}\gamma_\mu u)(CP)^{-1} = -\bar{u}\gamma^\mu s, \quad (I4)$$

the following relations among the form factors are derived,

$$\begin{aligned} F_V^{\bar{K}^0\pi^-} &= -F_V^{K^0\pi^+}, F_S^{\bar{K}^0\pi^-} = -F_S^{K^0\pi^+}, \\ F_V^{K^-\pi^0} &= -F_V^{K^+\pi^0}, F_S^{K^-\pi^0} = -F_S^{K^+\pi^0}. \end{aligned} \quad (I5)$$

In the isospin limit, we also obtain the relations,

$$\begin{aligned} F_V^{\bar{K}^0\pi^-} &= \sqrt{2}F_V^{K^-\pi^0}, F_S^{\bar{K}^0\pi^-} = \sqrt{2}F_S^{K^-\pi^0}, \\ F_V^{K^0\pi^+} &= \sqrt{2}F_V^{K^+\pi^0}, F_S^{K^0\pi^+} = \sqrt{2}F_S^{K^+\pi^0}. \end{aligned} \quad (I6)$$

Using Eq. (I2), Eq. (I3), Eq. (I5) and Eq. (I6), one can relate the form factor of  $K_s\pi^-$  of Eq. (I2) to that of  $K^+\pi^0$ ,

$$\langle K_s\pi^-|\bar{s}\gamma_\mu u|0\rangle = \langle K^+\pi^0|\bar{u}\gamma_\mu s|0\rangle. \quad (I7)$$

The contribution to the form factors is divided into two parts. One of them comes from 1 PI diagrams and the other comes from the diagrams which include the propagator of  $K^*$  meson,

$$F_V^{K^+\pi^0} = F_V^{1PI} + F_V^{K^*}, \quad (I8)$$

$$F_S^{K^+\pi^0} = F_S^{1PI} + F_S^{K^*}. \quad (I9)$$

Each contribution to form factors is given below (See also [6]),

$$F_V^{1PI} = -\frac{1}{\sqrt{2}}(1 - \frac{M_V^2}{2g^2 f^2}) + \frac{1}{\sqrt{2}} \left[ -\frac{3c}{2}(H_{K\pi} + H_{K\eta_8}) + \frac{cM_V^2}{8g^2 f^2}(10\mu_K + 3\mu_{\eta_8} + 11\mu_\pi) \right. \\ \left. - \frac{3}{8} \left( \frac{M_V^2}{g^2 f^2} \right)^2 (H_{K\pi} + H_{K\eta_8} + \frac{2\mu_K + \mu_\pi + \mu_{\eta_8}}{2}) - \frac{C_5^r}{2} \frac{Q^2}{f^2} \right. \\ \left. + \frac{M_V^2}{2g^2 f^2} \left\{ \frac{M_V^2}{2g^2 f^2} K_4^r \frac{m_K^2}{f^2} - 4L_5^r \frac{\Sigma_{K\pi}}{f^2} + \frac{2m_K^2 + m_\pi^2}{f^2} \left( \frac{M_V^2}{2g^2 f^2} K_5^r - 8L_4^r \right) \right\} \right], \quad (I10)$$

$$F_V^{K*} = -\frac{1}{2\sqrt{2}g} \frac{M_V^2}{M_V^2 + \delta A_{K*}} \left[ 4E + \sqrt{2} \frac{G + Q^2 \mathcal{H}}{f^2} - \frac{M_V^2}{gf^2} \right], \quad (I11)$$

$$F_S^{1PI} = \frac{1}{\sqrt{2}} \frac{1}{Q^2} \left[ \left( 1 - \frac{M_V^2}{2g^2 f^2} \right) \left\{ -\frac{\Delta_{K\pi} \bar{J}_{K\pi}}{8f^2} \{ 5cQ^2 - (5c-3)\Sigma_{K\pi} \} + \frac{\Delta_{K\eta_8} \bar{J}_{K\eta_8}}{8f^2} \{ 3cQ^2 - (3c-1)\Sigma_{K\pi} \} \right\} \right. \\ \left. + \frac{3\Delta_{K\pi}}{8f^2} \left( 1 - \frac{M_V^2}{2g^2 f^2} \right)^2 \left\{ \frac{\Delta_{K\pi}^2}{s} \bar{J}_{K\pi} + \frac{\Delta_{K\eta_8}^2}{s} \bar{J}_{K\eta_8} \right\} \right] \\ + \frac{1}{\sqrt{2}} \frac{\Delta_{K\pi}}{Q^2} \left[ -\left( 1 - \frac{M_V^2}{2g^2 f^2} \right) + \frac{c}{4} Q^2 \frac{3\mu_{\eta_8} + 2\mu_K - 5\mu_\pi}{\Delta_{K\pi}} + c \frac{M_V^2}{8g^2 f^2} (10\mu_K + 3\mu_8 + 11\mu_\pi) \right. \\ \left. - \frac{3}{16} \left( \frac{M_V^2}{g^2 f^2} \right)^2 (2\mu_K + \mu_\pi + \mu_{\eta_8}) - 4L_5^r \frac{Q^2}{f^2} \right. \\ \left. + \frac{M_V^2}{2g^2 f^2} \left\{ \frac{M_V^2}{2g^2 f^2} K_4^r \frac{m_K^2}{f^2} - 4L_5^r \frac{\Sigma_{K\pi}}{f^2} + \frac{2m_K^2 + m_\pi^2}{f^2} \left( \frac{M_V^2}{2g^2 f^2} K_5^r - 8L_4^r \right) \right\} \right], \quad (I12)$$

$$F_S^{K*} = -\frac{1}{2\sqrt{2}g} \frac{\Delta_{K\pi}}{Q^2} \frac{M_V^2}{M_V^2 + \delta A_{K*} + Q^2 \delta \tilde{B}_{K*}} \left[ 4(E + Q^2 \mathcal{F}) + \sqrt{2} \frac{G}{f^2} - \frac{M_V^2}{gf^2} \right], \quad (I13)$$

where  $G, \mathcal{H}, E$  and  $\mathcal{F}$  are given as,

$$G = \frac{1}{\sqrt{2}g} \{ M_V^2 + \delta A_{K*} + Q^2 \delta \tilde{B}_{K*} - \frac{3M_V^2}{2f^2} (L_{K\pi} + L_{K\eta_8}) \}, \quad (I14)$$

$$\mathcal{H} = \frac{1}{\sqrt{2}g} \{ Z_V^r - 2gC_4^r - \delta \tilde{B}_{K*} + \frac{3M_V^2}{2f^2} (M_{K\pi}^r + M_{K\eta_8}^r) \}, \quad (I15)$$

$$E = \frac{M_V^2}{4gf^2} - \frac{g}{2M_V^2} \{ (\delta A_{K*} + Q^2 \delta \tilde{B}_{K*}) (1 - \frac{M_V^2}{2g^2 f^2}) - C_1^r m_K^2 - C_2^r (2m_K^2 + m_\pi^2) \} \\ + \frac{M_V^2}{16gf^2} \{ -3(2\mu_K + \mu_\pi + \mu_{\eta_8}) + c(10\mu_K + 3\mu_{\eta_8} + 11\mu_\pi) - 32L_4^r \frac{2m_K^2 + m_\pi^2}{f^2} - 16L_5^r \frac{\Sigma_{K\pi}}{f^2} \} \\ + \{ \frac{g}{2M_V^2} (1 - \frac{M_V^2}{2g^2 f^2}) (\delta \tilde{B}_{K*} - Z_V^r) + \frac{C_3^r}{8f^2} \} Q^2, \quad (I16)$$

$$\mathcal{F} = -\{ \frac{g}{2M_V^2} (1 - \frac{M_V^2}{2g^2 f^2}) (\delta \tilde{B}_{K*} - Z_V^r) + \frac{C_3^r}{8f^2} \} + \frac{M_V^2}{8gf^4} \frac{1}{Q^2} \{ \Sigma_{K\pi} (\frac{3}{4} \bar{J}_{K\pi} + \frac{1}{12} \bar{J}_{K\eta_8}) \\ + c(Q^2 - \Sigma_{K\pi}) (\frac{5}{4} \bar{J}_{K\pi} + \frac{1}{4} \bar{J}_{K\eta_8}) \}. \quad (I17)$$

We obtain  $\delta\tilde{B}_{K^*}$  and  $\delta A_{K^*}$  in the above equations by taking the isospin limit of Eq. (C16) and Eq. (C15) and they are given respectively as follows,

$$\begin{aligned}\delta\tilde{B}_{K^*} &= Z_V^r(\mu) + 3g_{\rho\pi\pi}^2 \left[ M_{K\pi}^r + M_{K\eta_8}^r \right], \\ \delta A_{K^*} &= \Delta A_{K^{*+}} + C_1^r(\mu) M_{K^+}^2 + C_2^r(\mu) (2\bar{M}_K^2 + M_\pi^2) - Q^2 Z_V^r(\mu),\end{aligned}\quad (\text{I18})$$

where  $\Delta A_{K^*}$  is given by,

$$\Delta A_{K^*} = -3Q^2 g_{\rho\pi\pi}^2 \left[ M_{K\pi}^r + M_{K\eta_8}^r \right] + 3g_{\rho\pi\pi}^2 \left[ L_{K\pi} + L_{K\eta_8} - \frac{f^2}{2} \{2\mu_K + \mu_\pi + \mu_{\eta_8}\} \right]. \quad (\text{I19})$$

- 
- [1] R. Arnaldi *et al.* [NA60 Collaboration],  
Phys. Lett. B **757**, 437 (2016) [arXiv:1608.07898 [hep-ex]].
  - [2] M. Ablikim *et al.* [BESIII Collaboration],  
Phys. Rev. D **92**, no. 1, 012001 (2015) [arXiv:1504.06016 [hep-ex]].
  - [3] M. Bando, T. Kugo, S. Uehara, K. Yamawaki and T. Yanagida,  
Phys. Rev. Lett. **54**, 1215 (1985).
  - [4] G. Ecker, J. Gasser, A. Pich and E. de Rafael, Nucl. Phys. B **321**, 311 (1989).
  - [5] G. Ecker, J. Gasser, H. Leutwyler, A. Pich and E. de Rafael, Phys. Lett. B **223**, 425 (1989).
  - [6] D. Kimura, K. Y. Lee and T. Morozumi, PTEP **2013**, 053B03 (2013)  
[Erratum-ibid. **2014**, no. 8, 089202 (2014)] [arXiv:1201.1794 [hep-ph]].
  - [7] S. Anderson *et al.* [CLEO Collaboration],  
Phys. Rev. D **61**, 112002 (2000) [hep-ex/9910046 [hep-ex]].
  - [8] M. Fujikawa *et al.* [Belle Collaboration],  
Phys. Rev. D **78**, 072006 (2008) [arXiv:0805.3773 [hep-ex]].
  - [9] M. Davier, A. Hcker, B. Malaescu, C. Z. Yuan and Z. Zhang,  
Eur. Phys. J. C **74**, no. 3, 2803 (2014) [arXiv:1312.1501 [hep-ex]].
  - [10] B. Aubert *et al.* [BaBar Collaboration],  
Phys. Rev. D **76**, 051104 (2007) [arXiv:0707.2922 [hep-ex]].
  - [11] D. Epifanov *et al.* [Belle Collaboration],  
Phys. Lett. B **654**, 65 (2007) [arXiv:0706.2231 [hep-ex]].
  - [12] K. Inami *et al.* [Belle Collaboration], Phys. Lett. B **672**, 209 (2009) [arXiv:0811.0088 [hep-ex]].

- [13] P. del Amo Sanchez *et al.* [BaBar Collaboration],  
Phys. Rev. D **83**, 032002 (2011) [arXiv:1011.3917 [hep-ex]].
- [14] A. Pich, Prog. Part. Nucl. Phys. **75**, 41 (2014) [arXiv:1310.7922 [hep-ph]].
- [15] G. C. Wick, A. S. Wightman and E. P. Wigner, Phys. Rev. **88**, 101 (1952).
- [16] J. Wess and B. Zumino, Phys. Lett. B **37**, 95 (1971).
- [17] E. Witten, Nucl. Phys. B **223**, 422 (1983).
- [18] T. Fujiwara, T. Kugo, H. Terao, S. Uehara and K. Yamawaki,  
Prog. Theor. Phys. **73**, 926 (1985).
- [19] M. Bando, T. Kugo and K. Yamawaki, Phys. Rept. **164**, 217 (1988).
- [20] M. Hashimoto, Phys. Rev. D **54**, 5611 (1996) [hep-ph/9605422].
- [21] A. Bramon, A. Grau and G. Pancheri, Phys. Lett. B **344**, 240 (1995).
- [22] A. Bramon, R. Escribano and M. D. Scadron, Phys. Lett. B **503**, 271 (2001) [hep-ph/0012049].
- [23] C. Terschlüsen and S. Leupold, Phys. Lett. B **691**, 191 (2010) [arXiv:1003.1030 [hep-ph]].
- [24] C. Terschlüsen, S. Leupold and M. F. M. Lutz,  
Eur. Phys. J. A **48**, 190 (2012) [arXiv:1204.4125 [hep-ph]].
- [25] S. P. Schneider, B. Kubis and F. Niecknig,  
Phys. Rev. D **86**, 054013 (2012) [arXiv:1206.3098 [hep-ph]].
- [26] Y. H. Chen, Z. H. Guo and H. Q. Zheng,  
Phys. Rev. D **85**, 054018 (2012) [arXiv:1201.2135 [hep-ph]].
- [27] P. Roig, A. Guevara and G. Lopez Castro,  
Phys. Rev. D **89**, no. 7, 073016 (2014) [arXiv:1401.4099 [hep-ph]].
- [28] R. Escribano and S. Gonzalez-Sols, [arXiv:1511.04916 [hep-ph]].
- [29] R. Urech, Nucl. Phys. B **433**, 234 (1995) [hep-ph/9405341].
- [30] J. Gasser and H. Leutwyler, Nucl. Phys. B **250** (1985) 517.
- [31] A. Pilaftsis and C. E. M. Wagner, Nucl. Phys. B **553**, 3 (1999) [hep-ph/9902371].
- [32] K.A. Olive *et al.* [Particle Data Group], Chin. Phys. C **38**, 090001 (2014).
- [33] M. N. Achasov *et al.*, J. Exp. Theor. Phys. **107**, 61 (2008).
- [34] R. I. Dzhelyadin *et al.*, Phys. Lett. B **102**, 296 (1981); JETP Lett. **33**, 228 (1981).
- [35] R. R. Akhmetshin *et al.* [CMD-2 Collaboration],  
Phys. Lett. B **613**, 29 (2005) [hep-ex/0502024].
- [36] D. Babusci *et al.* [KLOE-2 Collaboration],

- Phys. Lett. B **742**, 1 (2015) [arXiv:1409.4582 [hep-ex]].
- [37] M. N. Achasov *et al.*, Phys. Lett. B **504**, 275 (2001).
- [38] A. Anastasi *et al.* [KLOE-2 Collaboration],  
Phys. Lett. B **757**, 362 (2016) [arXiv:1601.06565 [hep-ex]].
- [39] P. Adlarson *et al.* [WASA-at-COSY Collaboration],  
Phys. Lett. B **707**, 243 (2012) [arXiv:1107.5277 [nucl-ex]].
- [40] R. I. Dzhelyadin *et al.*, Phys. Lett. B **94**, 548 (1980);  
Sov. J. Nucl. Phys. **32**, 516 (1980); Yad. Fiz. **32**, 998 (1980).
- [41] P. Aguar-Bartolome *et al.* [A2 Collaboration],  
Phys. Rev. C **89**, no. 4, 044608 (2014) [arXiv:1309.5648 [hep-ex]].
- [42] R. I. Dzhelyadin *et al.*, Sov. J. Nucl. Phys. **32**, 520 (1980); Yad. Fiz. **32**, 1005 (1980).
- [43] T. D. Lee and C. N. Yang, Nuovo Cim. **10**, 749 (1956).
- [44] J. F. Donoghue, E. Golowich and B. R. Holstein,  
Camb. Monogr. Part. Phys. Nucl. Phys. Cosmol. **2**, 1 (1992).
- [45] J. Gasser and H. Leutwyler, Nucl. Phys. B **250**, 465 (1985).
- [46] K. Fujikawa and H. Suzuki, Oxford, UK: Clarendon (2004) 284 p.